Early Warning Generation for Process with Unknown Disturbance

by

©Mohammad Aminul Islam Khan

A Dissertation submitted to the School of Graduate Studies in partial fulfillment of the requirements for the degree of

Doctor of Philosophy

Faculty of Engineering and Applied Science

Memorial University of Newfoundland

May 2020

St. John's Newfoundland

Abstract

Process safety has paramount importance in a chemical process. A well designed control system is the first layer in a process system. The warning system works as the upper protection layer above the control system. It alerts the operators when the control system fails to prevent an undesired situation. A typical warning system issues warnings when a monitored variable exceeds the threshold. Often these do not allow operators sufficient lead-time to take corrective actions. With the motivation of improving the operator's working environment by providing lead-time, the current research develops a predictive warning scheme using a moving horizon technique.

The main hypothesis proposed in this thesis is given the current state of process system, the future states of the system can be predicted using a suitable model of process system. If an external input disturbs the system state, the controller will try to bring the system within the desired control/safety limits of the system. A warning is issued if it is determined that the control system will not be able to keep the system withing the safety limits. Based on the hypothesis, warning systems were developed for both linear and nonlinear systems. For linear systems, using the gain of the models, a linear constrained optimization problem was formulated. Linear programming (LP) was used to determine if the system will remain within the safety limits or not. In case the LP determines that there is no feasible solution within the constrained limits, warnings are issued.

The predictive warning scheme was also extended for nonlinear systems. A non-linear receding horizon predictor was used to predict the future states of the nonlinear system. However, for nonlinear system formulation leads to nonlinear constrained optimization problem, where the constraints are the safety limits. Controller's ability to keep the predicted states inside the safety limit was checked using a feasibility test algorithm. The algorithm uses a constraint separation method with weighting functions to determine the existence of a feasible solution. The algorithm calculates the global minimum of the objective function. If the global minimum of the objective function is positive, it signifies no feasible solution within the input and output constraints of the system and a warning is issued.

Prediction of the effect of the disturbances requires the knowledge of the disturbances. In process industries, disturbances are often unmeasured. This thesis also investigates the estimation of unknown disturbances. An iterative Expectation Minimization (EM) algorithm was proposed for the estimation of the unknown states and disturbances of nonlinear systems.

Efficacy of the proposed methods was shown through a number of case studies. The warning system for the linear system was simulated on a virtual plant of a continuous stirred tank heater (CSTH). The nonlinear warning system was implemented on a continuous stirred tank reactor (CSTR). Both case studies showed that, the proposed method was capable of providing a warning earlier than the traditional methods that issues warning based on the measured signals.

Acknowledgements

I would like to take the opportunity to thank my supervisors Dr. Syed Imtiaz, Dr. Faisal Khan and Dr. Salim Ahmed for all their generous help, support and valuable suggestions throughout my academic journey. Since the first day, they have been steady guides on this difficult voyage. There were times of frustration during research, when they encouraged me and provided me with directions, spending hours with me solving problems. I would like thank Dr. Shoukat Choudhury and Malik Tahiyat for their support to conduct my experiments for research.

The financial support provided by the Research and Development Corporation (RDC), Natural Sciences and Engineering Research Council (NSERC) and School Graduate Studies, Memorial University of Newfoundland and the Faculty of Engineering and Applied Science is much appreciated.I would like to thank my research colleagues and friends in Memorial University who helped me through the journey with the share of their knowledge and expertise. I would like to thank the stuffs of Faculty of Engineering and Applied Science Moya Crocker, Colleen Mahoney, Nicole Parisi and Tina Dwyer for their support throughout my Ph.D.

I would like to express the highest gratitude to my family in St. John's and in Bangladesh, especially my wife Gulshan Naher as well as my siblings and relatives for their encouragement and support. Finally, I express my greatest gratitude to my parents and dedicate this thesis to them.

Co-authorship Statement

I, Mohammad Aminul Islam Khan, hold primary author status for all the Chapters in this thesis. However, each manuscript is co-authored by my supervisors and co-researchers. Contributions of each of the co-authors are listed below:

- Mohammad Aminul Islam Khan, Malik Tahiyat, Syed Imtiaz, Mohammad Choudhury, Faisal Khan, **"Experimental evaluation of control performance of MPC as a regulatory controller"** has been accepted for publication in ISA transaction (2017).
  Statement: The research was conducted by Mohammad Aminul Khan as the first author. He prepared the manuscripts. Malik Tahiyat helped to conduct the experiment and gave access to the experimental set up. Other authors supervised to design experiment and reviewed the manuscript and provided feedback.

- Mohammad Aminul Islam Khan, Syed Imtiaz, Faisal Khan, **"Predictive alarm generation for chemical processes with unknown disturbance"** has been accepted for publication in Canadian Journal of Chemical Engineering (2018).
  Statement: The research is conducted by Mohammad Aminul Islam Khan as the first author. He prepared the manuscripts. Other authors supervised and reviewed the manuscript.

- Mohammad Aminul Islam Khan, Syed Imtiaz, Faisal Khan, **"Simultaneous**

estimation of hidden state and unknown input using expectation maximization (EM) algorithm" has been accepted for publication in Industrial Engineering and Chemistry Research (2019).

Statement: The research is conducted by Mohammad Aminul Islam Khan as the first author. He prepared the manuscripts. Other authors supervised and reviewed the manuscript and provided feedback.

- Mohammad Aminul Islam Khan, Syed Imtiaz, Faisal Khan, **"Predictive Warning System for Nonlinear Process"** to be submitted in a journal.

  Statement: The research is conducted by Mohammad Aminul Islam Khan as the first author. He prepared the manuscripts. Other authors supervised and reviewed the manuscript and provided feedback.

Table of Contents

List of Tables

List of Figures

Chapter 1

Introduction

1.1 Background and motivation

The number of measured variables of a typical process plant has increased significantly over the past decades with the advent of sensor technology. Currently, operators have access to more in-depth information about the plant through these variables. Safe and uninterrupted operation of a plant is understood by comparing the measured variables with predefined limits. Process systems are often affected by disturbances. When a disturbance affects a process, it changes the process states and may trigger a warning, when a state crosses the safety limits. A control system counteracts this phenomenon and tries to bring the process back to the original set points. If the actuator's capacity was unbounded, it can always bring the process back to safety. However, in most practical cases the controller's ability to mitigate the effect of a disturbance is limited by actuator capacity. When the controller cannot nullify the effect of the disturbance, one or more variables may exceed the safety limits. A well designed warning system identifies this type of situation and alerts the operators. A warning is triggered when the control system cannot keep the process variables within the desired limits. Currently, most warning systems monitor important process variables individually. Due to an increasing number of measured variables, many variables are interlinked and a large number of alarms may be triggered from a single violation of the safety limit and lead to alarm flooding. Alarm flooding creates a stressful environment, as the operator has to respond to a large number of alarms with corrective actions in a limited period of time. A number of researchers have attempted to improve the operator's environment by reducing the number of alarms. Some of the works focused on design techniques (e.g. delay timer, deadband, filter). These methods introduced an additional delay in detecting the fault. Others used multivariate statistical tools to reduce the number of alarms [Kresta et al., 1991, MacGregor et al., 1994, MacGregor and Kourti, 1995]. Multivariate statistical methods minimize the number of alarms and in some cases facilitate early warnings, compared to univariate methods. However, both multivariate and single variable methods use measured signals to generate the warning. This may be the only way of generating warnings for abrupt faults. However, process systems are frequently affected by disturbances which go through the system before they affect the states or measured outputs. Thus, there is a possibility to predict the impact of these disturbances as soon as they enter the system. However very little work has been done to generate warnings using a predictive signal. Due to extensive use of the model predictive controller (MPC) in the process industry, open loop models are typically known and process states are predicted in real time. This offers a unique opportunity to use process models for predicting states of the system using the existing control structure of the system. The motivation of the current research is to develop a 'predictive warning system' using the existing control structure of the system that is able to provide an early warning for disturbance type faults.

1.2 Objective

The objective of the current research is to develop a warning system that issues early warnings to give operators sufficient time to respond with corrective actions. Instead of using measured signals, predictive signals from a moving horizon predictor are used to issue warnings. Moving horizon predictors are integral parts of MPC. The idea of moving horizon prediction is demonstrated through the implementation of an MPC controller. An experimental study has compared the performance of MPC with intrincsic model control (IMC)-based proportional-integral-derivative (PID) controller. Next, a framework for a 'predictive warning system' for a linear system is developed. In an earlier study, a 'predictive warning' was developed for a linear system which assumed that the disturbance was known. The objective of the current study is to relax the assumption and develop a 'predictive warning' framework for more general cases when the disturbance is unknown. In the next step, the proposed warning system is extended for non-linear systems. Unknown input estimation of a non-linear system is a non-trivial problem and hence this step is has two stages. In the first stage, a simultaneous state and input estimation scheme has been developed, and then a warning system for nonlinear system has been developed. The major contributions of the thesis are:

Task 1: Evaluate the performance of the MPC and compare it with the PID as a regulatory controller.

Task 2: Design a predictive warning system for a linear system using receding horizon predictions and couple the system with a simultaneous state and input estimator.

Task 3: Develop a simultaneous state and input estimator for a nonlinear system.

Task 4: Develop a predictive warning system for a nonlinear system.

1.3 Brief overview of existing literature

The current study aims to use a receding horizon prediction in an MPC structure for warning generation. As stated in the previous section, the study will complete four tasks. This section presents a brief review of existing literature on the different topics of the current research. Instead of presenting a complete bibliography, the following subsections provide an overall summary of relevant literature and highlight significant works in control, monitoring and safety.

1.3.1 MPC as a regulatory controller

The PID is the most widely used controller in process industries due to its simplicity and reliability. Nevertheless, it has several limitations, such as being a SISO controller and thus structurally not optimal for highly interactive MIMO systems. Also, there is no universally accepted optimal tuning method for PID controllers. These limitations result in suboptimal tuning parameters for many PID loops in a process plant. To improve the performance of PID, different strategies were suggested by researchers, such as using of auto-tuning [Na, 2001] and a robust alternative structure [Ogunnaike and Mukati, 2006]. Many previous studies sought potential replacements for the PID of industrial settings, for example, state feedback observers, MPC, fuzzy controllers, constrained linear quadratic controllers (CLQ) and active disturbance rejection controllers (ADRC). Among the different alternatives, the MPC showed the most potential to replace PID controllers in process industries. Different comparative studies of the MPC with PID were performed to verify the superiority of the MPC in the supervisory layer. One such work showed the application of the MPC to optimize energy for a heat exchanger in the work of [Krishna Vinaya et al., 2012]. The authors concluded that the MPC is the better of these two structures. A performance comparison between the cascaded PID and hybrid MPC-PID structure was reported by [Singh et al., 2014], which used a PAT data management tool, OPC communication protocols, and a standard control platform for real time feedback control. This study suggested the potential of the MPC to replace the PID in the regulatory layer. Another study was performed in a pilot scale industrial setup by [Marzaki et al., 2014] which showed similar results. A hybrid MPC-PID control system was compared with a PID-only structure by [Sen et al., 2014] and the authors concluded that a hybrid structure has the potential to enhance the control performance and efficiency of pharmaceutical manufacturing operations.

Though there have been several studies to evaluate the performance of the MPC compared with the PID controller, there has been no prior study to compare the performances of an 'MPC directly manipulating actuator' with other structures. In Task 1 of the current research, an objective investigation of the performance of a direct MPC with its several other competing control structures was undertaken.

1.3.2 Warning generation for linear systems with unknown input

Next, predictive features of the MPC were used to develop an early warning generation framework. The objective of this study was to provide operators a lead-time to react to an abnormal situation. A predictive warning system was developed for a linear process with unknown input.

Typically, in process system, alarms are generated based on a measured variable exceeding the safety limits. Often, due to sensor noise, measurements momentarily exceed the threshold and this leads to a false alarm. Earlier approaches focused on improving the robustness of the alarm system by reducing false and missed alarms optimally. [Izadi et al., 2009] discussed the application of different signal processing and threshold design approaches such as filtering, deadband and delay-timer to reduce the false and missed alarms. A statistical approach to optimize the false and missed alarm is discussed in [Adnan et al., 2011]. As process systems are highly correlated, a single fault may excite several variables triggering multiple alarms. Thus, monitoring single variables sometimes leads to a high number of alarms. Multivariate statistics were used as an effective tool to generate alarms and monitor process systems [Kresta et al., 1991, MacGregor et al., 1994, MacGregor and Kourti, 1995]. All these methods relied on the measured signal to generate an alarm; thus they do not have much predictive capability. In recent years, there have been some studies which bring the predictive features into the warning system. Predictive warning generation provides a lead-time to the operator. [Juricek et al., 2001] showed an application of the Kalman filter based predictive warning method which was able to forecast an abnormal situation before it appeared. [Fernandez et al., 2005] proposed a neural network based supervisory method to generate a warning for an abnormal situation. A model based warning generation scheme with an open loop model was designed by [Khan et al., 2014]. Receding horizon predictions were used in this work to predict the future states. However, this work assumed that the disturbance input of the process was known, which is not realistic for most practical cases. To overcome the limitation, in the present study a simultaneous state and unknown input estimator were incorporated into the predictive alarm system. Next, the literature related to an unknown input estimator is reviewed.

1.3.3 State and unknown input estimator

[Radke and Gao, 2006] reviewed the observers used in the process industry and concluded that, the Luenberger based unknown input observer (UIO) shows promise for design simplicity and accurate estimation. [Corless and Tu, 1998] proposed a framework to estimate states and inputs simultaneously using 'Lyapunov-type characterization'. A fault reconstruction technique using UIO is shown in the work of [Lee and Park, 2012]. A more comprehensive review of observers used in chemical processes is provided by [Ali et al., 2015] with a conclusion that, despite their design simplicity, performance of the Luenberger observers suffer in the presence of model mismatch and higher noise levels. They also suggested the 'Bayesian estimator' as the possible replacement for these scenarios. An optimal recursive filter was proposed by [Kitanidis, 1987] for a process with unknown inputs, which was improved to become an unbiased minimum variance filter. This filter was used by [Hsieh, 2000] to estimate the unknown inputs. State and input estimators were linked together by [Gillijns and De Moor, 2007]. They proved that their estimation procedure showed optimal performance. This estimator was used to estimate the unknown disturbance and has been included in the 'model predictive warning' in Task 2.

1.3.4 Warning generation for nonlinear systems with unknown input

In most practical cases, processes show a certain amount of nonlinearity. Hence, it is necessary to improve the warning generation method for a nonlinear system with unknown disturbances. Estimation of unknown input for the process with hidden states is a challenging problem. So, the task of improving the warning generation system is divided into two sub-tasks. The goal of the first sub-task is to develop a procedure to estimate the state and unknown input simultaneously for a non-linear system. The second sub-task is to design a warning generation scheme for a non-linear process. Integration of these two sub-tasks provides a warning generation scheme for all general cases. Related research works for the sub-tasks are discussed separately in the following sections.

1.3.4.1 Simultaneous state and input estimation for a nonlinear system

State estimation is the focus of many researchers, as it is an integral part of control application. It is used for control and also for monitoring process health. It is more challenging when some of the inputs are unknown and hence a simultaneous estimation of both states and inputs is necessary. For linear cases, a Luenberger or Kalman based recursive filter solves the issue. However, these observers are not capable of handling the nonlinearity. A UIO based estimator was presented by [Imsland et al., 2007]. Another alternative was presented by [Korbicz et al., 2007] in the form of linear matrix inequality (LMI) based observer. A Bayesian framework provides a more general solution for state estimation. Some improved versions of the Kalman filter (e.g. extended Kalman filter(EKF), unscented Kalman filter(UKF)) are available to handle the system nonlinerity. A UKF based fault diagnosis and disturbance estimation method is discussed in [Zarei and Poshtan, 2010]. Both EKF and UKF use Gaussian approximation for process and measurement noises. A particle filter is more suitable for non-Gaussian nonlinear state estimation [Chen, 2003]. The Bayesian estimator for practical purposes requires constraint handling; hence optimization based estimation methods have been developed. One such work is presented by [Fang et al., 2013] to encompass simultaneous state and input estimation. In this work, state and input were estimated by optimizing the cost function. While implementing linearization based cost estimation, non-linearity propagates through the linearized point. For this, the accuracy of approximation deteriorates. Moreover, evaluating the derivative is challenging in most of the practical cases. The expectation maximization (EM) algorithm is an alternative tool to estimate the likelihood iteratively. It was used by [Andrieu and Doucet, 2003] to estimate the model parameters online. [Gopaluni, 2008] presented a particle filter based EM framework to estimate state and parameter simultaneously. In the work of [Güntürkün et al., 2014], an EM algorithm was used to estimate input. In the current study, the Bayesian solution is implemented to estimate state and input simultaneously using an EM algorithm. A particle filter was used in the E-step to estimate state, and gradient based optimization was used in the M-step to estimate input.

1.3.4.2 Predictive warning for nonlinear system

[Primbs et al., 1999] discussed two well known approaches for nonlinear optimum control: the control Lyapunov function and receding horizon control. They concluded that the control Lyapunov approach is more suitable for off-line computation, while a receding horizon works better in on-line control. In the work of [Albalawi et al., 2017], a comprehensive review is presented of current research efforts to design a control system that includes the safety consideration. They suggested one possible future research direction would be to use an MPC based triggering mechanism for a safety instrument. The proposed mechanism used closed loop state predictions to generate warning. One such effort by [Varga et al., 2009] predicted future states using a simulator based approach. They combined the Lyapunov criteria to check the last controllable point. Warning was generated when there was no controllable state in the prediction horizon. Lyapunov based model predictive controller (LMPC) was used by [Albalawi et al., 2016] to propose a safety scheme which varied the upper bound of the Lyapunov function to achieve the improved rate that drives the closed loop state to a safe operating region. [Aswani et al., 2013] combined safety with an MPC and proposed an MPC with an adaptive learning rate.

The Lyapunov approach is more suitable for off-line calculation, as suggested by [Primbs et al., 1999]. As the goal of this work is to generate warning based on the predictive signals from current measurements, on-line calculation is more suitable. Receding horizon or moving horizon estimates are attractive choices to predict future outputs and generate warnings on-line, based on the predictive signal. A receding horizon based model predictive safety (MPS) scheme was proposed by [Ahooyi et al., 2016] which used a moving horizon estimator to generate predictive warnings. If one of the output constraints was violated, the capacity of the controller was checked with the extreme value to determine whether the controller was able to nullify the disturbance. When multiple points of a moving horizon for multiple variables exceed the safety limit, determining the extreme condition for each variable would be difficult. Moreover, different variables are interconnected and hence control actions to nullify an extreme condition may cause other variables to exceed the safety limit.

1.4 Summary and knowledge gap

Reviewed literature of the previous section is summarized and the scope of further research is identified as follows:

i) The model predictive control was extensively used as a supervisory controller to a base layer PID. Many existing studies focused on the performance comparison of MPC and PID in a supervisory layer, but the potential of the MPC to replace the PID as a regulatory controller was not comprehensively studied. In our current study, performance of a regulatory MPC is compared with the two commonly used control structures: cascaded PID and PID cascaded to MPC.

ii) Different approaches were taken to improve the alarm system. The goal of most studies was to design a robust alarm to reduce false and missed alarms. Most of these methodologies used existing measurements and had no predictive features to generate an early warning. Predictive features of MPC can be used to improve warning generation. For most practical scenarios, the disturbance is unknown. Considering these two facts, a predictive warning scheme is proposed for the process with unknown inputs.

iii) Simultaneous state and input estimation of a nonlinear system is still an open problem. Different types of observers were able to solve the problem for specific systems, but Bayesian solutions showed the most promise for the general cases. In the current study an EM based framework is presented that iteratively estimates states and inputs. A particle filter is proposed as the tool for the E step to estimate state, and gradient based optimization was used in the M step to estimate input.

iv) Works on the predictive control and warning generation for non-linear systems can be classified into two types: Lyapunov based and receding horizon based. The former one was more suitable for off-line applications, while the latter showed promise for online monitoring. A solution for this problem was proposed by [Ahooyi et al., 2016] who compared the controllers' capacity to nullify a predicted extreme value. However, for a more complex system with a large number of interacting inputs and outputs, checking only extreme values will not be sufficient. Hence, a more general tool is required that considers safety limits of all outputs and actuator constraints of all manipulated variables. A warning scheme is proposed here that checks whether all the safety constraints and input constraints can be satisfied simultaneously. A constraint separation method was used to check the feasible solution of all safety constraints.

1.5 Implementation tools and expected outcome of the proposed tasks

Various tasks of the research were accomplished using proposed works identified from the literature review and knowledge gap. Implementation tools and outcome of the each task are reported in Tables 1.1 to 1.4.

Table 1.1: Description of Task 1

Properties	
Goal	Validate the potential of MPC as regulatory controller
Tool used	Dynamic matrix controller (DMC) as representative of MPC
Case study	Pilot plant of continuous stirred tank heater
Outcome	Result from comparative study of different control structures demonstrated MPC can deliver superior performance compared to PID.

Table 1.2: Description of Task 2

Properties	
Goal	Develop a predictive warning system for unknown disturbances
Tool used	Receding horizon prediction Kalman and Luenberger based observer for disturbance estimation
Case study	Virtual CSTH plant from literature
Outcome	A well designed warning generation scheme for linear process with unknown disturbance

1.6 Organisation of thesis

The thesis is written in manuscript format. Three published journal articles and one article under review are included in the thesis. Co-authorship statement is provided in the beginning of the thesis. Each task shown in Tables 1.1 to 1.4 is performed in each manuscript. Organaisation of the overall thesis is as follows:

Table 1.3: Description of Task 3

Properties	
Goal	Develop a simultaneous state and input estimation (SISE) scheme for non-linear system
Tool used	Expectation Maximization Algorithm
	Particle filter (E-step), gradient based optimization (M-step).
Case study	Simulation model of CSTR
	Simulated data of a four tank system
	Experimental four tank system.
Outcome	EM based estimation

Table 1.4: Description of Task 4

Properties	
Goal	Developed predictive warning scheme for nonlinear system
Tool used	Nonlinear receding horizon prediction
	Non-linear optimization
	Feasible region identification tool
Case study	Simulation model of CSTR
Outcome	Early warning generation scheme for nonlinear system.

Chapter 1 of the thesis describes the motivation and objective of the research. This chapter includes a brief review of the related work.

Chapter 2 describes the experimental comparison of PID and MPC controllers. The chapter shows that the MPC has the potential to replace the PID as a regulatory controller.

Chapter 3 presents a predictive warning system for a linear process with unknown input. Applicability of the warning system is shown for a continuous stirred tank heater (CSTH) system.

Chapter 4 describes an EM based estimator that was able to estimate the states and inputs of a non-linear system. Effectiveness of the proposed method is demonstrated for simulated and experimental case studies.

Chapter 5 presents a predictive warning generation scheme for a non-linear system. Moving horizon and constraint separation methods were used as the tools. Chapter 6 states the conclusions of the study and the scope of future work.

Bibliography

[Adnan et al., 2011] Adnan, N. A., Izadi, I., and Chen, T. (2011). On expected detection delays for alarm systems with deadbands and delay-timers. *Journal of Process Control*, 21(9):1318.

[Ahooyi et al., 2016] Ahooyi, T. M., Soroush, M., Arbogast, J. E., Seider, W. D., and Oktem, U. G. (2016). Model-predictive safety system for proactive detection of operation hazards. *AIChE Journal*, 62(6):2024–2042.

[Albalawi et al., 2016] Albalawi, F., Durand, H., Alanqar, A., and Christofides, P. D. (2016). Achieving operational process safety via model predictive control. *Journal of Loss Prevention in the Process Industries*.

[Albalawi et al., 2017] Albalawi, F., Durand, H., and Christofides, P. D. (2017). Process operational safety via model predictive control: Recent results and future research directions. *Computers & Chemical Engineering*.

[Ali et al., 2015] Ali, J. M., Hoang, N. H., Hussain, M. A., and Dochain, D. (2015). Review and classification of recent observers applied in chemical process systems. *Computers & Chemical Engineering*, 76:27.

[Andrieu and Doucet, 2003] Andrieu, C. and Doucet, A. (2003). Online expectation-maximization type algorithms for parameter estimation in general state space models. In *Acoustics, Speech, and Signal Processing, 2003. Proceedings.(ICASSP'03). 2003 IEEE International Conference on*, volume 6, pages VI–69. IEEE.

[Aswani et al., 2013] Aswani, A., Gonzalez, H., Sastry, S. S., and Tomlin, C. (2013). Provably safe and robust learning-based model predictive control. *Automatica*, 49(5):1216–1226.

[Chen, 2003] Chen, Z. (2003). Bayesian filtering: From kalman filters to particle filters, and beyond. *Statistics*, 182(1):1–69.

[Corless and Tu, 1998] Corless, M. and Tu, J. (1998). State and input estimation for a class of uncertain systems. *Automatica*, 34(6):757.

[Fang et al., 2013] Fang, H., De Callafon, R. A., and Cortés, J. (2013). Simultaneous input and state estimation for nonlinear systems with applications to flow field estimation. *Automatica*, 49(9):2805–2812.

[Fernandez et al., 2005] Fernandez, L. P. S., Pogrebnyak, O., and Marquez, C. Y. (2005). Neural network and trend prediction for technological processes monitoring. In *MICAI 2005: Advances in Artificial Intelligence*, pages 731–740. Springer.

[Gillijns and De Moor, 2007] Gillijns, S. and De Moor, B. (2007). Unbiased minimum-variance input and state estimation for linear discrete-time systems. *Automatica*, 43(1):111.

[Gopaluni, 2008] Gopaluni, R. (2008). A particle filter approach to identification of nonlinear processes under missing observations. *The Canadian Journal of Chemical Engineering*, 86(6):1081–1092.

[Güntürkün et al., 2014] Güntürkün, U., Reilly, J. P., Kirubarajan, T., et al. (2014). Recursive hidden input estimation in nonlinear dynamic systems with varying amounts of a priori knowledge. *Signal Processing*, 99:171–184.

[Hsieh, 2000] Hsieh, C.-S. (2000). Robust two-stage kalman filters for systems with unknown inputs. *Automatic Control, IEEE Transactions on*, 45(12):2374.

[Imsland et al., 2007] Imsland, L., Johansen, T. A., Grip, H. F., and Fossen, T. I. (2007). On non-linear unknown input observers–applied to lateral vehicle velocity estimation on banked roads. *International Journal of Control*, 80(11):1741–1750.

[Izadi et al., 2009] Izadi, I., Shah, S. L., Shook, D. S., and Chen, T. (2009). An introduction to alarm analysis and design. *IFAC Proceedings Volumes*, 42(8):645.

[Juricek et al., 2001] Juricek, B. C., Seborg, D. E., and Larimore, W. E. (2001). Predictive monitoring for abnormal situation management. *Journal of Process Control*, 11(2):111.

[Khan et al., 2014] Khan, M. A. I., Imtiaz, S. A., and Khan, F. (2014). Early warning system for chemical processes with time delay and limited actuator capacity. *Industrial & Engineering Chemistry Research*, 53(12):4763.

[Kitanidis, 1987] Kitanidis, P. K. (1987). Unbiased minimum-variance linear state estimation. *Automatica*, 23(6):775.

[Korbicz et al., 2007] Korbicz, J., Witczak, M., and Puig, V. (2007). Lmi-based strategies for designing observers and unknown input observers for non-linear discrete-time systems. *Technical Sciences*, 55(1).

[Kresta et al., 1991] Kresta, J. V., Macgregor, J. F., and Marlin, T. E. (1991). Multivariate statistical monitoring of process operating performance. *The Canadian Journal of Chemical Engineering*, 69(1):35.

[Krishna Vinaya et al., 2012] Krishna Vinaya, V., Ramkumar, K., and Alagesan, V. (2012). Control of heat exchangers using model predictive controller. In *2012*

International Conference on Advances in Engineering, Science and Management (ICAESM), pages 242 –246.

[Lee and Park, 2012] Lee, K.-S. and Park, T.-G. (2012). New results on fault reconstruction using a finite-time converging unknown input observer. *Control Theory & Applications, IET*, 6(9):1258.

[MacGregor et al., 1994] MacGregor, J. F., Jacckle, C., Kiparissides, C., and Koutondi, M. (1994). Process monitoring and diagnosis by multiblock pls methods. *American Institute of Chemical Engineers Journal*, 40 (5):826.

[MacGregor and Kourti, 1995] MacGregor, J. F. and Kourti, T. (1995). Statistical process control of multivariate processes. *Control Engineering Practice*, 3:403.

[Marzaki et al., 2014] Marzaki, M. H., Jalil, M. H. A., Shariff, H. M., Adnan, R., and Rahiman, M. H. F. (2014). Comparative study of model predictive controller (mpc) and pid controller on regulation temperature for ssisd plant. In *Control and System Graduate Research Colloquium (ICSGRC), 2014 IEEE 5th*, pages 136–140. IEEE.

[Na, 2001] Na, M. G. (2001). Auto-tuned PID controller using a model predictive control method for the steam generator water level. *IEEE Transactions on Nuclear Science*, 48(5):1664 –1671.

[Ogunnaike and Mukati, 2006] Ogunnaike, B. A. and Mukati, K. (2006). An alternative structure for next generation regulatory controllers: Part i: Basic theory for design, development and implementation. *Journal of Process Control*, 16(5):499 – 509.

[Primbs et al., 1999] Primbs, J. A., Nevistić, V., and Doyle, J. C. (1999). Nonlinear optimal control: A control lyapunov function and receding horizon perspective. *Asian Journal of Control*, 1(1):14–24.

[Radke and Gao, 2006] Radke, A. and Gao, Z. (2006). A survey of state and disturbance observers for practitioners. In *American Control Conference, 2006*, pages 6–pp. IEEE.

[Sen et al., 2014] Sen, M., Singh, R., and Ramachandran, R. (2014). A hybrid mpc-pid control system design for the continuous purification and processing of active pharmaceutical ingredients. *Processes*, 2(2):392–418.

[Singh et al., 2014] Singh, R., Sahay, A., Karry, K. M., Muzzio, F., Ierapetritou, M., and Ramachandran, R. (2014). Implementation of an advanced hybrid mpc–pid control system using pat tools into a direct compaction continuous pharmaceutical tablet manufacturing pilot plant. *International journal of pharmaceutics*, 473(1):38–54.

[Varga et al., 2009] Varga, T., Szeifert, F., and Abonyi, J. (2009). Detection of safe operating regions: a novel dynamic process simulator based predictive alarm management approach. *Industrial & Engineering Chemistry Research*, 49(2):658–668.

[Zarei and Poshtan, 2010] Zarei, J. and Poshtan, J. (2010). Design of nonlinear unknown input observer for process fault detection. *Industrial & Engineering Chemistry Research*, 49(22):11443–11452.

Chapter 2

Experimental Evaluation of Control Performance of MPC as a Regulatory Controller

Abstract: Proportional-integral-derivative (PID) control is widely practised as the base layer controller in the industry due to its robustness and design simplicity. However, a supervisory control layer over the base layer, namely a model predictive controller (MPC), is becoming increasingly popular with the advent of computer process control. The use of a supervisory layer has led to different control structures. In this study, we perform an objective investigation of several commonly used control structures such as 'Cascaded PI controller', 'DMC cascaded to PI' and 'Direct DMC'. Performance of these control structures are compared on a pilot-scale continuous stirred tank heater (CSTH) system. We used dynamic matrix control (DMC) algorithm as a representative of MPC. In the DMC cascaded to PI structure, the flow-loops are regulated by the PI controller. On top of that a DMC manipulates the set-points of the flow-loops to control the temperature and the level of water in the tank. The 'Direct

DMC' structure, as its name suggests, uses DMC to manipulate the valves directly. Performance of all control structures were evaluated based on the integrated squared error (ISE) values. In this empirical study, the 'Direct DMC' structure showed a promise to act as regulatory controller. The selection of control frequency is critical for this structure. The effect of control frequency on controller performance of the 'Direct DMC' structure was also studied. **Keywords**: Model predictive control, PI, Control Performance, CSTH

2.1 Introduction

In process industries model predictive controller (MPC) is typically used as a supervisory layer over the base level PID controller, especially in large-scale applications. This structure has gained acceptance as it allows the implementation of MPC with minimal changes to the existing base level controllers. Also, the PID layer can act as a fall back when the MPC is turned off for any reason. However, this structure does not allow harnessing full potentials of the MPC. In practice, it was observed that there are many incentives in breaking the PID loop, and directly manipulating the valves using the MPC. One common example is when trying to use the full valve capacity (e.g., maximizing feed, maximizing cooling capacities) it is common practice to manipulate the valve directly from MPC. Also, without PID controller layer, open loop models used in MPCs remain valid for a longer period, as they are independent of PID tuning parameters.

Recently, a software called MaxAPC from the original inventors of dynamic matix control (DMC) came to market, that uses a DMC type controller which directly manipulates the actuator. It is claimed that, this controller performs better than the 'MPC cascaded to PID' structure. Therefore, an objective investigation of the performances of these competing control structures is necessary. In this study, an experimental evaluation is carried out among three control structures: 'Cascade PI controller', 'DMC cascaded to PI' and 'DMC directly manipulating the valve output'. However, instead of using MaxAPC, an in-house DMC code developed in Matlab simulink was used in this study.

2.2 Literature Review

2.2.1 Current State of Regulatory Control Layer in process Industry

PID is the most widely used controller in process industries. Desborough and Miller estimated that 98 percent of the controllers in a typical chemical plant are PID controllers [Desborough and Miller, 2001]. Though it is widely used for its simplicity and reliability, it has several limitations. PID is a SISO controller, thus structurally it is not optimal for highly interactive MIMO systems. Van Oversee and De Moor [Van Overschee et al., 1997] reported 80 percent of industrial PID controllers are poorly tuned; 30 percent of the PID loops operate in manual mode; and 25 percent of the PID loops operate under default factory settings.

To overcome three limitations many improvements have been suggested by researchers of industry practitioners. A self-tuned PID controller to overcome the drawbacks of the conventional PID controllers with fixed tuning parameters, was proposed in [Na, 2001]. The PID gains are automatically tuned in order to keep a predefined cost function to a minimum. The auto tuned methodology improved the performance of the PID controller in both set point tracking and regulatory control. Another simple but robust technique is described in [Ogunnaike and Mukati, 2006] which combines the simplicity of PID and versatility of MPC. [Astrom and Hagglund, 2001] investigates potential alternatives for PID in industrial setting and recommended different techniques such as, discrete-time linear MISO controllers, state feedback and observers (SFO), model predictive controllers (MPC), and fuzzy controllers as alternative for PIDs. Controllers based on SFO require significant modelling effort, as such its use is justified only when modelling efforts are moderate. MPC is typically used as a supervisory layer to the base layer PID. The use of MPC provides a drastic improvement of set point tracking. However, computational complexity is a challenge for MPC. [Zhang et al., 2014] developed a new improved MPC approach using a state-space model for the air-supply system. This model is formulated through a rough linear representation of the process, which enables the controller design to be based on linear theory. This approach works best for plants where there is mismatch between the process and the model. Pannocchia et al. [Pannocchia et al., 2005] proposed an offset-free constrained linear quadratic (CLQ) controller as a potential candidate to replace PID, that outperformed PID in simulation studies. Hans described active disturbance rejection controller (ADRC) as an improved control scheme to replace PID [Han, 2009]. ADRC is error driven similar to PID, uses a state observer to utilize the power of non-linear feedback.

2.2.2 Comparative study between MPC and PID

Though various controllers have been proposed as alternatives to PID controllers, MPC shows most potential to replace a portion of the PID controllers in process industries. In this subsection, some of the articles that compared MPC with PID are reviewed.

A comparative study between standard PID and generalized predictive controller (GPC) is presented for a heat exchanger in [Bonivento et al., 2001], where an identified model is used to design both PID controller and GPC. GPC provides better performance for both set-point tracking and disturbance rejection. In [Krishna Vinaya et al., 2012], MPC was implemented for a heat exchanger to optimize and conserve energy. MPC and PID controller were designed and implemented to control the temperature of a fluid stream. MPC provided better performance based on the rise time, overshoot and settling time. A comparative study of PID controller, MPC and model free adaptive controller (MFA) is reported in [LUKÁČOVÁ and BORŽÍKOVÁ, 2010]. PID was found the fastest of the three controllers but with overshoot and steady state error, where both MFA and MPC were steady state error-free. MFA tracks the set point faster than MPC, but has significant overshoot. [Lim et al., 2014] presents finite-control-set model predictive control (FCS-MPC) for a five-phase induction motor drive. Both FCS-MPC were compared against steady-state and transient performance of a proportional-integral pulse width modulation (PI-PWM) based current control scheme. While a better transient performance was obtained with FCS-MPC, steady-state performance was always superior with PI-PWM control. An advanced hybrid MPC-PID control system was implemented in [Singh et al., 2014]. PAT data management tool, OPC communication protocols, and a standard control platform were used for real time feedback control. MPC relevant linear time invariant model was identified using step response test. The performance of hybrid MPC-PID control scheme was compared with a cascade PID scheme.

In [Marzaki et al., 2014], performances of MPC and PID were compared on a small scale industrial steam distillation pilot plant. The results show that MPC provided better performance compared to PIDs that are tuned based on Ziegler-Nichols tuning rule (PID-ZN) and Cohen-Coon tuning rule (PID-CC). Although the analysis are not exhaustive but the paper concludes that MPC has better performance against PID when the system has large dead time. [Ghadami et al., 2013] describes a comparative study of two feedback control methods for a microfluidic electroporation (EP) system. [Sen et al., 2014] presents a hybrid MPC-PID control system for the continuous purification and processing of active pharmaceutical ingredients (APIs). A comparative study between the performances of the hybrid MPC-PID and a PID-only control scheme showed that an enhanced control loop performance can be obtained under the hybrid control scheme and has high potential of improving the efficiency of pharmaceutical manufacturing operations.

The above literature survey shows that, even though there were several studies to evaluate the performance of MPC against PID controller, there was no prior study to compare the performances of two important control structures: 'MPC cascaded to PID' and 'MPC directly manipulating actuator'. A simulation based study was conducted in our prior work [Khan et al., 2014]. In this study we further conducted experimental study and compared the performances of the above mentioned control structures.

2.3 Control strategies

As current study is aimed to perform a comparative study among the different types of control structures, it is necessary to have an optimized control strategy for each control components. Two basic controllers are used in these structures: PI and MPC. IMC based tuning rules were used to tune PI whereas DMC is used as the MPC strategy. Brief overviews of IMC based tuning and DMC algorithm are presented in this section.

2.3.1 IMC based tuning for PI

IMC tuning method is based on an approximate process model. Thus a model is identified using step test and system identification technique to tune PI or PID controller. A two step PID design procedure is presented in [Seborg et al., 2010]. In the first stage process model is factored into two parts as follows

$$\tilde{G} = \tilde{G_+}\tilde{G_-} \tag{2.1}$$

where $\tilde{G_+}$ contains the time delay and right half plane (RHP) zeros of the process model and $\tilde{G_-}$ contains the invertible part of the model. The controller is given by,

$$G_c^* = \frac{1}{\tilde{G_-}} f \tag{2.2}$$

where f is a low pass filter and is typically defined as

$$f = \frac{1}{\tau_c s + 1} \tag{2.3}$$

where τ_c usually is the desired closed-loop time constant. The IMC tuning rules for different types of transfer functions are listed in [Seborg et al., 2010]. For this current work, the system was modelled as a first order time delay process (FOTPD) and its corresponding PI controller was designed based on IMC tuning rule. Tuning rules for generalized FOTPD is given in Table 2.1. In the Table, proportional gain of the PI controller are described as $K_C K$ and τ_i is the integral time constant, where K, τ and θ are the estimated model parameters.

Table 2.1: IMC tuning rules for First Order Time Delay (FOPTD process

Model	$K_c K$	τ_i
$\frac{Ke^{-\theta s}}{\tau s+1}$	$\frac{\tau}{\tau_c+\theta}$	τ

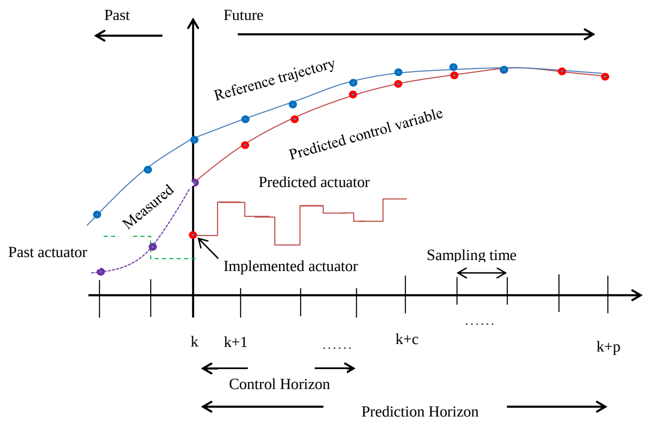

Figure 2.1: Receding horizon scheme (adopted from [Bemporad and Morari, 1999])

2.3.2 DMC Algorithm

This section briefly explains the steps for implementing DMC on a simple single input single output (SISO) system. A step response model for a SISO system can be written as

$$y_t = \sum_{i=1}^{\infty} a_i \Delta u_{t-i} \tag{2.4}$$

where y_t is the model output, a_i is the i-th coefficient of the step response model, and Δu_{t-i} contains the past input changes. Using the time-shifting and taking the constant disturbance into account, a future predicted value can be written as

$$\hat{y}_{t+k} = \sum_{i=1}^{\infty} a_i \Delta u_{t+k-i} + \nu_{t+k} \tag{2.5}$$

where $\hat{y}_{t+k}$ is the predicted output at time $t+k$, ν_{t+k} is the disturbance at time $t+k$. As the disturbance is assumed to be constant over the horizon, it is given by

$$\nu_{t+k} = \nu_t = y_m(t) - \hat{y}_t \tag{2.6}$$

where $y_m(t)$ is the measured output at time t. Replacing ν_{t+k} in Equation 2.5 we get the following form

$$\begin{aligned}\hat{y}_{t+k} =& \sum_{i=1}^{k} a_i \Delta u_{t+k-i} + \sum_{i=k+1}^{\infty} a_i \Delta u_{t+k-i} \\ &+ y_m(t) - \sum_{i=1}^{\infty} a_i \Delta u_{t-i}.\end{aligned} \tag{2.7}$$

The last three terms of Equation 2.7 express the output of the system if no control action is taken from time t to $t+k$, and is termed free response of the system, y^*_{t+k}. The free response of the system thus can be expressed mathematically as follows

$$y^*_{t+k} = y_m(t) + \sum_{i=k+1}^{\infty} (a_{k+i} - a_i)\Delta u_{t-i}. \tag{2.8}$$

If the process is asymptotically stable, the step response tends to reach a constant value after N samples. Therefore, finite step response of N samples can be used instead of infinite step response model as, $a_{k+i} - a_i \simeq 0$ for $i > N$. Using this finite step response model, free response of the system can be represented as,

$$y^*_{t+k} = y_m(t) + \sum_{i=k+1}^{N} (a_{k+i} - a_i)\Delta u_{t-i}. \tag{2.9}$$

Using the free response of the system, Equation 2.7 is rewritten in the following form

$$\hat{y}_{t+k} = \sum_{i=1}^{k} a_i \Delta u_{t+k-i} + y^*_{t+k} \tag{2.10}$$

Equation 2.10 will be used to predict system response for the entire prediction horizon *(k=1, 2, ..., p)* with m control actions. These calculated predicted values can be expressed in the following matrix form

$$\hat{\boldsymbol{y}} = \boldsymbol{y}^* + \boldsymbol{A}\boldsymbol{\Delta u} \tag{2.11}$$

where $\hat{\boldsymbol{y}}$ is a p dimensional vector containing the predicted output over prediction horizon, $\boldsymbol{y}^*$ is also a p dimensional vector which contains the free response of the system over the horizon, $\boldsymbol{\Delta u}$ is an m dimensional vector of control increments. $\boldsymbol{A}$ is the dynamic matrix of the system, which is defined in Equation 2.12

$$\boldsymbol{A} = \begin{bmatrix} a_1 & 0 & 0 & \dots & \dots & 0 \\ a_2 & a_1 & 0 & \dots & \dots & 0 \\ \dots & \dots & \dots & \dots & \dots & \\ a_m & a_{m-1} & a_{m-2} & \dots & \dots & a_1 \\ \dots & \dots & \dots & \dots & \dots & \\ a_p & a_{p-1} & a_{p-2} & \dots & \dots & a_{p-m+1} \end{bmatrix}. \tag{2.12}$$

Equation 2.11 expresses the relation between the predicted future output with control increment. The control actions are calculated by minimizing the objective function defined in Equation 2.13. The objective function calculates a set of control actions that minimizes the deviation between $\boldsymbol{r}$ and $\hat{\boldsymbol{y}}$, using penalty on the size of control increment and to avoid large movements in controller output.

$$J(\boldsymbol{\Delta u}) = (\boldsymbol{r} - \hat{\boldsymbol{y}})^T \boldsymbol{Q} (\boldsymbol{r} - \hat{\boldsymbol{y}}) + \boldsymbol{\Delta u}^T \boldsymbol{R} \boldsymbol{\Delta u} \tag{2.13a}$$

s.t.

$$\hat{y} = y^* + A\Delta y, \tag{2.13b}$$

where $\boldsymbol{Q}$ and $\boldsymbol{R}$ are the weighting matrix to penalize the control action. Minimization of the above objective function gives the following explicit expression for $\boldsymbol{\Delta u}$

$$\boldsymbol{\Delta u} = (\boldsymbol{A}^T \boldsymbol{Q} \boldsymbol{A} + \boldsymbol{R})^{-1} \boldsymbol{A}^T \boldsymbol{Q}^T (\boldsymbol{r} - \boldsymbol{y}^*). \tag{2.14}$$

This scheme can be easily generalized for a MIMO system.

2.4 Experiments on a pilot scale Continuous Stirred Tank Heater (CSTH)

Experiments were conducted in a Continuous Stirred Tank Heater (CSTH) pilot plant located in the Chemical Engineering Department of Bangladesh University of Engineering and Technology, Dhaka, Bangladesh. The CSTH serves as a MIMO system with two outputs and two inputs. A detailed description of the setup and experimental procedures are given below.

2.4.1 Plant description

A photograph of the CSTH plant appeared in Figure 2.2 and the schematics of the plant is shown in Figure 2.3. The setup is connected to Matlab Simulink through Advantech's ADAM-5000/TCP module and OPC server. Controllers were implemented using Simulink. The tank water level and the water temperature were considered as controlled variables (CVs). The schematic diagram shows that the readings of LT01 and TT02 sensors are the measured output of the system. Mesurement from the flow sensors FT01 and FT03 were used to design Proportional Integral (PI) controllers for the flow loops. Actuators of the flow loop valves are FCV01 and TCV01. Tank has a diameter of 26 inches, and inlet-outlet tubes have a diameter of 1 inch each.

Figure 2.2: Pilot scale CSTH set up

Because of the small inlet flow line compared to the tank size, the level of the tank requires an extended period of time to reach steady state. Thus, it is expected that the time constant of the tank is large and hence it acts similar to an integrating or lag dominant process.

2.4.2 Open-loop Model identification

The system described in the previous section can be represented structurally by the following transfer functions

$$\begin{bmatrix} y_1 \\ y_2 \end{bmatrix} = \begin{bmatrix} G_{11}(s) & 0 \\ G_{21}(s) & G_{22}(s) \end{bmatrix} \begin{bmatrix} u_1 \\ u_2 \end{bmatrix}, \tag{2.15}$$

where y_1 is the level, y_2 is the temperature, u_1 is the cold water valve position, u_2 is the steam valve position, and G_{ij} represents the transfer function that relates the ith output with the jth input. In the model identification stage, the first order transfer function models for all G_{ij} were identified by making step changes to u_1 and u_2. In

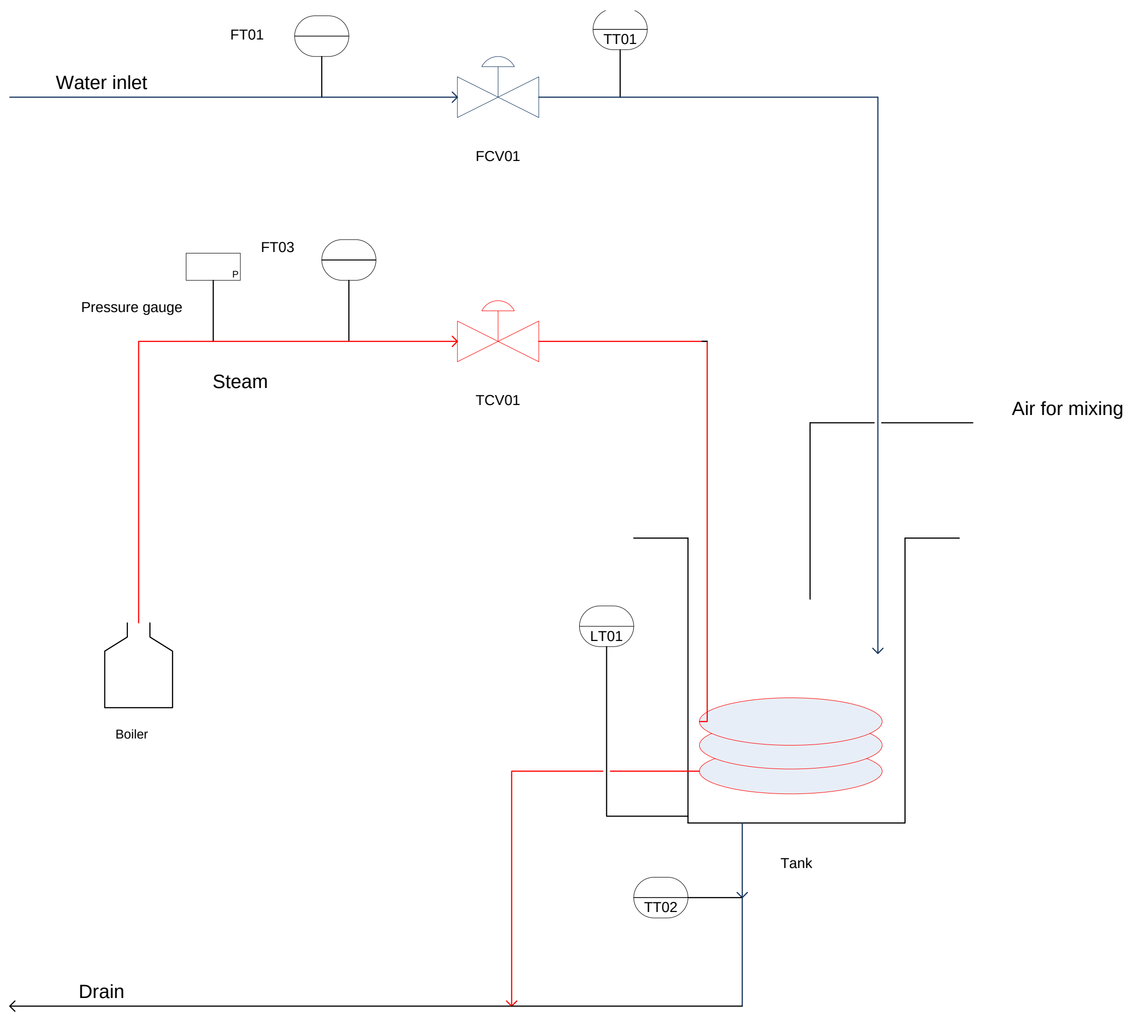

Figure 2.3: Schematic diagram of the CSTH

Table 2.2: Operating points of CSTH for different control structures

Variable	Op Pt
Level/percent	52
Temperature/Deg C	40
CW valve/mA	11.90
Steam valve/mA	9

order to avoid valve non-linearity effect, operating conditions were selected in such a way that both cold water valve and steam valve have linear effect on level and temperature.

Initially process was brought to the steady-state condition stated in Table 2.2. A step change from 11.9 mA to 12.38 mA is made in cold water valve at t= 189 min. Corresponding responses in cold water flow, level and temperature are shown in the first rows of Table 2.3 and 2.4 . After system reached steady state a step change was made on steam valve. Steam valve was changed from 9 mA to 12 mA at t=338 min. Responses of steam flow and temperature for step change in steam valve is shown in the second rows of Table 2.3 and 2.4. Graphical method was used to estimate the first order transfer function from the response curves. First order plus delay models were estimated in the form of

$$G(s) = \frac{Ke^{\theta s}}{\tau s + 1}, \tag{2.16}$$

where K is the total gain of the response for unit step change, θ is the delay time of the response after a step change is made, and τ is the time constant calculated from response curve. The identified first order transfer functions are reported in 2.5. These transfer functions plays an important role in designing the 'PI free DMC'. Using the Matlab 'step' function, the open loop step response of the transfer functions was obtained. The Finite Impulse Response (FIR) coefficients for the DMC algorithm was determined by sampling these step responses with an appropriate sampling time. A

Table 2.3: Step response plots of level and temperature from open loop step test

	Level	Temperature
Cold water valve	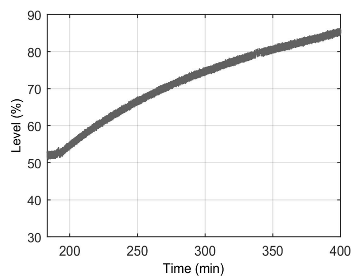	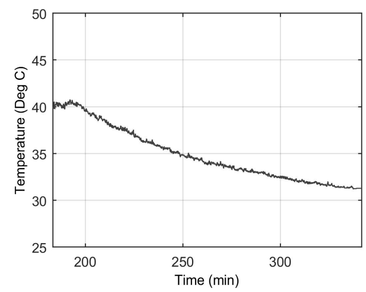
Steam valve		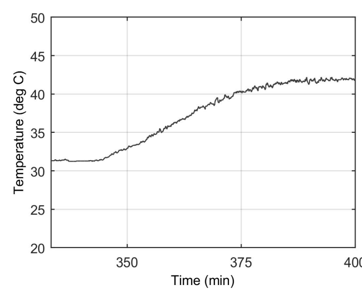

guideline for choosing the value of the sampling time and the number of FIR response coefficients can be found in [Shridhar and Cooper, 1998] and [Dougherty and Cooper, 2003].

2.5 Design of different control structures

This section describes the three different control structures implemented on the system.

Table 2.4: Step response plots of cold water flow and steam flow from open loop step test

	Cold water flow	**Steam flow**
Cold water valve	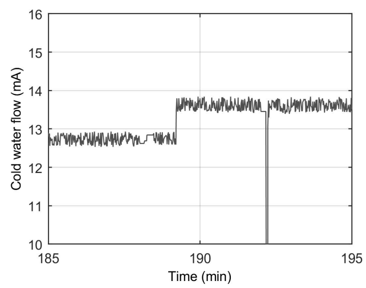	
Steam valve		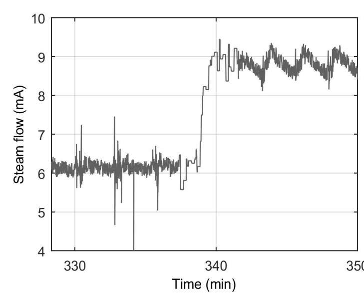

Table 2.5: Identified transfer function models from open loop step test (time unit in sec)

	Level	**Temperature**	**Cold water flow**	**Steam flow**
Cold water valve	$\frac{68.75e^{-50s}}{5800s+1}$	$\frac{-18.22e^{-350s}}{4000s+1}$	$\frac{1.875e^{-2s}}{3s+1}$	
Steam valve		$\frac{3.583e^{-293s}}{1603s+1}$		$\frac{0.7667e^{-15s}}{24s+1}$

Table 2.6: Tuning parameters for the cascaded PI structure

PI	P	I
Cold water flow PI (FIC1)	0.1778	0.06
Steam flow PI (FIC2)	1.16	0.048
Level PI (LIC)	0.053	9.24×10^{-6}
Temperature PI (TIC)	0.313	1.95×10^{-4}

2.5.1 Design of the 'Cascaded PI Structure'

The 'Cascaded PI' structure is presented in Figure 2.4, cold water flow rate and steam flow rate are the two measured variables used as the feedback to the base layer PI in the inner loop. The outputs of the base layer PI controllers manipulate the positions of the cold water flow control valve and steam flow control valve. Set-points of the base layer PI controllers are provided by the supervisory layer PI controllers.

IMC based tuning described in the previous section was used to tune PI controllers. However, as the identified open loop model between tank level and cold water valve has a large time constant, this system can be considered as an integrating system. For this reason, the tuning methods for the lag dominant systems were used for this case. There are different methods available to tune a lag-dominant system. In this work, controller was designed to provide good set point tracking performance [Seborg et al., 2010]. As the time constant is too large, selection of $\tau_1 = \tau$ would lead to a sluggish performance from the controller. As a remedy, we used Equation 2.17 to redesign the value of τ_1 as proposed in [Skogestad, 2003].

$$\tau_1 = min\{\tau_1, 4(\tau_c + \theta)\} \tag{2.17}$$

Tuning parameters of the PI controllers are reported in Table 2.6. Control intervals for both base layer and supervisory layer PIs were set to 1 sec.

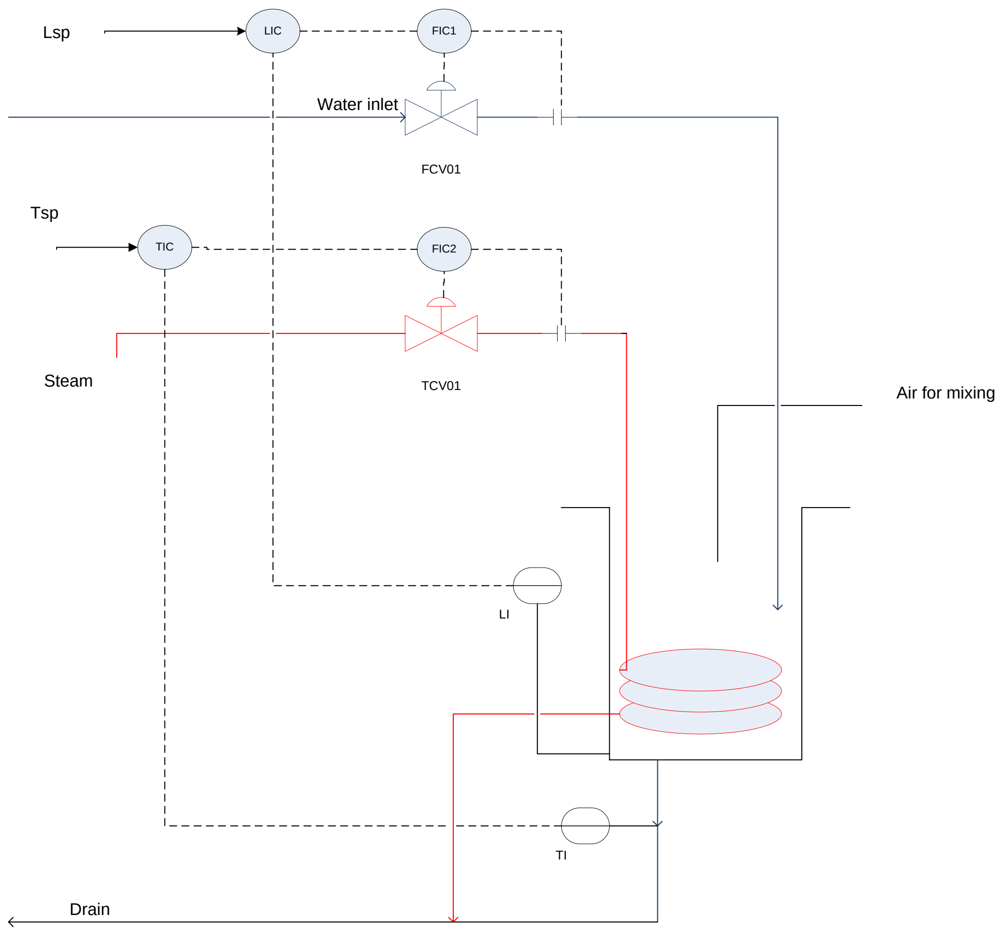

Figure 2.4: Two layer cascaded PI structure

Table 2.7: Identified transfer function models for flow PI set points (time unit in sec)

Variables	CW Flow	Steam flow
Level/%	$\frac{35e^{-100s}}{5463s+1}$	
Temperature/Deg C	$\frac{-9.65e^{-400s}}{4350s+1}$	$\frac{4.67e^{-350s}}{1950s+1}$

2.5.2 Design of the 'DMC Cascaded to PI' structure

This hybrid control structure is shown in Figure 2.5. In this structure, the supervisory layer is a DMC controller that controls the tank level and temperature by manipulating the set-points of the base layer PI flow controllers (i.e. FIC1, FIC2).

In order to design the DMC for this structure, models between controlled variables (level and temperature) and manipulated variables (cold water flow and steam flow) were identified. The identified first order transfer function models for this structure are given in Table 2.7. Here, the PI controller manipulates the valve at every 1 sec interval. Set point of the PI is changed according to the DMC output. Hence, the control frequency of DMC has to be less than 1 sec to allow the PI sufficient time to react to the base layer set point changes. In this case, control interval of DMC was set to 50 sec. Tuning parameters for DMC (e.g. prediction horizon, control horizon) were selected based on [Shridhar and Cooper, 1998] and [Dougherty and Cooper, 2003]. Prediction horizon and control horizon were set to 20 and 5 samples respectively for this case. Closed loop transfer function models stated in Table 2.7 were used to generate FIR coefficients. The built in Matlab function 'step' was applied to the models to evaluate the step response. The step response was sampled at 50 sec sampling interval to find the FIR coefficients. The FIR coefficients and the above stated tuning parameters were used to design the DMC as described in Section 3.

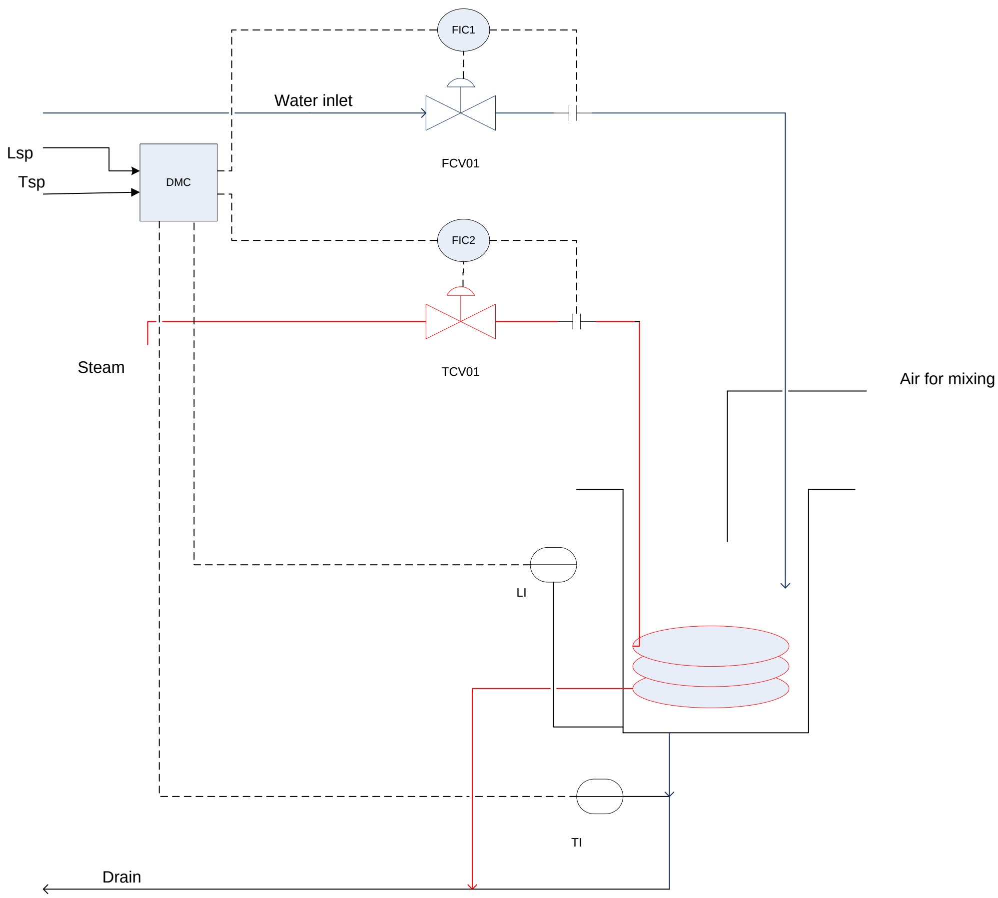

Figure 2.5: DMC cascaded with PI structure

2.5.3 Design of the 'Direct DMC' Structure

The 'Direct DMC' control structure is presented in Figure 2.6. In this control structure, the DMC controls the tank level and temperature by directly manipulating the positions of the cold water valve and the steam valve. The DMC algorithm was developed based on the open loop models stated in Table 2.5. Since model between the water valve and the level is a ramp, for controlling the level a modified DMC algorithm was used. Modifications for the tuning of this integrating system was done following the rules described in [Gupta, 1998]. As there is no base layer PI, DMC writes the control output directly to the control valve. As such DMC needs to execute at a much higher frequency compared to that of the DMC-PI structure. For the present work, the control interval of DMC was initially set to 10 sec. In the later stage, the effect of changing the control frequency was studied for 'Direct DMC structure'. The different tuning parameters (i.e. prediction horizon, control horizon, weight matrices) are chosen based on the guideline provided in [Shridhar and Cooper, 1998] and [Dougherty and Cooper, 2003]. The prediction horizon and the control horizon were 100 samples and 5 samples, respectively for this structure. These parameters along with the step response coefficients from the identified first order models were used to design the DMC controller. Due to the presence of high noise in the level measurements, a moving average filter was used to denoise the level signal.

2.6 Results: Comparison of the performances of three control structures

The control structures described in the previous sections, were implemented in the CSTH plant and performances of these controllers for set point tracking were evalu-

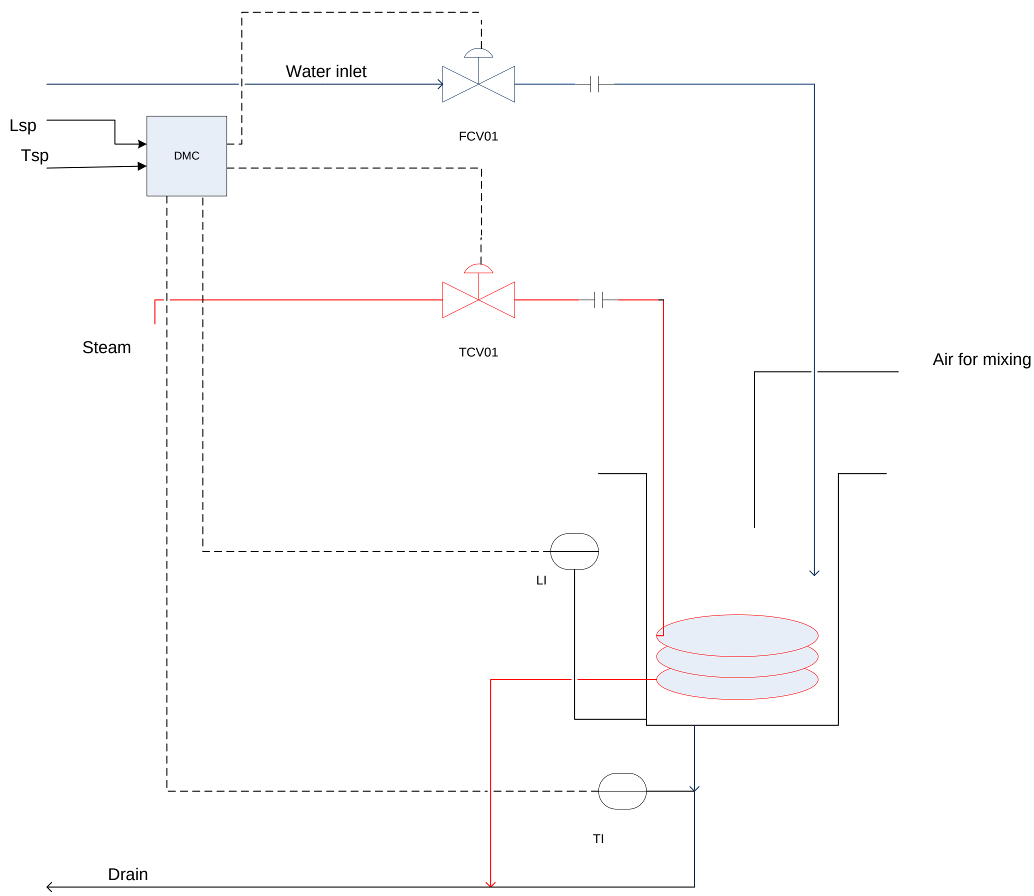

Figure 2.6: Direct DMC control structure

ated. For comparison purpose, the integrated squared error (ISE) values for process variables (i.e. level, temperature) were calculated for the set point changes. Another concern in application of a controller is the fluctuation of control valve, which is also reported in this study. The effect of control frequency on the 'Direct DMC structure' was also studied.

2.6.1 Set point tracking performance of the three control structures

To assess the set point tracking performances of the three control structures, step type set point changes of the same magnitude were made to all three controllers. At 50 min, set point of the level is changed from 60% to 65% and the data were collected until the level reached to a new steady state. In the 'DMC-PI structure' the control interval of DMC was set to 50 sec and for the 'Direct DMC structure' the control interval was set to 10 sec. The closed loop responses for these level set point change experiments for all three structures are shown in Figure 2.7. The 'DMC PI structure' has higher settling time compared to the other two structures. 'Direct DMC structure' is as good as 'Cascaded PI structure' except some errors after reaching the set point. The ISE values for level in the time span of 50 to 100 min are shown in Table 3.2. It shows that 'Cascaded PI' has the best performance among the three structures while the 'Direct DMC' proved to be better than the 'DMC PI structure'. The benefits of DMC is not reflected in this case due to the highly integrating nature of the system. The modified DMC algorithm for the integrating system is equivalent to a PID controller [Gupta, 1998]. The variations of the control output to cold water valve during the set point change of level for all three structures are shown in Figures 2.8 and 2.9. The variances of the control signal outputs were also calculated and shown in Table 3.2. From the results, it appears that there were

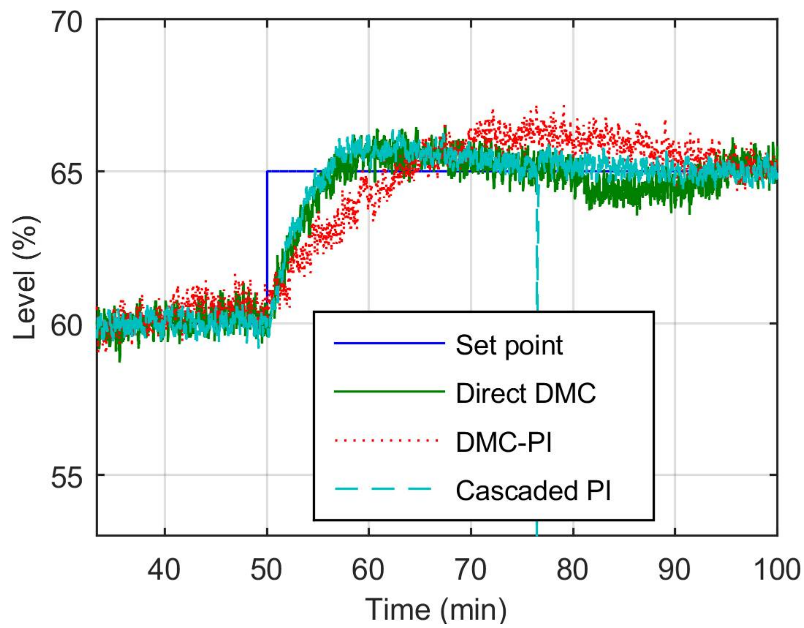

Figure 2.7: Performance comparison of three structures for level set point tracking

significant jitters in control output when DMC was directly manipulating the valve. This excessive movements of control output are because of the integrating nature of the level. The integrating system was approximated by a first order model with a large time constant, this caused some plant model mismatch. Also, in this experiment our objective was to track the level set point which may have also contributed to the fluctuations. In industrial scenario usually the level set-points are not tracked tightly, rather tank levels are allowed to move freely within a lower and upper bound. Thus the controller does not react to small disturbances and these jitters can be avoided. In the present DMC, we did not had the flexibility to implement such strategy. In commercial DMC, move suppression and move accumulation techniques are usually used. The controllers usually wait for control actions to exceed a certain threshold before passing the control actions to the actuators and thus reduce the high frequency movements of the valves significantly.

Temperature was the other controlled variable of the system. At 150 min, the

Table 2.8: Comparison of ISE values for level set point tracking and variance of control signal to cold water valve for three control structures

Control structure	ISE value	Variance
Cascaded PI	3380	0.2
DMC PI	7190	0.99
Direct DMC	5174	3.79

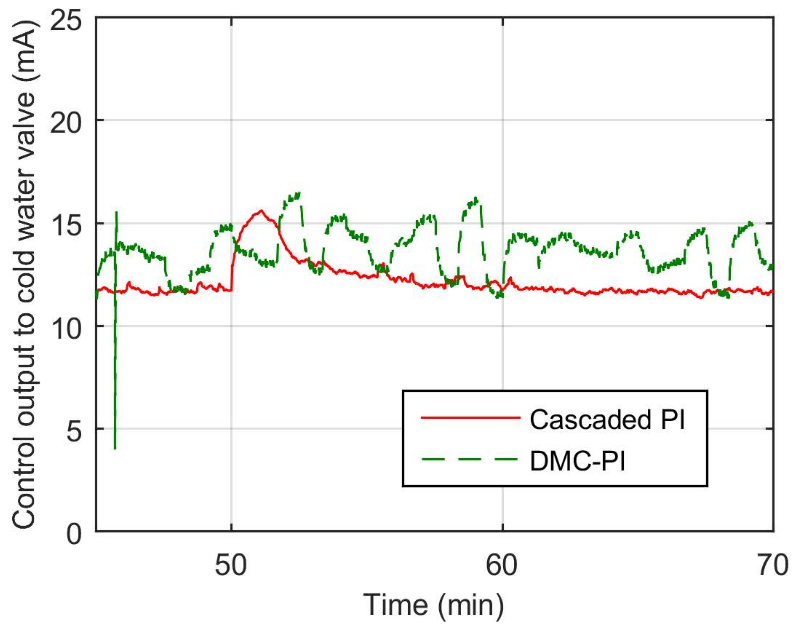

Figure 2.8: Control output to cold water valve due to level set point change(comparison between DMC-PI and cascaded structure)

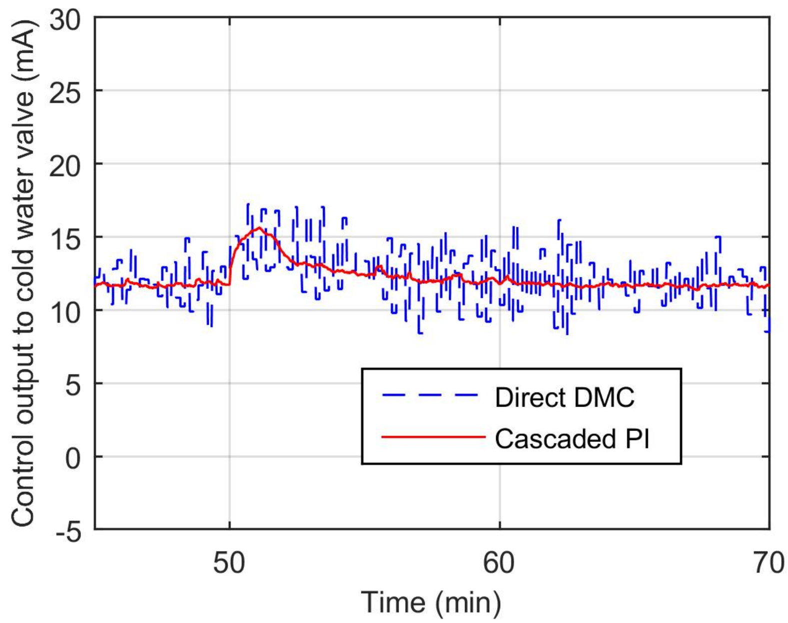

Figure 2.9: Control output to cold water valve due to level set point change(comparison between Direct DMC and cascaded structure)

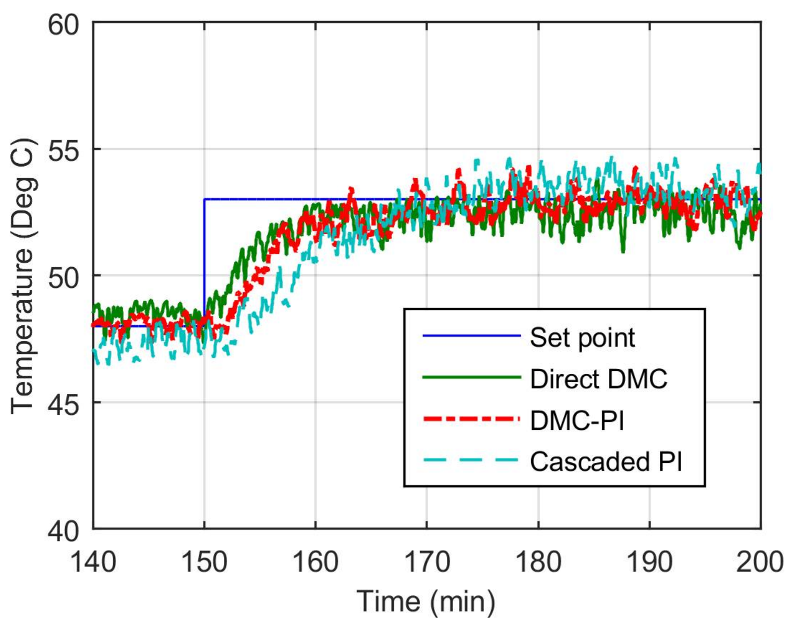

Figure 2.10: Performance comparison of three structures for temperature set point tracking

Table 2.9: Comparison of ISE for temperature set point tracking values and variance of control signal to steam valve for three control structures

Control structure	ISE value	Variance
Cascaded PI	13500	0.12
DMC PI	7490	0.24
Direct DMC	4482	0.25

temperature set point was changed from 48°C to 53°C and the response is observed till it reaches the new steady state. The closed loop responses for temperature set point change for all three structures are shown in Figure 2.10. The 'Cascaded PI structure' has longer settling time compared to the other two structures. The 'Direct DMC structure' has the fastest settling time of the three structures. The ISE values calculated for temperature for the span of 150 to 200 min are shown in Table 2.9. The 'Direct DMC structure' clearly shows the superior performance compared to the other two structures.

Steam valve position during the temperature set point change is shown in Figure 2.11. Valve movements are similar for all the structures. Variances of the control outputs were calculated and reported in Table 2.9. Results show that PI control structure provides less movement compared to the other two structures.

2.6.2 Effect of Control Frequencies on Direct DMC Performance

Next, we studied control performance of the 'Direct DMC structure' at 10 sec and 20 sec control intervals. At 50 min, level set point was changed from 60% to 65%. At 150 min, temperature set point was changed from 48°C to 53°C. The closed loop responses of both process variables were observed during the set point changes with 20 sec control interval. Then, the same experiment was replicated with 10 sec control interval. The

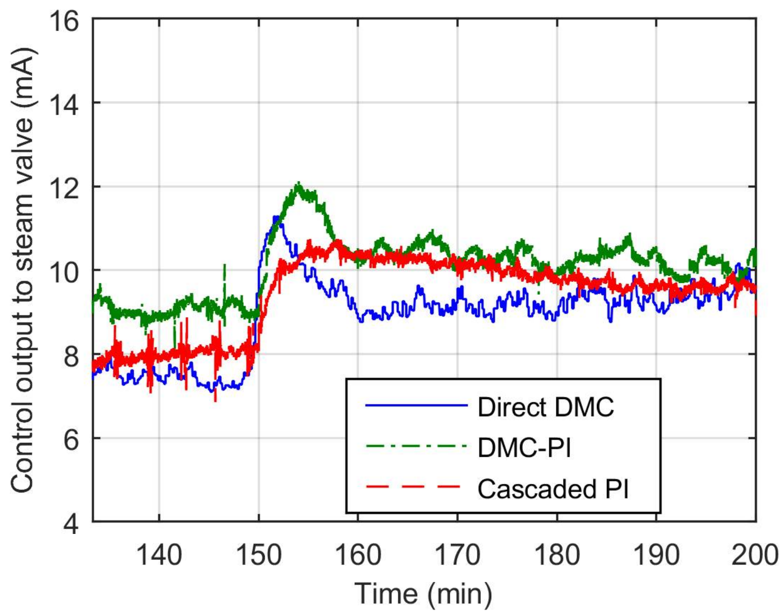

Figure 2.11: Control output to steam valve comparison of the three control structures

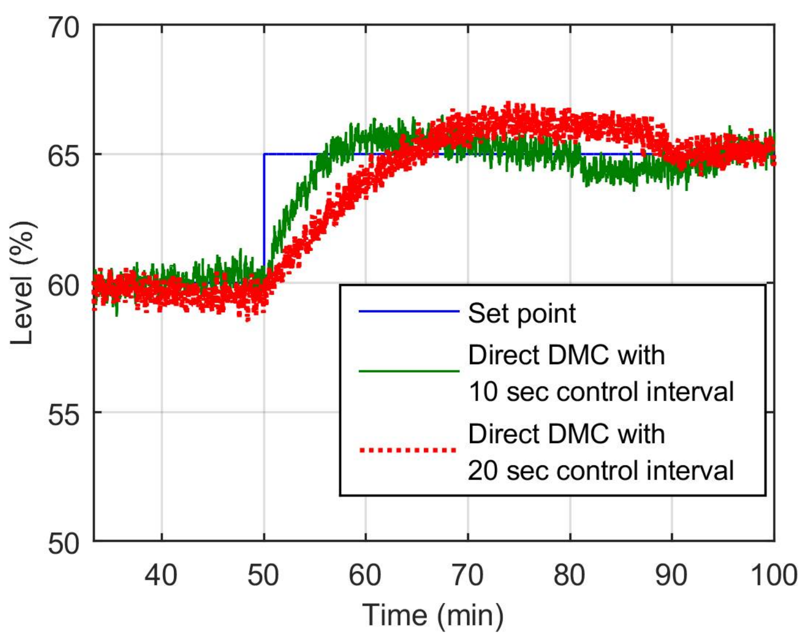

Figure 2.12: Comparison of Direct DMC structure with different control intervals for level set point tracking

Table 2.10: Comparison of ISE values for level set point change and variance of control output to cold water valve for level set point change in Direct DMC structure with different control intervals

Control interval	ISE value	Variance
20 sec	7190	0.29
10 sec	5174	3.79

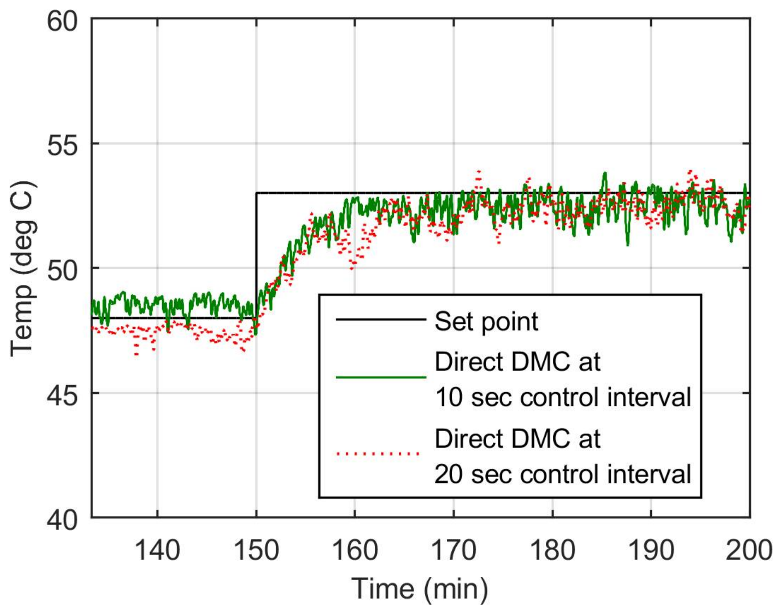

Figure 2.13: Comparison of Direct DMC structure with different control intervals for temperature set point tracking

Table 2.11: Comparison of ISE values for temperature set point change and variance of control output to steam valve in Direct DMC structure with different control intervals

Control interval	ISE value	Variance
20 sec	7490	0.55
10 sec	4482	0.25

closed loop responses of level and temperature for both cases are shown in Figures 2.12 and 2.13 respectively. Results suggest a significant improvement of performance with the decrease of control interval. The settling time for 10 sec controller is significantly lower compared to that of 20 sec. The ISE values for level and temperature during the set point changes are shown in Tables 2.10 and 2.11. The ISE values decreased significantly with the decrease of control intervals for both level and temperature variables. However, further increase of control frequency did not show any significant improvement in tracking performance.

The cold water valve for the above two experimental scenarios are shown in Figure 2.14. It appears that the controller output is jittery when DMC is executed at a lower control interval. Steam valve position for the above scenarios are shown in Figure 2.15. In these cases no jitters were observed but low frequency movements of control outputs were observed at higher control frequency. Variances of the control output to valve are reported in Table 2.10 and 2.11.

2.7 Conclusions and Suggestion for Additional Work

The present study experimentally evaluated performances of three control structures: 'Cascaded PI', 'DMC cascaded to PI' and a 'Direct DMC'. A CSTH system was used to carry out the experimental study. The findings of the experimental study broadly corroborates the results of the previous simulation studies [Khan et al., 2014]. On the basis of ISE, the 'Direct DMC' structure showed superior performance in set point tracking compared to the other two control structures at the expense of more valve movements. Performance of the 'Direct DMC' heavily relies on the control frequency. Control frequencies for the different control structures were set based on the current industrial practice so that the good performance can be achieved. In order

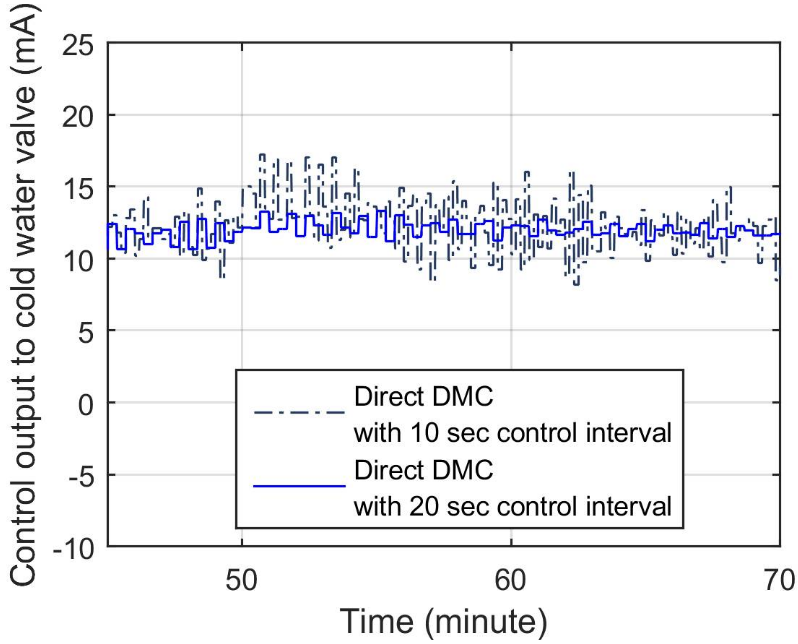

Figure 2.14: Comparison of the control output to cold water valve for Direct DMC structure with different control intervals

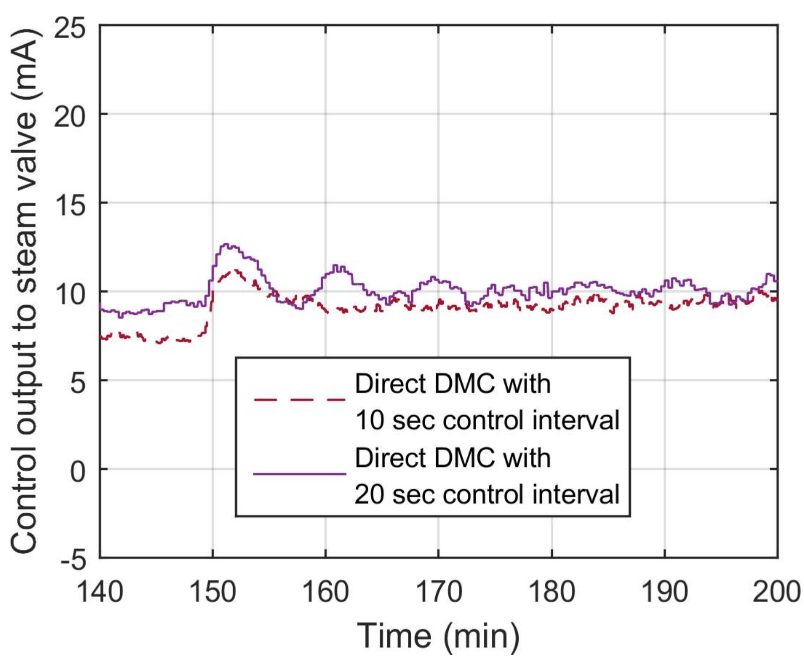

Figure 2.15: Comparison of the control output to steam valve for Direct DMC structure with different control intervals

to improve controller performance of the 'Direct DMC', it may be helpful to increase control frequency of DMC when plant is operating at low frequency. However, this may introduce unwanted fluctuations in the control outputs especially for an integrating system. A low pass filter can be used to reduce the high frequency control valve movements. It should be also noted that the control frequencies of these different controllers could not be compared on an equal basis because of the diverse structures of the controllers. Control frequency of 'Direct DMC' structure was five times higher than the control frequency of 'DMC cascaded to PI' structure. This is somewhat compensated by the fact that the base layer PI controller executed at a frequency ten times higher than the control frequency of the DMC in the 'Direct DMC' structure. As control frequency increases computational load also increases. The computational load imparted by the increased control frequency was modest for the 2 input and 2 output CSTH system. However, it may be a concern when implementing controllers on large scale industrial systems.

In this study we did not consider some other possible control structures, for example, a single layer PID controller where PID controls the secondary CV by directly manipulating the actuator. Direct PID is a preferred option when there is no local disturbance affecting the system. Also in this study, we used DMC algorithm which is optimal for linear system. As such we evaluated the controller performance within a narrow operating region to keep the system characteristics linear. Therefore, the effect of valve non-linearity and its impact on controller performance could not be evaluated.

Though the 'Direct DMC' structure demonstrated better performance than the 'Cascaded PI' or the 'DMC cascaded to PI', it is difficult to see that DMC/MPC will replace PI/PID controllers in near future only based on superior performance. The bigger issue here is the reliability of the controllers, in particular the reliability of the third party MPC software platform and their communication with DCS. In order to improve reliability and gain more operator confidence, a better approach is to integrate MPC with the DCS. There is already some initiative in that direction. For example, Emerson DeltaV offers some limited capability to implement MPC in their DCS. If MPC is available in this DCS platform. There is a possibility that in-house control engineers will try MPC for some difficult-to-control-loops (e.g., control loops with many feed forward variables) and thus MPC will slowly gain a ground as a regulatory controller.

Acknowledgement

The authors gratefully acknowledge the financial contributions of Research and Development Corporation (RDC) of Newfoundland and Natural Sciences and Engineering Research Council (NSERC) for this project.

Bibliography

[Astrom and Hagglund, 2001] Astrom, K. and Hagglund, T. (2001). The future of PID control. *Control Engineering Practice*, 9(11):1163 – 1175.

[Bemporad and Morari, 1999] Bemporad, A. and Morari, M. (1999). Robust model predictive control: A survey. In *Robustness in identification and control*, pages 207–226. Springer.

[Bonivento et al., 2001] Bonivento, C., Castaldi, P., and Mirotta, D. (2001). Predictive control vs PID control of an industrial heat exchanger. In *Proceedings of the 9th Mediterranean Conference on Control and Automation*.

[Desborough and Miller, 2001] Desborough, L. and Miller, R. (2001). Increasing customer value of industrial control performance monitoring - honeywell's experience.

[Dougherty and Cooper, 2003] Dougherty, D. and Cooper, D. J. (2003). Tuning guidelines of a dynamic matrix controller for integrating (non-self-regulating) processes. *Industrial & Engineering Chemistry Research*, 42(8):1739–1752.

[Ghadami et al., 2013] Ghadami, M., Shagoshtasbi, H., Mahjoob, M., and Lee, Y.-K. (2013). Comparative study of pid control and model predictive control for a microfluidic electroporation system. In *Nano/Micro Engineered and Molecular Systems (NEMS), 2013 8th IEEE International Conference on*, pages 895–898. IEEE.

[Gupta, 1998] Gupta, Y. (1998). Control of integrating processes using dynamic matrix control. *Chemical Engineering Research and Design*, 76(4):465 – 470. Process Operations and Control.

[Han, 2009] Han, J. (2009). From PID to active disturbance rejection control. *IEEE Transactions on Industrial Electronics*, 56(3):900 –906.

[Khan et al., 2014] Khan, M., Imtiaz, S., Khan, F., and Choudhury, M. (2014). Comparative study of different supervisory control structures. In *ADCONIP, Hiroshima*.

[Krishna Vinaya et al., 2012] Krishna Vinaya, V., Ramkumar, K., and Alagesan, V. (2012). Control of heat exchangers using model predictive controller. In *2012 International Conference on Advances in Engineering, Science and Management (ICAESM)*, pages 242 –246.

[Lim et al., 2014] Lim, C. S., Levi, E., Jones, M., Rahim, N. A., and Hew, W. P. (2014). Fcs-mpc-based current control of a five-phase induction motor and its comparison with pi-pwm control. *Industrial Electronics, IEEE Transactions on*, 61(1):149–163.

[LUKÁČOVÁ and BORŽÍKOVÁ, 2010] LUKÁČOVÁ, I. and BORŽÍKOVÁ, J. (2010). Comparison of advanced control methods with classical pid control for using in heating process control based on outdoor temperature compensation. *Journal of applied science in the thermodynamics and fluid mechanics*, 4.

[Marzaki et al., 2014] Marzaki, M. H., Jalil, M. H. A., Shariff, H. M., Adnan, R., and Rahiman, M. H. F. (2014). Comparative study of model predictive controller (mpc) and pid controller on regulation temperature for ssisd plant. In *Control and System Graduate Research Colloquium (ICSGRC), 2014 IEEE 5th*, pages 136–140. IEEE.

[Na, 2001] Na, M. G. (2001). Auto-tuned PID controller using a model predictive control method for the steam generator water level. *IEEE Transactions on Nuclear Science*, 48(5):1664 –1671.

[Ogunnaike and Mukati, 2006] Ogunnaike, B. A. and Mukati, K. (2006). An alternative structure for next generation regulatory controllers: Part i: Basic theory for design, development and implementation. *Journal of Process Control*, 16(5):499 – 509.

[Pannocchia et al., 2005] Pannocchia, G., Laachi, N., and Rawlings, J. B. (2005). A candidate to replace PID control: Siso-constrained lq control. *AIChE Journal*, 51(4):1178–1189.

[Seborg et al., 2010] Seborg, D. E., Mellichamp, D. A., Edgar, T. F., and Doyle III, F. J. (2010). *Process dynamics and control*. John Wiley & Sons.

[Sen et al., 2014] Sen, M., Singh, R., and Ramachandran, R. (2014). A hybrid mpc-pid control system design for the continuous purification and processing of active pharmaceutical ingredients. *Processes*, 2(2):392–418.

[Shridhar and Cooper, 1998] Shridhar, R. and Cooper, D. J. (1998). A tuning strategy for unconstrained multivariable model predictive control. *Industrial & Engineering Chemistry Research*, 37(10):4003–4016.

[Singh et al., 2014] Singh, R., Sahay, A., Karry, K. M., Muzzio, F., Ierapetritou, M., and Ramachandran, R. (2014). Implementation of an advanced hybrid mpc–pid control system using pat tools into a direct compaction continuous pharmaceutical tablet manufacturing pilot plant. *International journal of pharmaceutics*, 473(1):38–54.

[Skogestad, 2003] Skogestad, S. (2003). Simple analytic rules for model reduction and pid controller tuning. *Journal of process control*, 13(4):291–309.

[Van Overschee et al., 1997] Van Overschee, P., Moons, C., Van Brempt, W., Vanvuchelen, P., and De Moor, B. (1997). Rapid: the end of heuristic pid tuning. *JOURNAL A*, 38:6–10.

[Zhang et al., 2014] Zhang, R., Xue, A., Lu, R., Li, P., and Gao, F. (2014). Real-time implementation of improved state-space mpc for air supply in a coke furnace. *Industrial Electronics, IEEE Transactions on*, 61(7):3532–3539.

Chapter 3

Predictive Alarm Generation for Chemical Processes with Unknown Disturbance

Abstract A predictive warning generation scheme for chemical processes with unknown disturbances is proposed in this paper. The proposed methodology uses predicted states of a process system evaluated from the open loop process model and disturbance estimates. Alarms are issued for two conditions, during a time delay period and at the steady state. Disturbances are estimated using unknown input estimators. 'Moving horizon' predictor combined with bias correction is used to predict the dynamic state of a process for a time-delay period. To generate warnings for actuator limitations, steady state gain for disturbances, along with input constraints, are used to check for a feasible solution for using linear programming. A warning is generated to the operator when a feasible solution does not exist. The proposed methodology is demonstrated in a simulated model for a continuous stirred tank heater system (CSTH). Results show an early detection of an abnormal situation that provides the

operator a lead time to react in the case of a disturbance affecting the system.

3.1 Introduction

A well-designed warning generation system is imperative for a safe and uninterrupted operation of a process plant. Process variables are required to be kept inside certain limits for operational requirements and process safety. The purpose of a warning system is to issue alarms to operators when abnormal events are triggered. Usually, process control is the first layer of protection. A warning is triggered when the control system cannot keep the process variables within the desired limits. An effective warning system is required to have a reduced number of false alarms and missed alarms. A missed alarm may bring dire consequence to process facilities. A false alarm may lead to alarm flooding which is exhausting for an operator and reduces the work efficiency in an abnormal situation. In addition, the early detection of an abnormal situation provides an operator a lead time to respond with corrective actions.

Significant research has been performed to design optimized warning systems to keep false and missed alarms to a minimal level. Filtering, deadband, and delay are the conventional approaches to minimize false alarms which lead to detection delay. Some earlier efforts were made to strike a balance between false alarms and detection delay [Izadi et al., 2009a, Izadi et al., 2009b, Adnan et al., 2011]. To reduce false alarms, the process variables were compressed using multivariate statistical tools. Since the pioneering work by [Kresta et al., 1991], multivariate statistical tools have been used for process monitoring in many other studies [Kresta et al., 1991, MacGregor et al., 1994, MacGregor and Kourti, 1995]. All these methods relied on the process measurements for alarm generation, as they emphasised the robustness of the alarm system. Inclusion of predictive features make the warning system capable of forecasting an abnormal system significantly earlier. Significant work in this area includes a Kalman filter based predictor, proposed by [Juricek et al., 2001], which was extended by [Zamanizadeh et al., 2008] for nonlinear systems. They used an extended Kalman filter as the tool to handle the nonlinearity. [Fernandez et al., 2005] proposed a neural network based supervisory method to generate an alarm for an abnormal situation. These methodologies demonstrated good performance in forecasting abnormal situations, with some drawbacks. The main drawback of the predictive methodologies is that the prediction horizon of the warning systems is not large enough to take full advantage of the predictive features. In order to predict for a longer time horizon, a closed loop model is required to predict system behaviour.Thus the monitoring system becomes dependent on the controller tuning parameter and has to be updated as the tuning parameter changes.

In our prior work [Khan et al., 2014], a warning generation framework was proposed for systems with time delay and actuator capacity limitations using open loop models. The main benefit of using an open loop model is that it remains unchanged in the event of any change in the control structure. A receding horizon algorithm and linear programming are used as the tools for the warning system for a time-delay period and constrained actuator scenario respectively. The limitation of the proposed method was that it assumed the disturbance input to be known, which may not be the case for most practical cases. The motivation of this work is to improve the previously proposed methodology for unmeasured disturbance inputs. Estimation of unknown inputs varies depending on the nature of the process model. We limit our scope of work to linear systems only.

A state observer is widely used in control systems to estimate the hidden states. In the last few decades, the functionality of the state observer was broadened to estimate the disturbance inputs along with hidden states. [Radke and Gao, 2006] provided a review of the observers used in the process industry. They concluded that computation simplicity is as important as accurate state estimation. The Luenberger based unknown input observer (UIO) shows promise for both criteria. [Chang et al., 1994] presented an initial work on the unknown input observer explaining its design procedure for a linear system. The initial design was focused on estimating the states of the system. [Xiong and Saif, 2003] addressed the simultaneous estimation of the states and inputs for the process. A framework to estimate the state and input simultaneously was proposed by [Corless and Tu, 1998]. This framework used 'Lyapunov-type characterization' to obtain an estimator which was able to estimate the unmeasured disturbance inputs based on the measured output. [Xiong and Saif, 2003] focused on reducing the computational complexity of the designed observer with a lower order. [Mattavelli et al., 2005] used a disturbance observer for voltage control and estimation of unknown input. [Sundaram and Hadjicostis, 2008] demonstrated the use of UIO for time-delay systems and [Lee and Park, 2012] discussed a fault reconstruction scheme using finite time UIO.

A more comprehensive review of observers used in chemical processes is provided by [Ali et al., 2015]. They stated that, though Luenberger based observers are easy to implement, they require perfect knowledge of the system. Performance of this observer is limited if there exists a model mismatch and high level of noise. They also suggested a Bayesian estimator (e.g, Kalman filter) as the suitable tool for fast estimation results. The two-stage Kalman filter were proposed in an earlier work by [Friedland, 1969] for some restrictive conditions, where state and input were decoupled. [Kitanidis, 1987] used an optimal recursive filter with no prior information of unknown inputs, which was extended by [Darouach and Zasadzinski, 1997] with an unbiased minimum variance filter. They also provided stability and convergence criteria of the proposed filter. Both the work of [Kitanidis, 1987] and [Darouach and

Zasadzinski, 1997] estimated the hidden state in presence of unknown inputs. Connecting these filters, [Hsieh, 2000] proposed an input estimation method. [Gillijns and De Moor, 2007] proposed a recursive filter which can simultaneously estimate the states and inputs using an unbiased minimum variance filter. They also proved the optimality of the input estimation method proposed by [Hsieh, 2000].

In our work, we have used the Kalman filter based observer proposed by [Gillijns and De Moor, 2007] for estimation of unknown inputs and states simultaneously. For comparison, the Luenberger based unknown input observer described in [Zarei and Poshtan, 2010] was also used for input reconstruction.

3.2 Proposed Predictive 'Warning Generation' System

Due to extensive use of the model predictive controller, open loop process models of chemical processes are usually available. In the current study, we used open loop process models to our advantage to generate warnings for two limiting conditions when the process is vulnerable to a disturbance input. These conditions are briefly explained below.

Monitoring during delay period:

A dynamic system with disturbance entering into the system can be written in the following state space form given by Equations 3.1 and 3.2:

$$x_{k+1} = \mathbf{A}x_k + \mathbf{B}u_{k-t_d} + \mathbf{E}u_k^d + w_k \tag{3.1}$$

$$y_k = \mathbf{C}x_k + v_k, \tag{3.2}$$

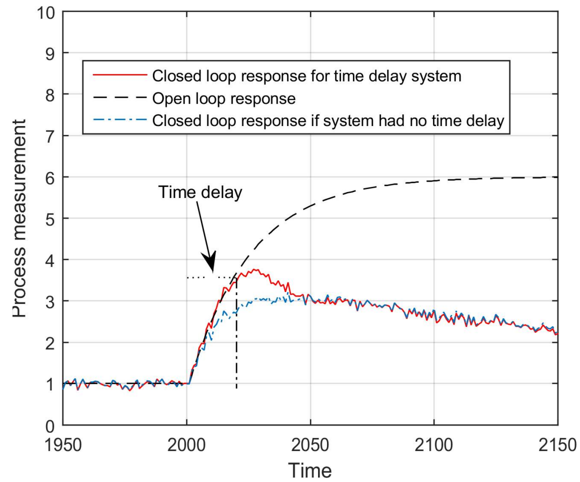

Figure 3.1: Different responses of process variable in presence of disturbance

where x_k is the state vector with dimension n, u_{k-t_d} is the process inputs delay t_d with dimension m, u_k^d is the disturbance to the system, y_k is the process outputs with dimension p, and w_k and v_k are the process and measurement noise. It is assumed that w_k and v_k are mutually uncorrelated, zero mean, white noise with known covariance matrices Q and R respectively. When a disturbance u_k^d enters into the system, process outputs will start to change. Figure 3.1 shows the different responses of the process measurement based on the availability of the controller and nature of the system.

If the process has no controller, process variables will increase and settle to steady state value. This response can be estimated from the open loop process and disturbance models. As soon as disturbance affects the outputs, the controller counteracts and try to bring the process back to its original state. However, if the process has a time-delay, controller action is delayed until the delay period is over. Thus, the process is vulnerable in this period and needs to be monitored. From the figure, it is evident that the closed loop response followed the predicted open loop response when controller has no effect. We call this window the ‘ time-delay monitoring horizon’. The proposed methodology monitors the process continuously over this horizon using the open loop predictions. As it is evident from Figure 3.1, though the closed loop response follow the open loop response during the 'monitoring horizon', there are some deviations due to the presence of noise. Proposed methodology uses lumped bias correction to nullify these deviations.

Monitoring system for limited actuator capacity:

Next we consider the steady state of a system with a limited actuator. If disturbance enters the system, the steady state of a system will be disturbed and the process will settle to a new steady state, provided the system is stable and there is no effect of the controller. But, similar to the previous scenario, the controller will counteract the effect of the disturbance and try to maintain the original steady state value. If the actuator capacity is not limited, a well tuned controller will bring the process back to the original steady state irrespective of the size of the disturbance. However, if the actuator capacity is constrained, it cannot make the input changes calculated by the controller and the original state of the system may not be restored. Figure 3.2 shows the different steady states of the process. When the actuator is saturated, the process variables settle to a different state compared to the nominal one. Steady state conditions are analysed to check whether the actuator has the capacity to counteract a certain disturbance and bring process outputs within the safety limit at steady state. If it is identified that with a certain disturbance, the input actuator cannot bring back the process within safety limit, an alarm is generated.

In [Khan et al., 2014], it was assumed that the disturbance entering the system is known. Future states of process variables were predicted using the known disturbance and an open loop model. In the current study, disturbance inputs are assumed to be unknown, which is a more realistic scenario, and are estimated before proceeding to generate a warning for the system. The estimation procedure is performed using observers. Receding horizon prediction and linear programming (LP) are the main tools

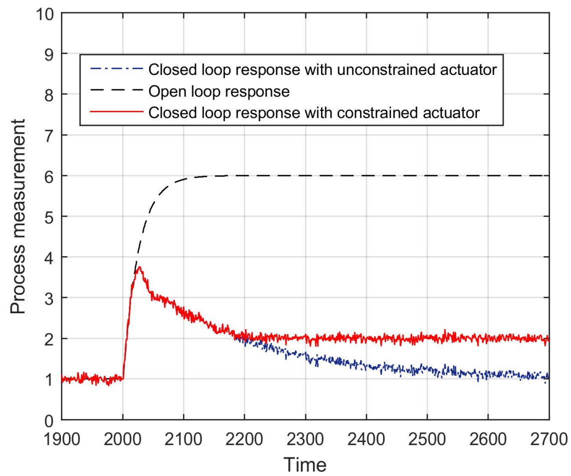

Figure 3.2: Different responses of process variables in presence of disturbance

used for the warning system.

Figure 3.3 shows the detailed implementation scheme. The alarm system works in three steps. In the first step, observers use the filtered outputs to estimate the unknown disturbance. The estimated disturbance is used in the next steps. Next, LP checks for a feasible solution for the actuator constrained scenario. In the case of non-existence of a feasible solution, an alarm is generated. If LP finds a feasible solution, the system will proceed to the next step. In this step, calculations are performed for the 'time-delay monitoring horizon' condition using the open loop prediction from process models, inputs and estimated disturbances. If predicted values cross the threshold over the 'time-delay monitoring horizon', an alarm is generated; otherwise the alarm system will proceed to the next time step where measurement is filtered and is sent to the estimation step of next iteration. Filtered data is also used at the bias correction stage in the next iteration. Different steps of the implementation scheme are described in the following subsections in detail.

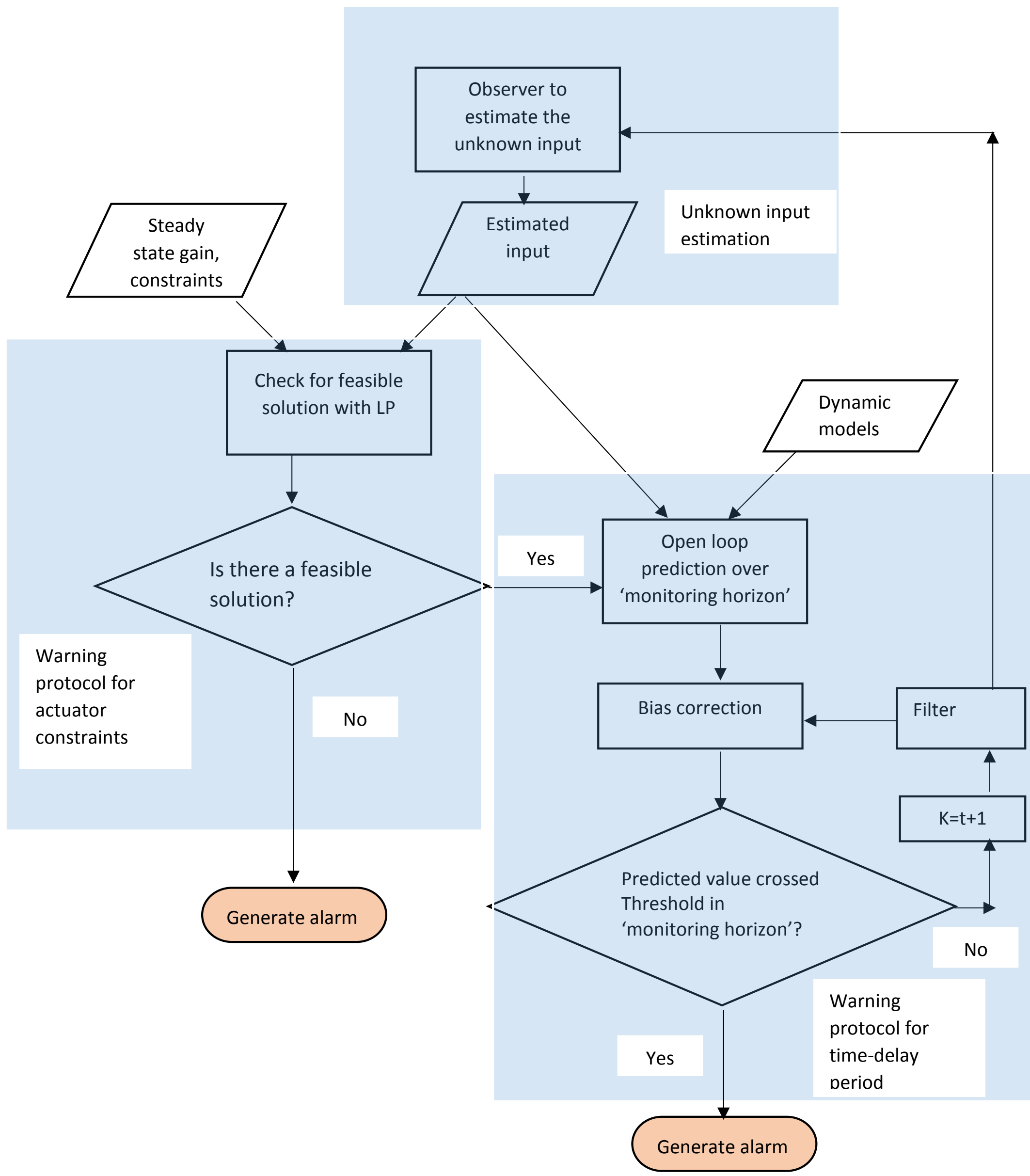

Figure 3.3: Proposed alarm generation protocol with observer

3.2.1 Unknown disturbance estimation

Observers were used in this work for reconstructing the unknown inputs (i.e. disturbances). Estimated inputs from observers were used as inputs to the warning generation system. Design procedures of the observers used in the monitoring system are briefly explained in this subsection.

3.2.1.1 Unknown input observer

The main feature of an unknown input observer (UIO) is that it is able to estimate the states in the presence of unknown inputs; more precisely, the state estimation error asymptotically approaches to zero, even in the presence of unknown inputs. The UIO estimates the states in such a way that disturbance is decoupled in the estimation process.

$$z_{k+1} = \mathbf{F} z_k + \mathbf{T}\mathbf{B} u_{k-t_d} + \mathbf{K} y_k \tag{3.3}$$

$$\hat{x}_{k+1} = z_{k+1} + \mathbf{H} y_{k+1}, \tag{3.4}$$

$$\mathbf{K} = \mathbf{K}_1 + \mathbf{K}_2, \tag{3.5}$$

where $\hat{x}_k \in R^n$ is the estimated state, $z \in R^n$ is the new state of the unknown input observer, and $\mathbf{F}$, $\mathbf{T}$, $\mathbf{K}_1$, $\mathbf{K}_2$, $\mathbf{H}$ are the design matrices to achieve the the unknown input decoupling. The matrices are designed from the primary condition of unknown input observer, that state estimation error e_{k+1} approaches zero asymptotically, where

$$e_{k+1} = x_{k+1} - \hat{x}_{k+1}. \tag{3.6}$$

From the unknown input observer theory it can be shown that, for the estimated state to converge asymptotically, the following conditions must hold.

$$(\mathbf{HC} - \mathbf{I})\mathbf{E} = 0 \tag{3.7}$$

$$\mathbf{T} = \mathbf{I} - \mathbf{HC} \tag{3.8}$$

$$\mathbf{F} = \mathbf{A} - \mathbf{HCA} - \mathbf{K}_1\mathbf{C} \tag{3.9}$$

$$\mathbf{K}_2 = \mathbf{FH}. \tag{3.10}$$

When these conditions hold, we will have:

$$e_{k+1} = \mathbf{F}e_k + E_{N,k}, \tag{3.11}$$

where $E_{N,k}$ is the error term due to process and measurement noise. It is evident from Equation 3.11 that e_{k+1} does not depend on u_k^d. Therefore, the estimation error remains bounded asymptotically in the presence of the unknown disturbance if the designed matrix $\mathbf{F}$ is stable. UIO is designed solving Equations 3.8 to 3.10 with the proper choice of $\mathbf{F}$ and $\mathbf{K}_1$. In our work, we have used the result of [Zarei and Poshtan, 2010] for choosing a $\mathbf{K}_1$ that minimizes the variance of estimation errors and estimates $\hat{x}_{k+1}$. The estimated state is used to estimate the disturbance $\hat{u}_k^d$ using the following equation

$$\hat{u}_k^d = (\mathbf{CE})^+[\mathbf{C}\hat{x}_{k+1} - \mathbf{CA}x_k - \mathbf{CB}u_k], \tag{3.12}$$

where $(\mathbf{CE})^+$ is the pseudo-inverse matrix of $\mathbf{CE}$.

Kalman based input estimation approach

[Gillijns and De Moor, 2007] proposed a Kalman filter based observer that estimates the hidden states and unknown inputs of the system simultaneously. Consider the dynamic system described in Equation 3.1 and 3.2. First, we concatenate the input and disturbance vectors and their corresponding model matrices and describe them as $u_{k,d} = [u_k \; u_k^d]^T$ and $G = [B \; E]$. A recursive filter was used as the estimation tool for this system. Use of the recursive filter is only applicable for this system when the following conditions hold:

Assumption 1: rank $CG_k =$ rank G_k ;

Assumption 2: $n > m$, $p > m$.

Upon fulfilling the necessary conditions, the recursive filter is described as follows:

$$\hat{x}_{k/k-1} = A_k \hat{x}_{k-1/k-1}, \tag{3.13}$$

$$\hat{u}_{d,k-1} = M_k (y_k - C\hat{x}_{k/k-1}), \tag{3.14}$$

$$\hat{x}^*_{k/k} = \hat{x}_{k/k-1} + G\hat{u}_{d,k-1}, \tag{3.15}$$

$$\hat{x}_{k/k} = \hat{x}^*_{k/k} + K_k (y_k - C_k \hat{x}^*_{k/k}). \tag{3.16}$$

M_k and K_k are the tuning parameters with dimensions of $m \times p$ and $n \times p$. A detailed tuning procedure and proof of optimality are stated by [Gillijns and De Moor, 2007]. M_k is tuned from the least square solution of the innovation and K_k is tuned by minimizing the state variance. For tuning these parameters, initially the covariance matrix for state innovation is defined as $P_{k/k} \equiv \mathbb{E}\ [\tilde{x} \; \tilde{x}^T]$, where $\tilde{x}$ denotes the difference between the true state and the unbiased estimated state. The value of $P_{k/k}$ changes at each time sample and used to define the error variance of biased estimate state ($\hat{x}_{k/k-1}$). Error variance of biased estimate is defined from

$P_{k-1/k-1}$ as $P_{k/k-1} = AP_{k-1/k-1}A^T + Q$. It can be shown from further calculation that, $\tilde{R}_k = CP_{k/k-1}C^T + R$, where $\tilde{R}_k$ is the expected value of e_k, where e_k is defined from the model parameters as $e_k = C(A\tilde{x}_k + w_{k-1}) + v_k$. It has been shown in [Gillijns and De Moor, 2007], using the above defined parameters, that optimal tuning of M_K and K_k is given by the following equations:

$$M_k = (F^T \tilde{R}_k^{-1} F)^{-1} F^T R_k^{-1}, \tag{3.17}$$

$$K_k = P_{k/k-1} C \tilde{R}_k^{-1}, \tag{3.18}$$

where $F = CG$. Using these rules, the unknown disturbance and states can be obtained. M_k was used to estimate input from measurement and biased state, as shown in Equation 3.14. Estimated input was used to update the estimated state using Kalman gain K_k, as shown in Equation 3.16.

3.2.2 Warning generation for time-delay condition

As stated in the first limiting condition, within the monitoring horizon, the open-loop and closed-loop predictions remain the same. Process variables are predicted over the entire *monitoring horizon* using the open loop models, process and estimated inputs. Predictions are then bias corrected to reduce the effect of process noise. An alarm will be generated if an open-loop prediction exceeds the alarm threshold within the monitoring horizon. The detailed procedure is described below step by step.

Step 1 is to identify the process and disturbance vectors using one of the observers described. Estimated disturbance $\hat{u}_k^d$ will be used to predict process responses over the 'time-delay monitoring horizon'.

Step 2 predicts the future states from the open loop model and estimates inputs from Step 1. Process variables are predicted over the *monitoring horizon*, considering the disturbance model of the process. The monitoring horizon is chosen based on the time delay of the process. For a given process with time delay t_d, the monitoring horizon $t_p \geq t_d$.

For the system described in Equations 3.1 and 3.2, the l sample ahead predicted output is described by the Equation 3.19.

$$y_{k+l} = C[A^l x_k + \sum_{i=1}^{l} A^{i-1} B u_{k-t_d+l-i} + A^{i-1} E u^d_{k+l-i}], \tag{3.19}$$

where l=[*1,2,3,...,P*] and P is the horizon defined based on the process knowledge. Equation 3.19 predicts the i-th output over the horizon P.

Step 3 is a correction step to account for the noise and process model mismatch. Predicted outputs are updated using the current process measurements. At each time step, measured outputs are compared with the predictions from the previous time step. The deviation of these two values is defined as bias error. The bias error at time t is defined as Equation 3.20:

$$b_k = y_k - y^*_k \tag{3.20}$$

where y^*_k is the predicted value of the variable y for discrete time sample *k-1* and y_k is the output of the filter at discrete time k. This bias error is used to update all the predicted outputs over the horizon as given in Equation 3.21:

$$\hat{y}_{k+l} = y^*_{k+l} + b_k, \tag{3.21}$$

where l= *1,2,...* P. As updated predictions use both process and disturbance models, they are able to forecast the effect of disturbance before it actually appears in the measurement.

However, measured output cannot be used directly if it is heavily affected by the measurement noise. In such cases, measured data need to be preprocessed passing through a filter and filtered measurements will be used for warning generation. For the Kalman based approach, filtered process variables can be extracted from the estimated state.

Step 4 analyses the updated prediction and generates the alarm. Maximum and minimum limits for safe operation of each variable are defined. Predicted values are checked to determine if they exceed the limits. When predictions cross the limits, an alarm will be generated to the operator.

Step 5 improves the robustness of the alarm. If an alarm is generated based on a single value exceeding the threshold, there will be false alarms in a noisy measurement or a model mismatch scenario. To improve the robustness, an alarm is issued only when three consecutive predictions exceed the limit. However, the heuristic can be changed based on the nature of the process variable, the defined threshold value and the consequence for such limit violation.

3.2.3 Warning generation for limited actuator capacity

This protocol is developed for a constrained actuator scenario. The concept hinges on the idea that an actuator has a limited capacity, as such, it may not be possible to counteract a large disturbance effect. The decision is made based upon the disturbance effect on the process which is predicted using the 'process model' and 'disturbance model', available control actions based on the actuator capacity and the various input-output limits. The steady state values without any control action are calculated for process gain and estimated changes in the disturbance variable. In our previous work [Khan et al., 2014], known disturbance inputs were used to calculate the open loop steady state value. In the current work, disturbance input is unknown and is estimated with the procedure described in 'Unknown disturbance estimation'. Let us consider a disturbance size estimated as Δu^d entering the system at time step k. If there is no controller, the steady state value of the 'i-th' output variable is given by Equation 3.22:

$$y_i^{ss} = y_{i,k} + G_i \Delta u_k^d,. \tag{3.22}$$

where G_i is the gain of 'i-th' output to the disturbance. The controller will try to negate the effect of disturbance by manipulating the actuator so that process output remains inside the desired safety limits. If the maximum and minimum safety limits for the i-th output are $y_{i,low}$ and $y_{i,high}$ respectively, the following condition needs to be satisfied for safe operation:

$$y_{i,low} \leq y_i^{ss} + \Delta y_i^{ss} \leq y_{i,high}, \tag{3.23}$$

where Δy_i^{ss} is the steady state change in the i-th variable due to controller manipulation of the actuators. Input and output relations at the steady state can be described using process gain as follows:

$$\Delta y_i^{ss} = \sum_{j=1}^{m} G_{ij}(0) \Delta u_j \tag{3.24}$$

where $G_{ij}(0)$ is the process gain of a step which is the step response at the steady state.

Combining Equations 3.23 and 3.24, safe operational condition in terms of input variables is derived as:

$$y_{i,low} - y_i^{ss} \leq \sum_{j=1}^{m} G_{ij}(0) \Delta u_j \leq y_{i,high} - y_i^{ss}. \tag{3.25}$$

Actuator capacity at a certain steady state is the difference between the steady state and the two limiting positions (maximum and minimum) of the actuator (e.g., valve). It is expressed as follows:

$$u_{j,low} - u_{j,t} \leq \Delta u_j \leq u_{j,high} - u_{j,t}, \tag{3.26}$$

where $u_{j,low}$ and $u_{j,high}$ are the maximum and minimum positions of the actuator.

Controllers will be able to bring the output variables inside safety limits at the steady state when inequalities 3.25 and 3.26 are satisfied simultaneously. Thus, these inequalities are the necessary criteria for safe operation of a process at the steady state. When any of the inequalities cannot be satisfied, a warning will be issued to operator. These criteria are checked using a linear programming (LP) algorithm. LP can confirm if there exists a region where all constraints are satisfied. Similarly, the methodology can be scaled for any number of variables.

3.3 Case Study for a Simulated CSTH Model

The proposed predictive warning scheme was demonstrated using the Simulink model of a continuous stirred tank heater (CSTH) presented in Thornhill et el [Thornhill et al., 2008]. The model mimics an experimental CSTH system located in the Department of Chemical and Material Engineering at the University of Alberta. The model is mild nonlinear as outflow is nonlinearly related to the height of the tank. Moreover, the model provides a complete characterization of actuators and sensors based on experimental data. This nonlinear model was used as a benchmark system for implementation of the warning protocol. The CSTH system is shown schematically in Figure 3.4. Level and temperature of the tank water are the process outputs. Manipulated variables for the system are, steam flow and cold water flow regulated by

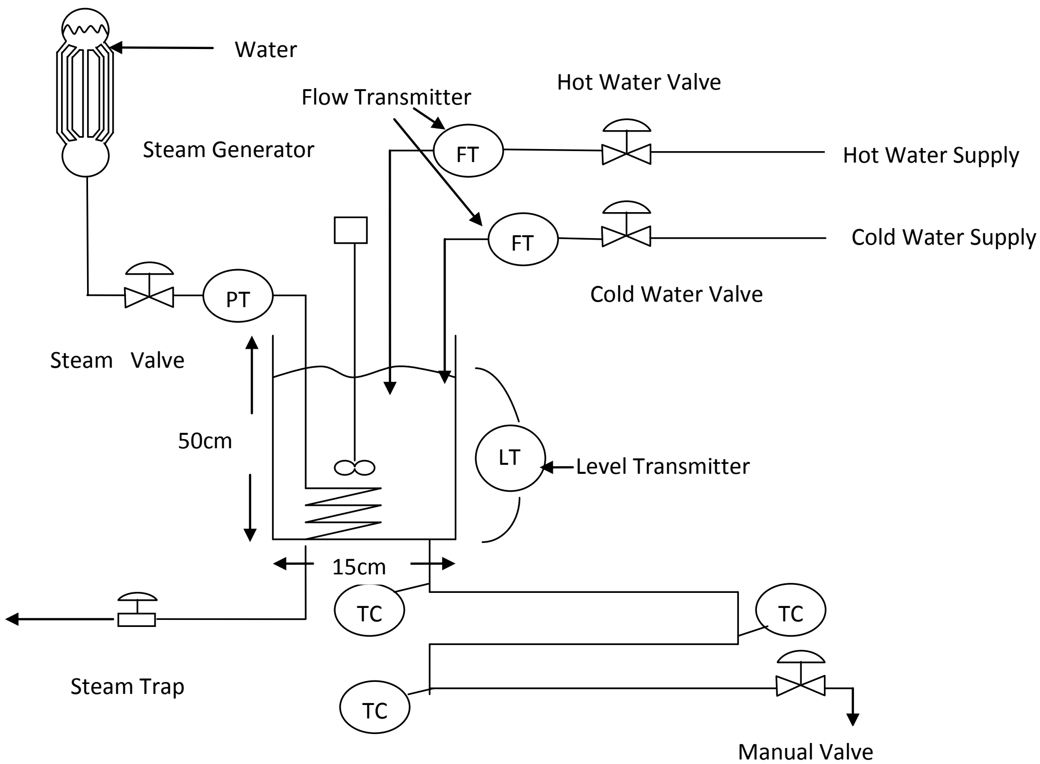

Figure 3.4: Schematic Diagram of the CSTH plant

control valves. The other input to the system is hot water flow. For our current study, we consider this to be the disturbance. Any change in hot water flow affects both of the process outputs.

For implementing the model predictive controller and the predictive monitoring system, we used the linear state space model provided in Thornhill et el. [Thornhill et al., 2008]. The process is described in state space form as follows:

$$\dot{\boldsymbol{x}} = \boldsymbol{A}\boldsymbol{x} + \boldsymbol{B}\boldsymbol{u'} + \boldsymbol{E}\boldsymbol{u^d} \tag{3.27a}$$

$$\boldsymbol{y'} = \boldsymbol{C}\boldsymbol{x}, \tag{3.27b}$$

where $\begin{bmatrix} u_1'(t) \\ u_2'(t) \end{bmatrix} = \begin{bmatrix} u_1(t-1) \\ u_2(t) \end{bmatrix}$, $\begin{bmatrix} y_1(t) \\ y_2(t) \\ y_3(t) \end{bmatrix} = \begin{bmatrix} y_1'(t) \\ y_2'(t) \\ y_2'(t-8) \end{bmatrix}$ and $u^d(t) = u_3(t)$

Here, u_1 is the cold water valve position, u_2 is the steam valve position, u_3 is the hot water valve position, y_1 is the level measurement, y_2 is the flow measurement of the water going out, y_3 is the water temperature, x_1 is tank volume, x_2 is output of valve transfer function and x_3 is the total enthalpy in the tank. $\boldsymbol{A}$, $\boldsymbol{B}$, $\boldsymbol{C}$ and $\boldsymbol{E}$ are the model matrices for the system linearized at a given operating point. The model was operated at the nominal operating conditions stated in Table 3.1. Model matrices for the given operating point when all the input and output variables are measured in mA, are as follows:

$$A = \begin{bmatrix} -3.7313 \times 10^{-3} & 1.5789 \times 10^{-6} & 0 \\ 0 & -2.6316 \times 10^{-1} & 0 \\ 4.158 \times 10^{3} & 1.5842 \times 10^{-1} & -2.7316 \times 10^{-2} \end{bmatrix}, \quad B = \begin{bmatrix} 0 & 0 \\ 1 & 0 \\ 0 & 0.64 \end{bmatrix},$$

Table 3.1: Typical operating point of the CSTH

Variable	Op Pt
Level	20.50 cm
Temperature	42.50°C
CW valve	17.7%
Steam valve	9.8 %
HW valve/percent	9.4%

$$C = \begin{bmatrix} 2690 & 0 & 0 \\ 0 & 1.5132 \times 10^{-1} & 0 \\ -1979.2 & 0 & 1.1226 \times 10^{-2} \end{bmatrix} \text{ and } \quad E = \begin{bmatrix} 4.29 \times 10^{-5} \\ 0 \\ 8.8712 \end{bmatrix}.$$

Note that, the measurement delay in the system for temperature is 8 s which is an important factor for the proposed warning system, since it is developed for systems with output time-delay. Dynamic Matrix Control (DMC) was used to control the level and temperature of the tank water. The DMC regulated the cold water valve and steam valve to control the level and temperature of the water. The hot water valve position is the unknown disturbance that gives rise to measured outputs (e.g, level and temperature of water). The plant was initially steadied at a temperature of 42.5°C. High alarm limit for temperature is set at 43.8°C. In closed loop, the hot water valve position was changed as a disturbance input and the temperature was monitored. The warning system was configured to issue warning to the operator when the temperature of the water exceeded the high alarm limit.

3.3.1 Warning generation for time-delay

In this section, we show the performance of the warning system for monitoring the process during the time delay period. As shown in 'Proposedpredictive 'warning generation' system', the estimated open loop response is the same as the closed loop re-

Table 3.2: ISE of estimation for different observers at different duration

	600-650 s	620-650 s
UIO	10.08	1.16
Kalman based observer	16.72	0.38

sponse over the 'time-delay monitoring horizon' due to the delay in controller action. Unknown input was estimated from the state space model of the system described above, using Luenberger based and Kalman Filter based unknown input observers. Estimated input along with the open loop model were used to generate a warning for the plant. The robustness of the method was checked for two levels of measurement noise.

3.3.1.1 Warning generation for low measurement noise

In the first scenario a moderate noisy environment with temperature noise variance $\sigma_T^2 = 0.0044^\circ\ C^2$ was considered. At $t = 600$ s, a disturbance was introduced to the system by opening the hot water valve from 9.4% to 11.3%. Disturbance affects both level and temperature. From the measured value, unknown input was estimated using the observers and validated against actual change of valve position. Figure 3.5 shows the estimated changes of the hot water valve from the UIO and the Kalman based observers. From the figure, it is evident that both observers were able to estimate the disturbance magnitude. Integral squared error (ISE) is calculated to quantify the performance comparison. ISE was calculated for the whole duration of a step change and at the steady state separately. Calculated ISE values are given in Table 3.2. It is observed that the UIO was able to estimate the step change more quickly compared to the Kalman based observer. However, the Kalman based observer estimated the disturbance more precisely at the steady state, as is evident from ISE.

As, the temperature has a time-delay of 8 s, any control action to the system affects

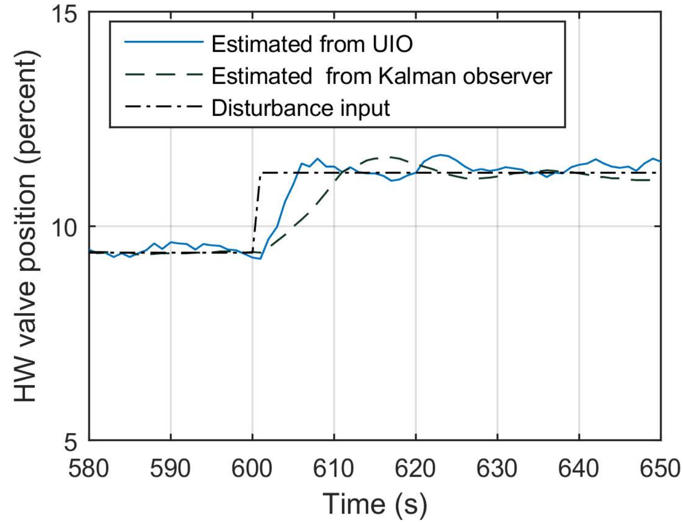

Figure 3.5: Estimated disturbance from observers for low noise scenario

temperature after the delay period. Hence, temperature is continuously monitored for a horizon of 8 s at each instant. The estimated disturbance and open loop model together evaluate the open loop process response over the 'monitoring horizon'.

Predicted temperature using the UIO over the monitoring horizon for different instances are shown in Figure 3.6. This shows that predicted values started to cross the threshold at 633 s. However, to improve robustness, a warning was generated only when three consecutive predicted values crossed the threshold. Hence, a warning was issued to the operator at $t = 634$ s. The predicted temperature over the monitoring horizon using the Kalman based observer is shown in Figure 3.7.

The measured value and the Kalman estimation of temperature are shown in Figure 3.8. This shows that the Kalman filter provides a good estimate of temperature which is less noisy compared to the original measurement. Moreover, it is observed that the temperature originally crossed the threshold at $t = 641$ s. Hence, the warning system was successfully able to forecast an abnormal situation 7 s earlier in a less noisy

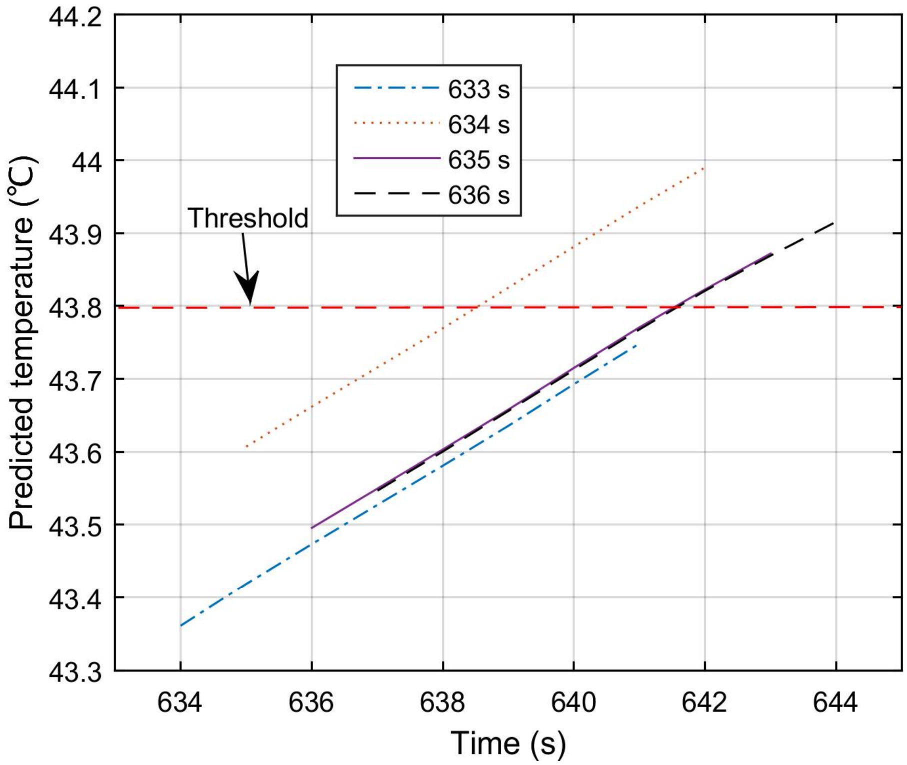

Figure 3.6: Predicted values over 'monitoring horizon' using UIO

environment. From the identified model provided by Thornhill et el. [Thornhill et al., 2008], the time constant for temperature, $\tau = 36.6$ s. As such the proposed warning system provided a lead time of 19.1% of the process time constant.

3.3.1.2 Warning generation for noisy measurements

Chemical processes usually have significant noise in the system. In this section we investigate the effect of measurement noise in the proposed warning system. Variance of temperature noise is increased by a factor of 10 compared to the previous scenario.

At $t = 600$ s, a disturbance is introduced into the system by changing the hot water valve position from 9.4% to 11.3%. The estimated disturbance from the UIO and the Kalman based observer are shown in Figure 3.17. ISE for this scenario is reported in Table 3.3. Though the UIO was able to estimate the disturbance faster, ripples of

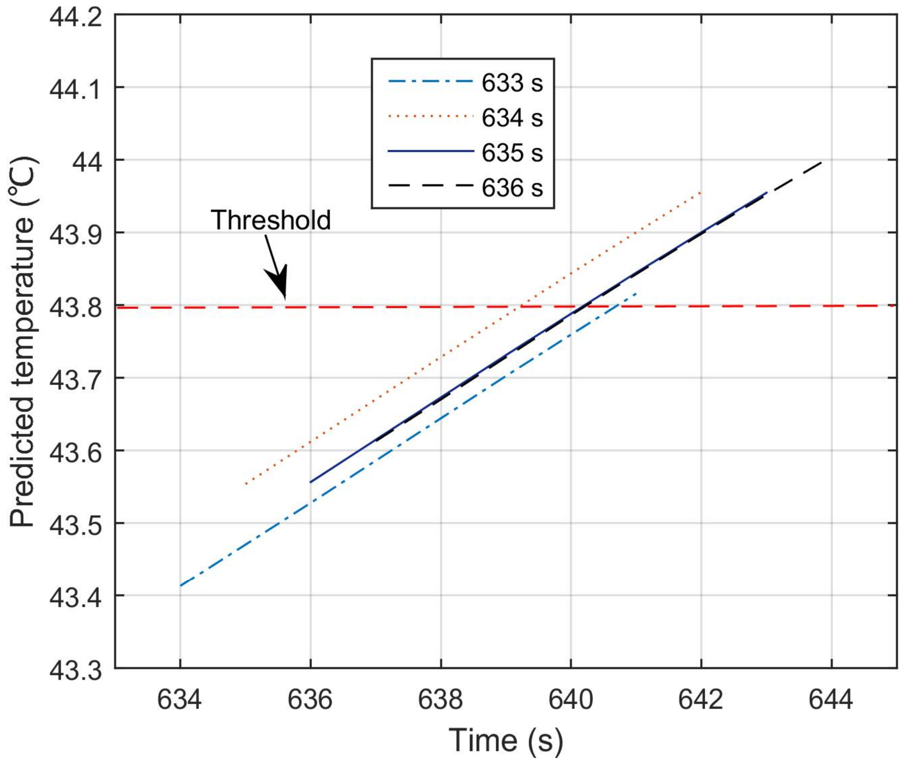

Figure 3.7: Predicted values over ‘monitoring horizon’ using Kalman based observer

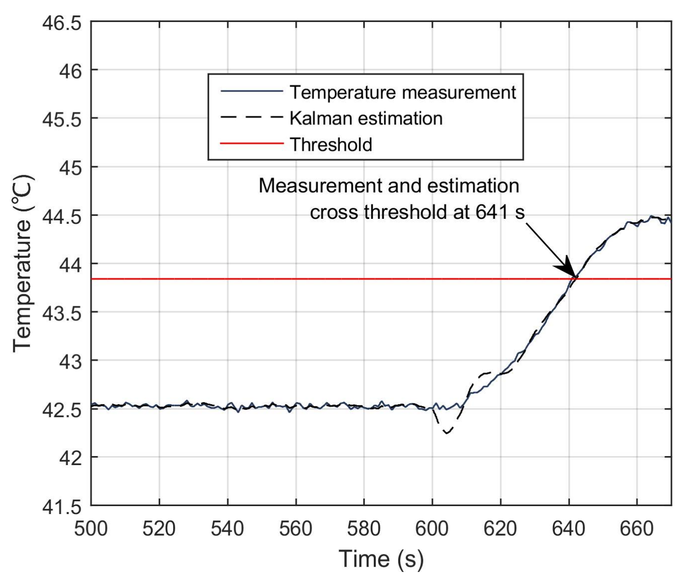

Figure 3.8: Temperature measurement with estimated value from Kalman filter

Table 3.3: ISE of estimation for different observers at different duration

	600-650 s	620-650 s
UIO	18.54	4.98
Kalman based observer	20.10	0.96

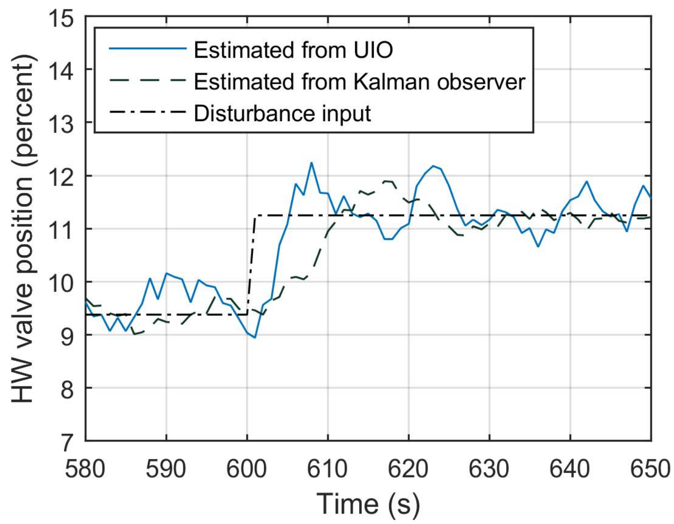

Figure 3.9: Estimated disturbance from observers for high noise scenario

the estimated signal increased significantly compared to the previous scenario. The Kalman based observer estimated more accurately compared to the UIO at a steady state in noisy environment. However, estimation accuracy deteriorated more in the noisy case compared to the previous scenario. Temperature was predicted using this estimated disturbance and a warning issued using the proposed warning system. Predicted values of the temperature using the UIO at different instances are shown in Figure 3.10. It is observed that at t=634, three of the predicted values crossed the threshold and a warning was generated. However, at t = 635 and 636 s, the predictions remained within threshold and the process is in a non-warning state. At t = 637 s, all the predictions again crossed the threshold and the warning was reissued. A flip-flop behaviour of the alarm was observed in this scenario due to the oscillation in the estimated disturbance.

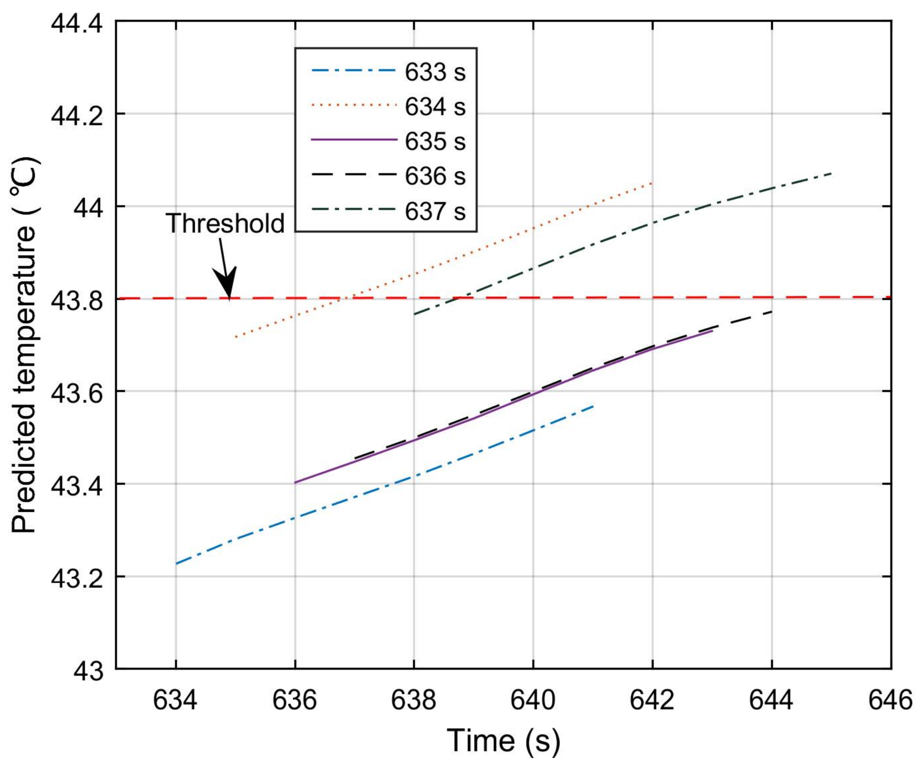

Figure 3.10: Predicted values over 'monitoring horizon' using UIO

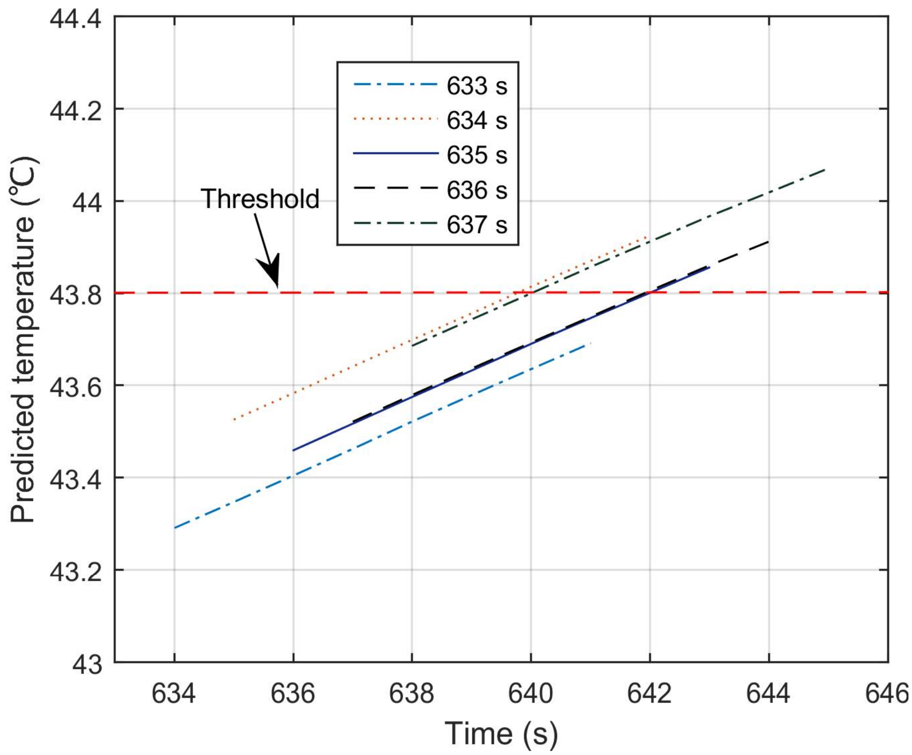

Figure 3.11: Predicted values over 'monitoring horizon' using Kalman based observer

The predicted temperature values over the monitoring horizon using the Kalman based observer are shown in Figure 3.11. The warning is stable and a more consistent behaviour is observed. At $t = 637$ s, three of the predictions crossed the threshold value and a warning was generated to the operator.

The measurement and Kalman estimation of temperature for the 'high noise scenario' are shown in Figure 3.12. It shows that the Kalman filter was able to track the temperature, even in the presence of high noise. Moreover, the temperature crossed the threshold at $t = 641$ s. Using this proposed warning system, the abnormal situation was predicted 4 s earlier. Comparing the time constant of the temperature, $\tau = 36.6$ s, it can be said that the proposed framework provides a lead time of 10.9% of the process time constant.

It is clear from the results reported above that the warning system requires a lit-

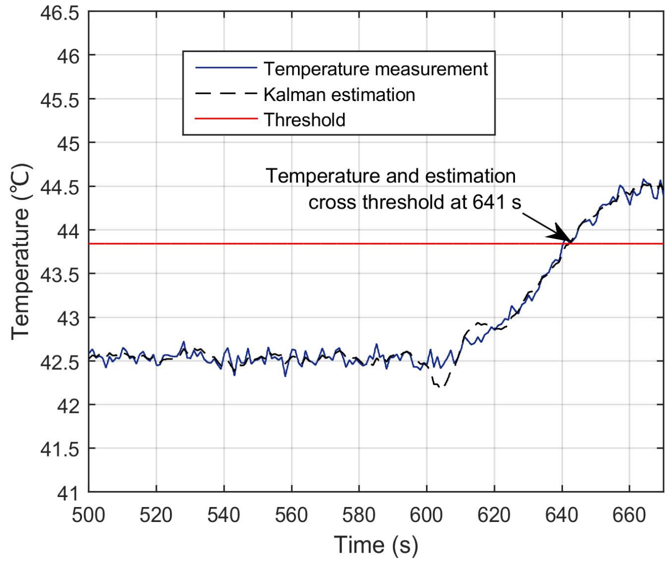

Figure 3.12: Temperature measurement with estimated value from Kalman filter

tle longer time to respond to the increase of noise and gives the operator less lead time. The noise to disturbance ratio is around 10% for the second case. Even in the presence of large noise, the proposed methodology is able to provide a warning to the operator and allow the time to respond before the temperature actually exceeds the safety limit.

3.3.2 Warning generation for limited actuator capacity

Necessary criteria for safe operation of a process is described by output constraints, whereas input constraints describe the availability of the actuator capacity. Violation of any of these constraints will trigger a warning. For the current scenario, our output constraints are on level (y_1) and temperature (y_2), and input constraints are on the steam valve position (u_1) and cold water valve position (u_2). Also, the inputs and outputs are related in the system at the steady state through process gain. These relationships are used to formulate an LP problem for the system.. At a steady state, the CSTH system model is given by:

$$\Delta y_1^{ss} = 2.766\Delta u_1 \tag{3.28a}$$

$$\Delta y_2^{ss} = -0.293\Delta u_1 + 0.369\Delta u_2, \tag{3.28b}$$

where Δy_1^{ss}, Δy_2^{ss} are the changes in level and temperature at a steady state, respectively, and Δu_1 and Δu_2 are the changes in the position of the cold water valve and steam valve. The inequality limits arise from the operational limits of the output variables and the capacities of the actuators. Maximum and minimum operator limits for the tank level are 15.8 cm and 52 cm; for temperature, the limits are 39.2°C and 43.2°C. Both the steam valve and cold water valve can be either fully open or fully closed; thus, the maximum and minimum limits for both valves are 100% and 0%. Based on these values, the inequality constraints are given by Equation 3.29.

$$15.8 - y_1^{ss} \leq \Delta y_1^{ss} \leq 25.2 - y_1^{ss} \tag{3.29a}$$

$$39.2 - y_2^{ss} \leq \Delta y_2^{ss} \leq 43.2 - y_2^{ss} \tag{3.29b}$$

$$0 - u_{1,t} \leq \Delta u_1 \leq 100 - u_{1,t} \tag{3.29c}$$

$$0 - u_{2,t} \leq \Delta u_2 \leq 100 - u_{2,t} \tag{3.29d}$$

In the work of Khan et el. [Khan et al., 2014], two different sizes of disturbances were used to check the authenticity and robustness of the warning system. The hot water valve was opened from 7.1% to 7.6% in the first scenario to check the robustness. It was found from the LP that there exists a feasible region, as shown in Figure 3.13 and the process measurements were consistent with the generated ‘no warning’ state.

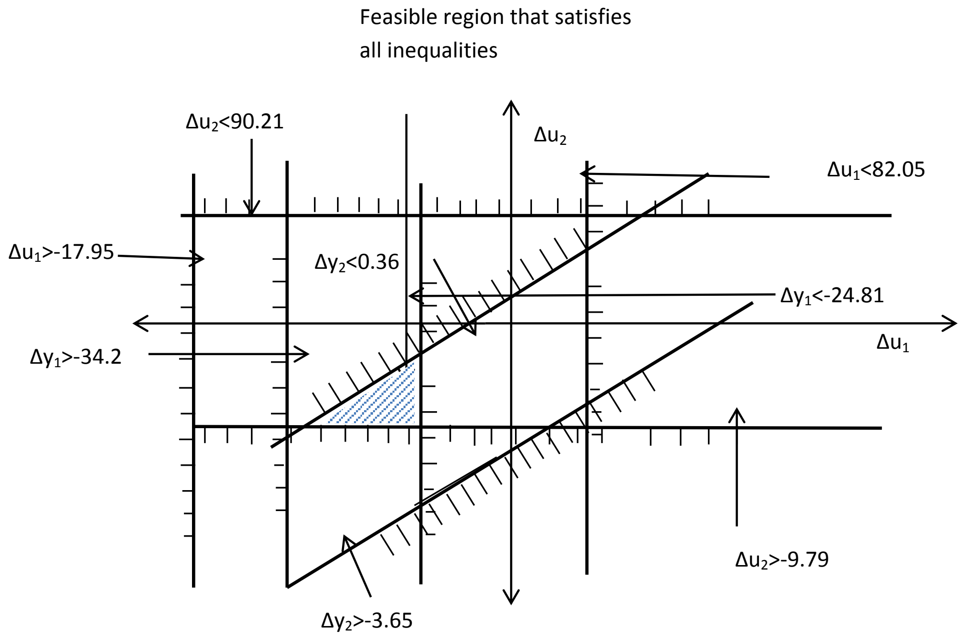

Figure 3.13: Constraints inequalities for the robustness check ([Khan et al., 2014])

In the second scenario, the hot water valve was opened from 7.1% to 9.5%, which resulted in changes in the system. LP calculation revealed that there was no feasible region, as shown in Figure 3.14 and hence an alarm was generated. The temperature at the steady state was measured outside threshold and the robustness of alarm is justified.

As, a step disturbance was used in previous case, feasibility checks at the initial and final values of the transition were made to generate a warning. However, as the disturbance was unknown for current case, the estimated inputs from observers were used. As estimated input was changed gradually, LP needed to check for a feasible region at each instance. From the Equation 3.29, it is clear that input constraint inequalities represent the limiting actuator capacity only and do not change with the disturbance size. It is observed from the two LP plots shown in Figures 3.13 and 3.14 that output constraint inequalities for temperature depend on disturbance size.

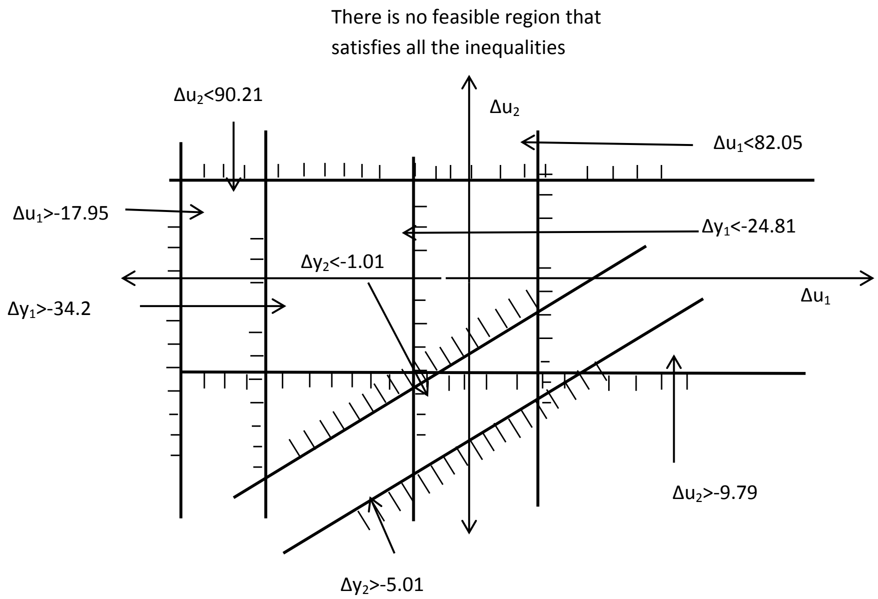

Figure 3.14: Constraints inequalities for authenticity check ([Khan et al., 2014])

When disturbance size increases, the upper temperature constraint line in the LP plot tends to slide towards the origin point. Whenever this line slides far from the origin, a feasible region no longer exists. This property of LP was used for our current case study.

We have upper constraint inequality in 3.29b. Using the value of Δy_2^{ss} from 3.28b, this inequality can be written in terms of input change:

$$-0.293\Delta u_1 + 0.369\Delta u_2 \leq 43.2 - y_2^{ss} \tag{3.30}$$

From the property of the straight line we can say that the constraint line will cross origin when we have, $y_2^{ss} = 43.2°\text{C}$. So, whenever disturbance input is large enough to bring the steady state of temperature over 43.2°C, there will be no feasible solution and hence an alarm is generated.

A step type disturbance was introduced into the system by changing the hot water

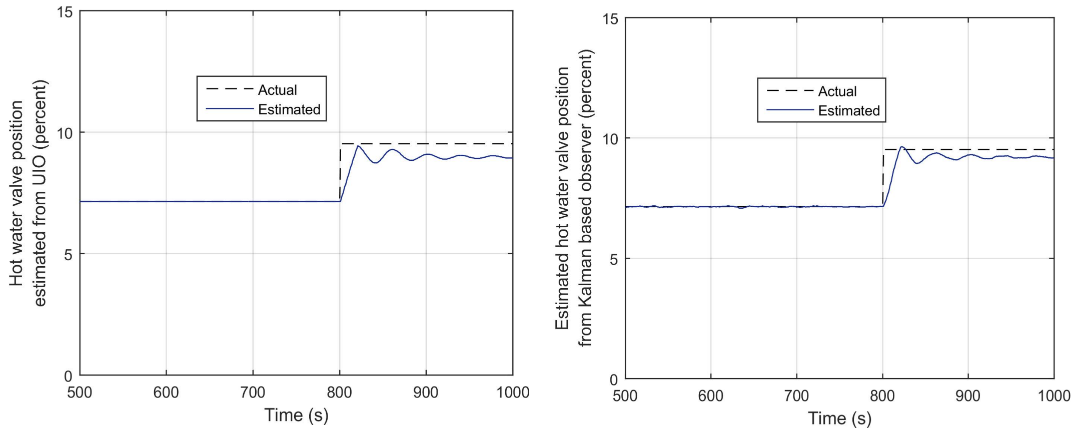

(a) Estimated disturbance using UIO

(b) Estimated disturbance using Kalman based observer

Figure 3.15: Estimated disturbance from observers

valve position from 7.1% to 9.5% at t=800 s. Disturbance was estimated from the change in measurements using two observers. Estimated values of disturbance from different observers are shown in Figures 3.15a and 3.15b.

Due to the system dynamics, the effect of the disturbance on the output is not immediate. This is reflected in the estimated values of the disturbance. The estimated values of disturbance show a second order system dynamics and gradually reaches from 7.1% to 9.5%. At each instant the estimated disturbance value is used by LP to check for a feasible solution. An alarm is generated at 812 s and 814 s for the UIO and Kalman based observer respectively. In both instances the disturbance size is around 8.84% and the predicted steady state value of the temperature is 43.5°C. An LP plot for this condition is shown in Figure 3.16. Closed loop responses for the above disturbance scenario are shown in Figure 3.17a and 3.17b. It is observed that, the temperature settled to a new steady state outside the high alarm limit and thus validates the alarm generated based on the estimated value from observers.

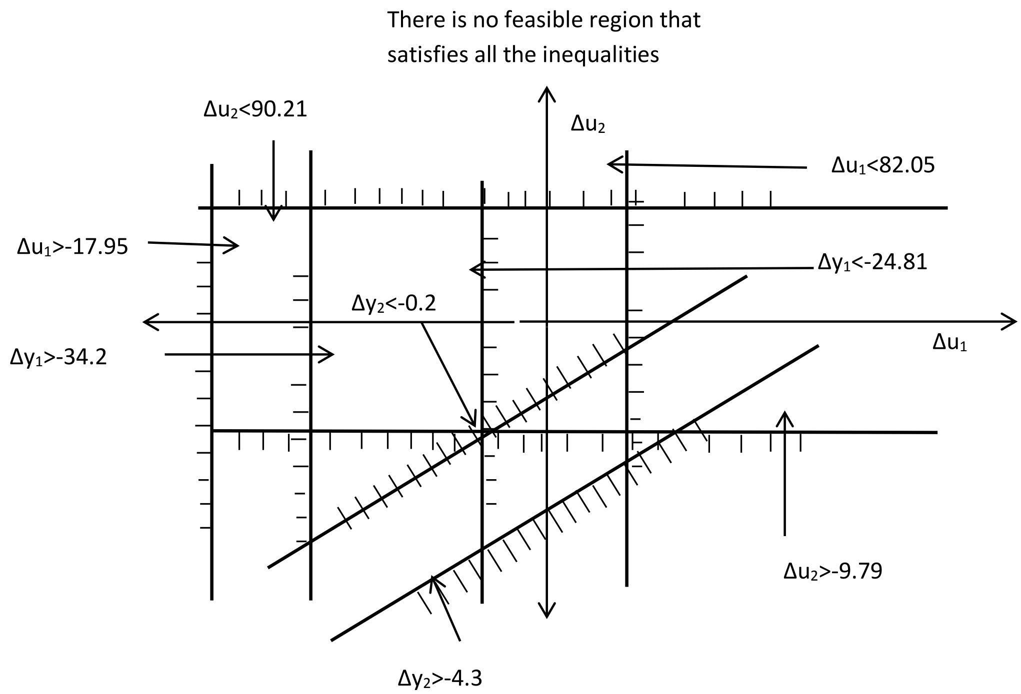

Figure 3.16: LP plot for inequalities with marginal value of disturbance showing no feasible solution

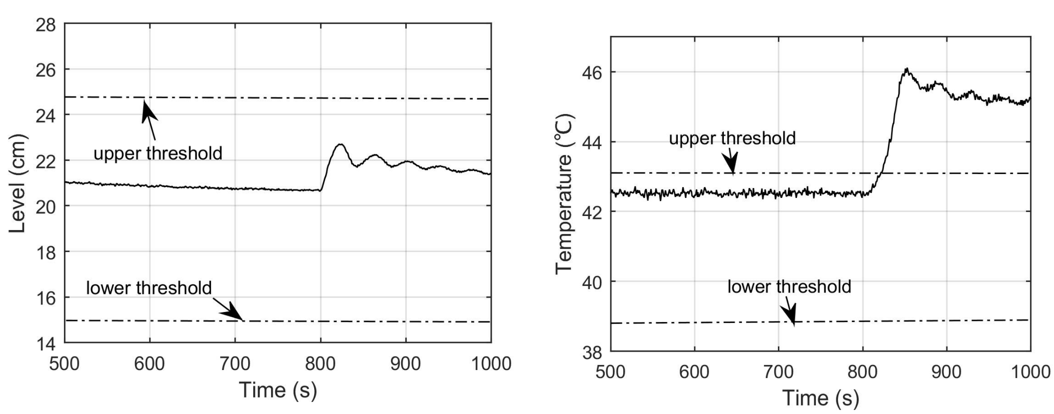

(a) Level measurement and the limits (b) Temperature measurement and the limits

Figure 3.17: Process measurements and the limits

3.3.3 Performance comparison of the proposed framework with an existing method

The proposed warning system is an extension of the work presented by [Khan et al., 2014]. Case studies for the proposed method were performed on the same CSTH system and similar disturbance scenarios were considered to compare the performance of the current warning system with the framework proposed by [Khan et al., 2014]. Performance comparison for the different disturbance scenarios are discussed in following subsections.

3.3.3.1 Performance comparison for monitoring during delay period

To monitor temperature during the time delay period, a disturbance was introduced to the system by opening the hot water valve from 9.4% to 11.3% at $t = 600$ s. Disturbance affects both level and temperature and temperature crossed threshold at $t = 640$ s. Warning would have been issued at this instance, if it was generated based on the measured signal. Predictive methods issued warning early to provide a lead time to take corrective action.

Table 3.4 reported the lead time for different scenarios of the proposed predictive method. These are also compared to the lead time generated by the warning system of [Khan et al., 2014]. Lead time of the current system decreases compared to the previous one in a noisy scenario. However, the previous method assumed that the disturbance was known, which limits its applicability. The proposed method considers disturbance to be unknown and hence relaxes the restrictive assumption of the previous work at the cost of a slight decline in performance.

Table 3.4: Lead time of different scenarios for monitoring time delay period

	Lead time (s)
UIO low noise	7
Kalman based observer low noise	7
UIO high noise	4
Kalman based observer high noise	4
Known input [Khan et al., 2014]	7

3.3.3.2 Performance comparison for monitoring for limited actuator capacity

To monitor process's vulnerability to a limited actuator capacity at steady state, disturbance was introduced at $t = 800$ s. The hot water valve was opened from 7.1% to 9.5%, which resulted in changes in the system. In Khan et el. [Khan et al., 2014], it was assumed that disturbance was known and LP revealed that, there was no feasible region and warning was generated at $t = 800$ s. For the proposed method, unknown disturbance was used and estimated disturbance for estimator increased gradually and warning generation was delayed.

Comparison of the warning generation instances for different scenarios are presented in Table 3.5. It is observed that the warning generation of the current method is delayed compared to the case where the disturbance was known [Khan et al., 2014]. This is due to the fact that the estimator requires time to estimate the step change and the disturbance increases gradually, in contrast to the previous case, where the known input changed instantly at 800 s. However, proposed method was able to generate warning earlier than a monitoring system that would issue warning based on measured signal.

Table 3.5: Comparison of different warning systems to monitor the system with constrained actuators

Warning system	Alarm generation instant (s)
UIO based predictive for unknown input	812
Kalman based predictive for unknown input	814
Predictive for known input [Khan et al., 2014]	800
Based on measured signal	825

3.4 Conclusions

The present work extended the predictive alarm system proposed by [Khan et al., 2014] to consider a more realistic scenario where disturbance is unmeasured. A methodology was developed where the unknown input estimator was combined with the warning system. Luenberger based and Kalman filter based unknown input observers were used to estimate disturbance. As expected, the Luenberger observer based method was good for noise free cases, but did not perform well in a noisy scenario. The Kalman filter based method gave consistent results in a noisy scenario. Detailed implementation steps of the methodology are described in the paper. The proposed methodology showed consistent performance in generating an early alarm. However, the lead time to detect the alarm reduced with the increase of measurement noise.

The proposed methodology generates a warning for the system during the time-delay period and at steady state condition only; the dynamic change period of the process is not covered by the alarm generation system. Moreover, the developed warning system is applicable to a linear system only. For a nonlinear system, a more elaborate set of conditions are required for alarm generation; also, the disturbance estimator needs to be adapted for a nonlinear system.

Acknowledgement

The authors thank Natural Sciences and Engineering Research Council (NSERC) for financial support.

Nomenclature

$\mathbf{A}, \mathbf{B}, \mathbf{C}, \mathbf{D}$ System matrices for the linear state space system

ΔH Reaction heat

Δu_k^d Step change in disturbance at time k ($unit$)

Δy_i^{ss} Change in steady state controller made to the i-th variable ($unit$)

ϵ Threshold value for two iterations

γ_i Valve opening of i-th pump

$\hat{u}_{k-1}^+$ Estimated input after M-step

$\hat{u}_k^d$ Estimated disturbance ($unit$)

$\hat{u}_{k-1}$ Estimated input at time step $k-1$

$\hat{x}_k$ Estimated state at time step k

$\hat{x}_k$ Estimated state ($unit$)

$\hat{y}_k$ Estimation of process variables from estimated state $\hat{x}_k$ at time step k

ν_k Measurement noise at time-step k

ρ Density of the reactant

$\sigma^2\mathbf{I}$ Variance of measurement noise of four tank system

σ_T^2 Noise variance of temperature ($^\circ$ C^2)

$\mathbf{A}$,$\mathbf{B}$ $\mathbf{C}$ and $\mathbf{E}$ Matrices of state space system

$\mathbf{F}$, $\mathbf{T}$, $\mathbf{K}_1$, $\mathbf{K}_2$, $\mathbf{H}$ Design matrices for UIO

A_i Cross section area of i-th tank of Four tank system

a_i Cross section are of the flow line coming out of ith tank of Four tank system

A_r Area of heat transfer

b_k Bias error ($unit$)

C_A Concentration of the reactant

C_p Specific heat of the reactant

C_{Ai} Feed concentration

e_k Estimation error ($unit$)

$E_{N,k}$ Error due to noise ($unit$)

G_i Gain of 'i-th' output

$G_{ij}(0)$ Step response at steady state

h_i Water level of ith tank of Four tank system

$k_0 e^{-E_A/T} C_A$ Reaction rate

$k_i v_i$ Flow of of i-th pump

m Number of total inputs

M_k,K_k Design matrices for Kalman based observer

N Total number of particles

n Number of states

P Monitoring horizon

p Number of measurements

Q Variance of process noise w_k

$q(x_k/x_{k-1}, Y_{k-1})$ Proposal distribution

Q_r Variance of process model mismatch of CSTR

q_r Flow rate of feed at CSTR

R Variance of measurement noise ν_k

R_r Variance of measurement noise of CSTR

T Temperature in the reactor

T_c Temperature of the cooling fluid

T_i Feed temperature

U Effective heat co-efficient

u_k^d Disturbance to the system ($unit$)

u_{k-1}^{d+} Estimated disturbance after M-step

u_{k-1}^{d-} Initial value of unknown disturbance at time step k

u_k^d Unknown input at time-step k

u_k^{in} Known input at time-step k

u_1 Cold water valve position (%)

u_2 Steam valve position (%)

u_3 Hot water valve position (%)

u_k Process inputs ($unit$)

u_l Left pump input of Four tank system

u_r Right pump input of Four tank system

V Volume of the feed at CSTR

v_i Applied voltage of i-th pump

v_k Measurement noise ($unit$)

w Unmodelled dynamics of CSTR

w_k Process noise ($unit$)

W_k Importance weight at time step k

w_k Process noise at time-step k

W_k^i Importance weight of i-th particle at time step k

x_k^i Random particle at time step k

$x_{k,resamp}^i$ Resampled particles

x_1 Tank volume

x_2 Output of valve transfer function

x_3 Enthalpy of tank

x_k Unknown state of the system (*unit*)

x_k Unknown states at time-step k

y_1 Level measurement (cm)

y_2 Flow measurement (m^3/s)

y_3 Temperature measurement ($^\circ C$)

y_i^{ss} the steady state of the 'i-th' output variable (*unit*)

y_k Process measurement (*unit*)

y_k Process measurement at time-step k

$y_{i,high}$ Maximum safety limit of 'i'th output (*unit*)

$y_{i,k}$ Measurement of i-th' output at time k

$y_{i,low}$ Minimum safety limit of 'i'th output (*unit*)

z_k State of UIO (*unit*)

$u_{j,high}$ Minimum position of actuator (*unit*)

$u_{j,low}$ Maximum position of actuator (*unit*)

y_k^* predicted value of the variable y for at time sample *k-1* (*unit*)

Bibliography

[Adnan et al., 2011] Adnan, N. A., Izadi, I., and Chen, T. (2011). On expected detection delays for alarm systems with deadbands and delay-timers. *Journal of Process Control*, 21(9):1318.

[Ali et al., 2015] Ali, J. M., Hoang, N. H., Hussain, M. A., and Dochain, D. (2015). Review and classification of recent observers applied in chemical process systems. *Computers & Chemical Engineering*, 76:27.

[Chang et al., 1994] Chang, S.-K., You, W.-T., and Hsu, P.-L. (1994). General-structured unknown input observers. In *American Control Conference, 1994*, volume 1, pages 666–670. IEEE.

[Corless and Tu, 1998] Corless, M. and Tu, J. (1998). State and input estimation for a class of uncertain systems. *Automatica*, 34(6):757.

[Darouach and Zasadzinski, 1997] Darouach, M. and Zasadzinski, M. (1997). Unbiased minimum variance estimation for systems with unknown exogenous inputs. *Automatica*, 33(4):717.

[Fernandez et al., 2005] Fernandez, L. P. S., Pogrebnyak, O., and Marquez, C. Y. (2005). Neural network and trend prediction for technological processes monitoring. In *MICAI 2005: Advances in Artificial Intelligence*, pages 731–740. Springer.

[Friedland, 1969] Friedland, B. (1969). Treatment of bias in recursive filtering. *Automatic Control, IEEE Transactions on*, 14(4):359.

[Gillijns and De Moor, 2007] Gillijns, S. and De Moor, B. (2007). Unbiased minimum-variance input and state estimation for linear discrete-time systems. *Automatica*, 43(1):111.

[Hsieh, 2000] Hsieh, C.-S. (2000). Robust two-stage kalman filters for systems with unknown inputs. *Automatic Control, IEEE Transactions on*, 45(12):2374.

[Izadi et al., 2009a] Izadi, I., Shah, S. L., Shook, D. S., and Chen, T. (2009a). An introduction to alarm analysis and design. *IFAC Proceedings Volumes*, 42(8):645.

[Izadi et al., 2009b] Izadi, I., Shah, S. L., Shook, D. S., Kondaveeti, S. R., and Chen, T. (2009b). A framework for optimal design of alarm systems. *IFAC Proceedings Volumes*, 42(8):651.

[Juricek et al., 2001] Juricek, B. C., Seborg, D. E., and Larimore, W. E. (2001). Predictive monitoring for abnormal situation management. *Journal of Process Control*, 11(2):111.

[Khan et al., 2014] Khan, M. A. I., Imtiaz, S. A., and Khan, F. (2014). Early warning system for chemical processes with time delay and limited actuator capacity. *Industrial & Engineering Chemistry Research*, 53(12):4763.

[Kitanidis, 1987] Kitanidis, P. K. (1987). Unbiased minimum-variance linear state estimation. *Automatica*, 23(6):775.

[Kresta et al., 1991] Kresta, J. V., Macgregor, J. F., and Marlin, T. E. (1991). Multivariate statistical monitoring of process operating performance. *The Canadian Journal of Chemical Engineering*, 69(1):35.

[Lee and Park, 2012] Lee, K.-S. and Park, T.-G. (2012). New results on fault reconstruction using a finite-time converging unknown input observer. *Control Theory & Applications, IET*, 6(9):1258.

[MacGregor et al., 1994] MacGregor, J. F., Jacckle, C., Kiparissides, C., and Koutondi, M. (1994). Process monitoring and diagnosis by multiblock pls methods. *American Institute of Chemical Engineers Journal*, 40 (5):826.

[MacGregor and Kourti, 1995] MacGregor, J. F. and Kourti, T. (1995). Statistical process control of multivariate processes. *Control Engineering Practice*, 3:403.

[Mattavelli et al., 2005] Mattavelli, P., Spiazzi, G., and Tenti, P. (2005). Predictive digital control of power factor preregulators with input voltage estimation using disturbance observers. *Power Electronics, IEEE Transactions on*, 20(1):140.

[Radke and Gao, 2006] Radke, A. and Gao, Z. (2006). A survey of state and disturbance observers for practitioners. In *American Control Conference, 2006*, pages 6–pp. IEEE.

[Sundaram and Hadjicostis, 2008] Sundaram, S. and Hadjicostis, C. N. (2008). Partial state observers for linear systems with unknown inputs. *Automatica*, 44(12):3126.

[Thornhill et al., 2008] Thornhill, N. F., Patwardhan, S. C., and Shah, S. L. (2008). A continuous stirred tank heater simulation model with applications. *Journal of Process Control*, 18(3-4):347 – 360.

[Xiong and Saif, 2003] Xiong, Y. and Saif, M. (2003). Unknown disturbance inputs estimation based on a state functional observer design. *Automatica*, 39(8):1389.

[Zamanizadeh et al., 2008] Zamanizadeh, E., Salahshoor, K., and Manjili, Y. (2008). Prediction of abnormal situation in nonlinear systems using ekf. In *Networking, Sensing and Control, 2008. ICNSC 2008. IEEE International Conference on*, pages 681–686. IEEE.

[Zarei and Poshtan, 2010] Zarei, J. and Poshtan, J. (2010). Design of nonlinear unknown input observer for process fault detection. *Industrial & Engineering Chemistry Research*, 49(22):11443.

Chapter 4

Simultaneous Estimation of Hidden State and Unknown Input Using Expectation Maximization (EM) Algorithm

Abstract: An expectation maximization (EM) algorithm-based simultaneous state and input estimator for nonlinear systems is developed. This study uses a Bayesian solution to estimate the states and unknown inputs simultaneously. It was assumed that a joint distribution between states and inputs exist. The joint distribution was estimated sequentially using an EM algorithm. The EM algorithm has two steps: expectation step (E-step) and maximization step (M-step). In the E-step, a particle filter was used to estimate the conditional probability of states. The expected state was also estimated for an assumed value of input. The conditional distribution of the measurement conditioned on the estimated states was maximized with respect to input in the M-step, and inputs were estimated. These two steps were performed

alternatively until both states and inputs converged to a solution. The effectiveness of the proposed method was demonstrated using simulation and experimental case studies.

4.1 Introduction

Safe and uninterrupted operation is the top priority in a process plant. The control system works as the first layer of safeguard to keep the process variables inside the desired limit. When a disturbance enters into the process, the existing controller reacts to it and tries to nullify the effect of the disturbance. However, in some instances, available control actions are not sufficient in size or dynamically not quick enough to reject the disturbance effect. Due to this, it is important to monitor process health and check its vulnerability to abnormal situation. Monitoring process states can often give an early indication of a fault. Many of the states are not measured directly, and hidden states need to be estimated from the available process measurements. Estimation of the state is more challenging when a process is perturbed by unknown disturbances. If a disturbance is unknown, it needs to be estimated and reconstructed to forecast an abnormal situation. The motivation of this work is to develop an estimation technique for nonlinear systems that estimates the hidden states and reconstructs unknown inputs from the available measured variables.

State observers and Kalman-based estimators have been widely used over the last several decades to recursively estimate system states [Luenberger, 1971,Kalman, 1960]. In recent years, these two types of observers were modified and several improved versions are in use. Application of different types of observers in a chemical process is extensively discussed by [Mohd Ali et al., 2015]. The most common type of observer is classical Luenberger observer and its improved versions such as extended Luenberger observer, sliding mode observer, and adaptive state observer (e.g. [Dochain, 2003], [Floquet et al., 2004], [Vries et al., 2010], and [Spurgeon, 2008]). These observers are easy to implement but not suitable for a complex dynamic system with plant model mismatch and measurement noise. Luenberger observers were modified to disturbance observers or unknown input observers to handle the model mismatch and disturbance. [Radke and Gao, 2006] presented the design advantages of disturbance observers and concluded that computation simplicity popularized the UIO, especially for simple processes. A Lyapunov characterization was used by [Corless and Tu, 1998] to design an estimator that was able to estimate the state and input simultaneously. A similar approach was used by [Xiong and Saif, 2003] to estimate input and state with an observer with reduced order. Disturbance observers were used to reconstruct the disturbances by [Mattavelli et al., 2005], [Lee and Park, 2012] and [Sundaram and Hadjicostis, 2008].

Bayesian estimators fall into another group of observers. This group of observers estimates the states and inputs from the joint posterior distribution of states and inputs, and can handle the complex process with measurement noise. A wide variety of filters such as the Kalman filter, particle filter, and moving horizon estimators belong to this observer group. For estimating state and input, a two-stage Kalman-based estimator was proposed by [Friedland, 1969] which was further modified as a recursive filter by [Kitanidis, 1987]. [Hsieh, 2000] and [Gillijns and De Moor, 2007] proposed a recursive filter with minimum variance and proved their optimality. They used Kalman-based tuning to minimize the state. An application of UIO for lateral vehicle velocity estimation is presented by [Imsland et al., 2007]. They concluded that designing a UIO is more challenging for nonlinear systems and synthesis criteria are difficult to obtain. A novel linear matrix inequality (LMI)-based observer for a nonlinear system was proposed by [Korbicz et al., 2007]. LMI was defined from the Lipschitz constant, using the Lyapunov theorem to check the stability and calculate the observer gain. Applicability of this method is limited to a Lipschitz type system. Kalman filter-based approaches are not optimal for nonlinear systems, and many modifications have been done to deal with the system nonlinearity. Bayesian solutions are applicable for more general cases of state estimation problems. [Patwardhan et al., 2012] presented an exhaustive review on recent developments of Bayesian nonlinear state estimation. Bayesian estimators were classified based on nonlinearity handling approaches. Early attempts to handle nonlinearity (e.g., extended Kalman filter (EKF) and versions of EKF [Söderström, 2012]) are based on Taylor series approximation. This approach has several limitations. First of all, nonlinearity propagates through the mean value, and hence, accuracy of approximation is compromised. Moreover, evaluating the derivative is nontrivial in most of the practical cases. These problems are addressed with a statistical linearization approach. An unscented Kalman filter (UKF) proposed by [Julier and Uhlmann, 2004] is most popular among this type of estimators. [Kandepu et al., 2008] and [Zarei and Poshtan, 2010] used UKF to design a nonlinear unknown input observer and applied it for fault handling and disturbance estimation. However, both EKF and UKF assume Gaussian distribution for process and measurement noises and initial states. A group of filters that approximates the posterior using random samples is known as a particle filter (PF). [Rawlings and Bakshi, 2006] discussed the several state estimators for nonlinear systems and concluded that the PF has the potential to estimate state without restrictive assumptions. [Chen, 2003] discussed the application of PF in the field of computer vision and target tracking. Some of the implementation challenges of PF were resolved in [Imtiaz et al., 2006]. [Jampana et al., 2010] used PF to develop a vision sensor for an oil sand separation unit. Implementation of PF to estimate the state and input is shown in [Mejri et al., 2013].

Implementation of a Bayesian estimator for practical purposes requires constraint handling. Thus, optimization-based estimation methods were developed. The moving horizon estimator (MHE) is one of the most common of this genre. MHE estimates the conditional density and calculates the arrival cost using MLE or MAP. As arrival cost approximation is crucial for estimation accuracy, researchers have used different methods to estimate arrival cost. [Qu and Hahn, 2009] used UKF to update the covariance of the arrival cost. An optimization-based framework is used by [Fang et al., 2013] and [Fang and de Callafon, 2015] for simultaneous state and input estimation (SISE). While [Fang and de Callafon, 2015] used the ensemble approach to handle nonlinearity, [Fang et al., 2013] linearized using the nonlinear function using the first-order Taylor's series. They developed the SISE scheme that was applied for flow field estimation.

The expectation maximization (EM) algorithm is a sequential method to estimate the states and parameters from joint distribution. The EM algorithm proposed by [Dempster et al., 1977] optimizes the likelihood iteratively instead of seeking for an analytical solution. Many researchers have used this as an efficient tool to identify the hidden model from incomplete data. [Zia et al., 2008] used the EM algorithm to estimate the state of a nonlinear process with model uncertainty, and [Andrieu and Doucet, 2003] applied the EM algorithm to estimate the model parameter online. [Gopaluni, 2008] presented a framework to estimate state and parameter simultaneously, using a particle filter as the approximation tool in the E-step and an optimization method to perform the M-step. A particle filter-based EM algorithm was also used by [Zhao et al., 2013] for estimating the model parameters for a batch process. The EM algorithm was used by [Güntürkün et al., 2014] to estimate the hidden driving force from incomplete a priori knowledge. The EM algorithm-based framework was used to estimate state and identify the time varying random latency probability of measurements by [Wang et al., 2017, Wang et al., 2016]. A Gaussian filter smoother and standard maximization procedure were used in the E-step and the M-step, respectively. A stochastic counterpart of the EM algorithm called data augmentation has also been used for parameter estimation. Data augmentation is a iterative optimization or sampling algorithm which was popularized by [Tanner and Wong, 1987] to estimate the posterior distribution of parameter. This algorithm solves the incomplete-data problem by repeatedly solving the available complete-data problem. The relation between data augmentation and the EM algorithm is discussed by [Wei and Tanner, 1990]. They also showed a Monte Carlo implementation of the EM algorithm. From the efficient results of the related works, we conclude that the EM algorithm is an attractive optimization-based choice for SISE.

The proposed estimator used the EM-based framework to simultaneously estimate states and unknown inputs. However, instead of evaluating the expected value of log-likelihood in the E-step, the conditional probability density of state is approximated in a sample space similar to data augmentation shown in [Wei and Tanner, 1990]. A particle filter was used to implement this step. In the M-step, the unknown input is estimated by maximizing the conditional posterior of input. Multiple iterations of the E-step and M-step of the EM algorithm were performed sequentially at each time step until the state and input converged. The proposed method is significantly different from existing literature [Wang et al., 2017, Wang et al., 2016]. The proposed estimator uses a particle Filter in contrast to a Gaussian filter used in [Wang et al., 2017, Wang et al., 2016, Wang et al., 2014]. As such, the estimator is optimal for a nonlinear non-Gaussian system as well. Also, from an application point of view the estimator is designed for estimating states and unknown inputs, while [Wang et al., 2016] estimates unknown or time-varying latency probability and system states.

The article is organized as follows: In Section 2, the estimation problem is defined and a Bayesian solution framework is described. In Section 3, the proposed scheme is derived for a simple linear system. In Section 4, three case studies are presented to demonstrate the effectiveness of the proposed method. Section 5 describes the conclusions and future work.

4.2 Problem formulation and theoretical framework

4.2.1 Problem formulation

Let us consider a discrete time nonlinear system described by Equations 4.1 and 4.2:

$$x_k = f(x_{k-1}, u_{k-1}) + w_k, \tag{4.1}$$

$$y_k = g(x_k) + \nu_k, \tag{4.2}$$

where $x_k \in \mathbf{R}^n$ is the state vector, $y_k \in \mathbf{R}^p$ is the measurement, u_k= $[u_k^{in}\ u_k^d]$ where $u_k^d \in \mathbf{R}^m$ is the unknown input to the system, u_k^{in} is the known inputs to the system, and w_k and ν_k are the process and measurement noises, respectively. Process and measurement noises are assumed to be uncorrelated and can be any arbitrary distribution. State is updated by a nonlinear relation $f(.)$, and the measurement is related to the state by nonlinear function $g(.)$. It is assumed that u_k is uncorrelated with w_k, ν_k. Further, no prior distribution for u_k is available except their relation with the state as given in Equation 4.1. Full information on measurement variable y_k up to current timestep 'k' is available and stored in $Y_k = \{y_1,\ y_2,\ ...\ ,y_k\ \}$. Without loss of the generality, in the derivation we ignore the known inputs u_k^{in} and consider u_k^d as the input to the system.

The objective of this estimation problem is to estimate state x_k and input u_{k-1} from available Y_k. In case u_{k-1} is a manipulated variable. Its values are set by the operators, and u_{k-1} is a deterministic signal. Our interest is in unknown inputs or disturbances, which can be either deterministic or stochastic. However, there is uncertainty in these inputs; as such, we assume the input u_{k-1} to be stochastic. Further, it was assumed that there exists a joint distribution between x_k and u_{k-1}. Our ultimate goal is to estimate the joint distribution $p(x_k, u_{k-1}/Y_k)$.

4.2.2 Bayesian framework

Estimation of the joint distribution is a difficult problem. A stepwise process is much simpler to implement. Using Bayes' rule and invoking the results in data augmentation [Tanner and Wong, 1987], we can formulate a two step iterative procedure. Using Bayes' rule, we can write:

$$p(u_{k-1}, x_k/Y_k) = p(x_k/Y_k)p(u_{k-1}/Y_k, x_k). \tag{4.3}$$

Integrating both sides with respect to x_k, we have the following relation

$$p(u_{k-1}/Y_k) = \int p(x_k/Y_k)p(u_{k-1}/Y_k, x_k)dx_k. \tag{4.4}$$

Similarly, from the Bayes' rule, joint posterior is expressed as follows:

$$p(u_{k-1}, x_k/Y_k) = p(u_{k-1}/Y_k)p(x_k/Y_k, u_{k-1}). \tag{4.5}$$

Integrating both sides with respect to u_{k-1}, we obtain,

$$p(x_k/Y_k) = \int p(u_{k-1}/Y_k)p(x_k/Y_k, u_{k-1})du_{k-1}. \tag{4.6}$$

Observation 1: For integrating Equation 4.6, we should be able to sample from $p(u_{k-1}/Y_k)$, and for integrating Equation 4.4, we should be able to sample from $p(x_k/Y_k)$. Equations 4.4 and 4.6 together suggest an EM-like iterative scheme between these two equations. According to [Tanner and Wong, 1987], if iterations are performed for an extended period, $p(u_{k-1}/Y_k)$ and $p(x_k/Y_k)$ will converge to the joint distribution $p(x_k, u_{k-1}/Y_k)$.

Observation 2: In Equation 4.6, if u_{k-1} is known, estimation of $p(x_k/Y_k, u_{k-1})$ is essentially a state estimation problem. For any given input u_{k-1}^{-}, we can use any Bayesian filter (e.g., particle filter) to estimate $p(x_k/Y_k, u_{k-1}^{-})$. Since there is uncertainty in input, it is integrated over du_{k-1} to reduce the uncertainty and make the estimate independent of u_{k-1}. In discrete form:

$$p(x_k/Y_k) = \frac{1}{m}\sum_{i=1}^{m} p(x_k/Y_k, u_{k-1}^{i}) \tag{4.7}$$

where u_{k-1}^{i} is sampled from $p(u_{k-1}/Y_k)$. Finally, the expected value of x_k is given by

$$E[x_k] = \int x_k p(x_k/Y_k, u_{k-1}^{-}) dx_k \tag{4.8}$$

Observation 3: In Equation 4.4, $p(u_{k-1}/Y_k, x_k)$ is not defined, rather $p(Y_k/x_k, u_{k-1})$ is easy to define given that x_k and noise distribution of Y_k are known. For an estimated state $\hat{x}_k$, input u_{k-1} can be estimated through maximization of density function $p(Y_k/\hat{x}_k, u_{k-1})$

4.2.3 Proposed Expectation Maximization (EM) algorithm

Based on the above observations, we propose an EM-like algorithm. The algorithm is initiated with a assumed value of input. In the expectation step (E-step), a Bayesian filter can be used to estimate $p(x_k/Y_k, u_{k-1}^-)$. However, the choice of the filter will depend on the characteristics of the system and noise distribution. For example, for a linear Gaussian system a Kalman filter can be used. In this study, we describe the use of a particle filter to make the estimation problem general for nonlinear non-Gaussian system. Subsequently, in the maximization step (M-step), we use maximum likelihood estimation (MLE) technique to estimate u_{k-1} from $p(Y_k/x_k, u_{k-1})$. These two steps are described in the following sections.

4.2.3.1 Expectation step (E-step)

The goal of this step is to estimate the posterior distribution $p(x_k/u_{k-1}, Y_k)$. The algorithm is initiated with an assumed u_{k-1}^- and prior distribution of x_{k-1}. Particles are sampled from the prior distribution. These particles along with u_{k-1}^- are passed through the prediction equation to predict $p(x_k/Y_{k-1}, u_{k-1}^-)$. As soon as measurement y_k becomes available, prior distribution is updated to $p(x_k/Y_k, u_{k-1}^-)$. Exact evaluation of $p(x_k/Y_k, \hat{u}_{k-1}^-)$ is nontrivial for a nonlinear non-Gaussian process. For this reason a SIR filter is used to approximate the posterior. In this approach, particles are sampled using a known importance function $q(x_{1:k}/y_{1:k}, u_{k-1})$ and importance weight
$W_k = \frac{p(x_{1:k}/Y_k, u_{k-1})}{q(x_{1:k}/Y_k, u_{k-1})}$.
Using the Markovian chain rule on the state, importance weights can be factored as follows:

$$
\begin{aligned}
W_k &= \frac{p(x_{1:k}/Y_k, u_{k-1})}{q(x_{1:k}/Y_k, u_{k-1})} \\
&= \frac{p(x_k/Y_k, p(x_{1:k-1})u_{k-1})p(x_{1:k-1}/Y_{k-1}, u_{k-1})}{q(x_k/Y_k, x_{1:k-1}u_{k-1})q(x_{1:k-1}/Y_{k-1}, u_{k-1})} \\
&= \frac{p(x_k/Y_k)p(x_{1:k-1})u_{k-1}}{q(x_k/Y_k, x_{1:k-1}u_{k-1})} \quad W_{k-1}
\end{aligned}
\tag{4.9}
$$

It is shown in [Fang and de Callafon, 2011] that

$\frac{p(x_k/Y_k, p(x_{1:k-1})u_{k-1})}{q(x_k/Y_k, x_{1:k-1}u_{k-1})} \propto p(y_k/x_k)$.

Thus we have a recursive relation of the importance weight W_k as follows:

$$W_k \propto p(y_k/x_k)W_{k-1}. \tag{4.10}$$

The recursive property of the SIR filter is used to estimate the target posterior distribution. The implementation steps of the SIR filter are as follows:

Step 1: Random particles $x^i \sim q(x_k/x_{k-1}, Y_{k-1})$ are generated where $i = 1, 2, ...N$, N is the number of particles. Particles are passed through the state equation to predict prior distribution in the next timestep.

Step 2: Importance weights are calculated in this step. The importance weight of a any particle i is calculated as:

$$W_k^i = \frac{p(y_k/x_k^i)p(x_k^i/x_{k-1}^i, u_{k-1})}{q(x_k^i/x_{k-1}^i, u_{k-1}, Y_K)} W_{k-1}^i. \tag{4.11}$$

Step 3: Information of the calculated weight is transferred to the next time sample through resampling using importance weight W_k^i. After resampling, all particles' weights are reset to $1/N$. The resampled particles $x_{k,resamp}^i$ constitute an approximate distribution of the target posterior $p(x_k/Y_k, u_{k-1}^-)$. This conditional pdf will be used to derive the arrival cost function in the M-step. The expected value of the state from the distribution can be calculated directly from the average of the resampled particles as follows:

$$\hat{x}_k = \frac{1}{N} \sum_{i=1}^{N} x_{k,resamp}^i. \tag{4.12}$$

4.2.3.2 Maximization step (M step)

In this step, the cost function is defined from the conditional posterior distribution of states $p(x_k/Y_k, u_{k-1}^-)$ evaluated in the E-step. By augmenting estimated $\hat{x}_k$, the conditional distribution of Y_k, $p(Y_k/\hat{x}_k, u_{k-1})$can be written easily. This augmented posterior is maximized for u_{k-1}.

$$\hat{u}_{k-1}^{+} = \underset{u_{k-1}}{argmax} \quad p(y_k/\hat{x}_k, u_{k-1}) \tag{4.13}$$

A gradient-based optimization approach was used to maximize the distribution. For Gaussian distribution
$p(y_k/\hat{x}_k, u_{k-1}) = \frac{1}{\sqrt{2\pi}R^{0.5}} e^{-\frac{1}{2}(y_k-\hat{y}_k)^T R^{-1}(y_k-\hat{y}_k)}$
leads to the following log likelihood function:

$$\ell(u_{k-1}) = \delta - (y_k - \hat{y}_k)^T R_k^{-1}(y_k - \hat{y}_k) \tag{4.14}$$

where δ is a constant and $\hat{y}_k = g(\hat{x}_k/u_{k-1}, Y_{k-1})$. Input u_{k-1} is estimated by minimizing $\ell(u_{k-1})$. The estimated input $\hat{u}_{k-1}$ is supplied back to the E-step.

The E-step and M-step are performed alternatively several times at each time step to update $\hat{x}_k$ and $\hat{u}_{k-1}$ until the difference between the two iterations is smaller than the specified threshold value, ϵ.

Implementation of the proposed methodology is shown in Figure 4.1.

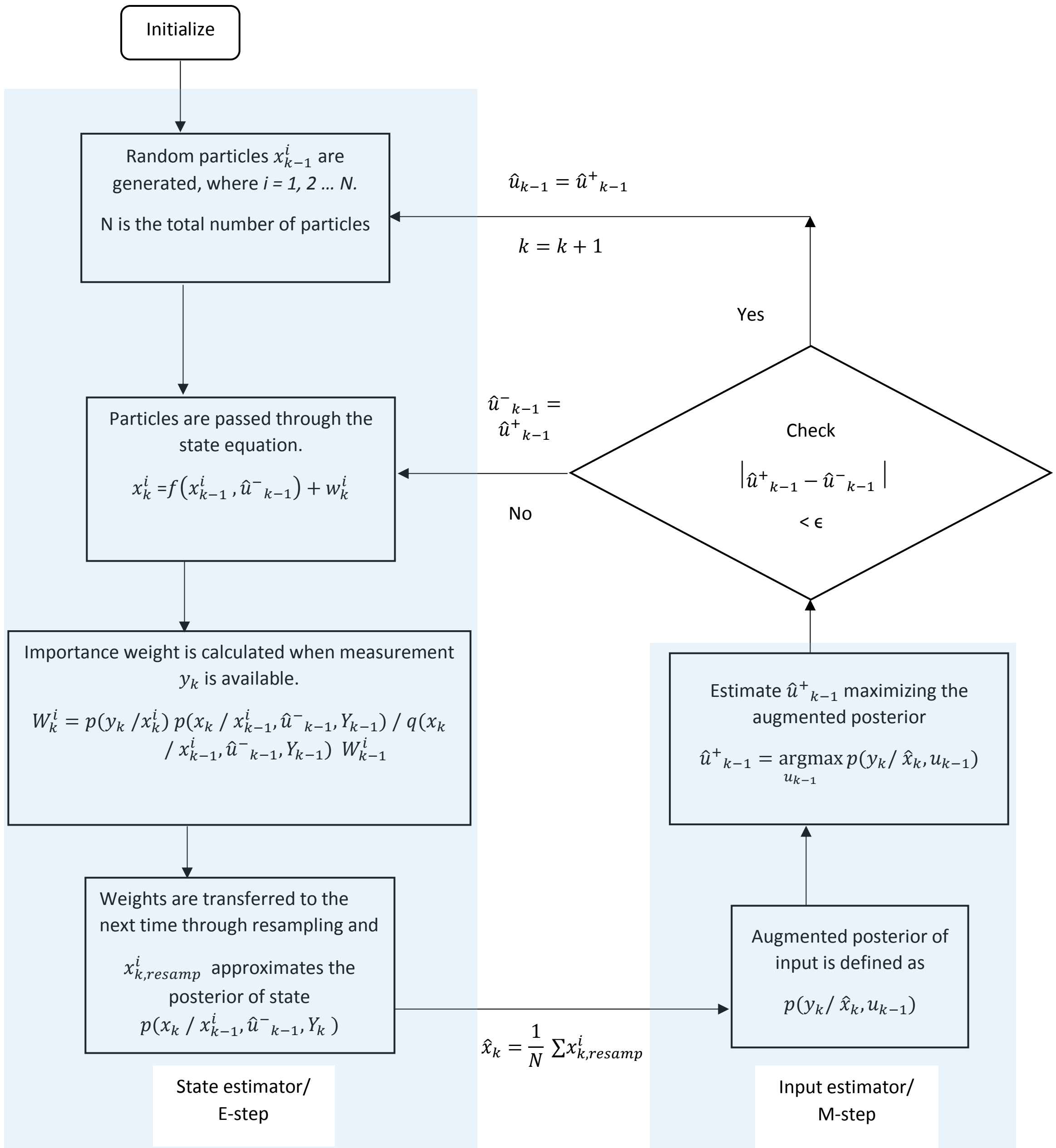

Figure 4.1: Implementation procedure of the proposed methodology.

4.3 Implementation of the proposed method for a simple linear system

In this section, the proposed methodology is implemented on a simple linear system. Let us consider the following linear state space system:

$$x_k = \mathbf{A}x_{k-1} + \mathbf{B}u^{in}_{k-1} + \mathbf{D}u^{d}_{k-1} + w_k, \tag{4.15}$$

$$y_k = \mathbf{C}x_k + \nu_k. \tag{4.16}$$

where, x_k is the state of the system at time k, y_k is the measurement, u^{in}_{k-1} is the known input, and u^{d}_{k-1} is the unknown input to the system. $\mathbf{A}$, $\mathbf{B}$, $\mathbf{C}$, and $\mathbf{D}$ are matrices describing the system dynamics, and w_k and ν_k are the Gaussian process and measurement noise with a zero mean and covariance of Q and R, respectively.

First, the unknown inputs, u^{d-}_{k-1}, and states, x_{k-1}, are initialized. Next, particles are sampled randomly from a proposed distribution $x^i_k \sim q(x_k/x_{k-1}, \hat{u}_{k-1})$. These particles are passed through the state equation to evaluate the estimate of particles after state transition $\hat{x}^i_k$ as follows:

$$\hat{x}^i_k = \mathbf{A}x^i_{k-1} + \mathbf{B}u^{in}_{k-1} + \mathbf{D}u^{d-}_{k-1} \tag{4.17}$$

Next, importance weight of the i-th particle is calculated using the following equation:

$$W^i_k = \frac{exp(-\frac{1}{2}(y_k - \mathbf{C}x^i_k)^T(Q + \mathbf{C}^T R\mathbf{C})(y_k - \mathbf{C}x^i_k))}{\sum_{i=1}^{N} exp(-\frac{1}{2}(y_k - \mathbf{C}x^i_k)^T(Q + \mathbf{C}^T R\mathbf{C})(y_k - \mathbf{C}x^i_k))} W^i_{k-1}, \tag{4.18}$$

where N is the total number of particles, and y_k is the measurement of the system. In the next step, information on the weight is transferred to the particles through resampling. W^i_k is used to get the resampled particles $x^i_{k,resamp}$. After calculating $x^i_{k,resamp}$, all the weights are set to $\frac{1}{N}$ and the estimated state $\hat{x}_k$ is calculated to complete the E-step.

$$\hat{x}_k = \frac{1}{N}\sum_{i=1}^{N} x^i_{k,resamp} \tag{4.19}$$

In the M-step, $\hat{x}_{k-1}$ and u_{k-1} are used to construct the cost function. The log likelihood function is given as follows:

$$\begin{aligned}\ell(u^d_{k-1}) = \delta - &(y_k - \mathbf{C}(\mathbf{A}\hat{x}_{k-1} + \mathbf{B}u^{in}_{k-1} + \mathbf{D}u^d_{k-1}))^T(Q + \mathbf{C}^T R\mathbf{C}) \\ &(y_k - \mathbf{C}(\mathbf{A}\hat{x}_{k-1} + \mathbf{B}u^{in}_{k-1} + \mathbf{D}u^d_{k-1})).\end{aligned} \tag{4.20}$$

Input for the system can be estimated by maximizing the cost function.

$$\hat{u}^{d+}_{k-1} = \underset{u_{k-1}}{argmax} \quad \ell(u^d_{k-1}) \tag{4.21}$$

At each time step k, the E-step and M-step are repeated several times until some convergence criteria are met.

4.4 Case studies

The proposed methodology is demonstrated on two systems. First, a simulated model nonlinear continuous stirred tank reactor (CSTR) system is used with different process and measurement noise scenarios. The second system is a laboratory-scale four-tank plant.

4.4.1 Non-linear CSTR system

A schematic diagram of a CSTR is shown in Figure 5.4. Nonlinear state equations of

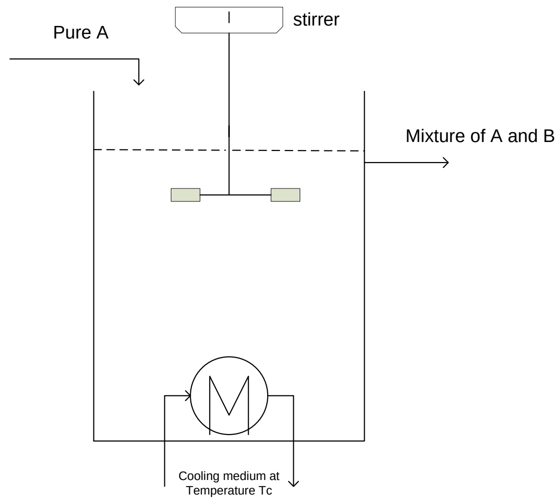

Figure 4.2: Schematic diagram of a CSTR.

the process are given as follows:

$$\frac{dC_A}{dt} = \frac{q}{V}(C_{Ai} - C_A) - k_0 e^{-E_A/T} C_A + w_1 \tag{4.22}$$

$$\frac{dT}{dt} = \frac{q}{V}(T_i - T) - \frac{\Delta H}{\rho C_p} k_0 e^{-E_A/T} C_A - \frac{UA_r}{\rho C_p V}(T - T_c) + w_2, \tag{4.23}$$

where C_A is the concentration of the reactant, T is the temperature in the reactor, q and V are flow-rate and volume of feed, respectively, C_{Ai} and T_i are feed concentration and temperature respectively, $k_0 e^{-E_A/T} C_A$ is the reaction rate, ΔH is the heat of reaction, ρ is the density, C_p is the specific heat, A_r is the area of heat transfer, U is the effective heat coefficient and T_c is the temperature of the cooling fluid. $w = [w_1 \; w_2]^T$ is the unmodeled dynamics of the system modeled as an additive process Gaussian noise with variance $Q_r = diag\ [0.001 \quad 0.001]$. The operating range of process inputs and different parameters of the system were chosen from [Henson and Seborg, 1997]. Nonlinear state equations at the given operating conditions were solved to evaluate the simulated open loop response.

This model was used by [Imtiaz et al., 2006] to estimate C_A and T from a noisy measurement scenario. For the current case study, the estimation objective was different. We considered that the feed temperature, T_i, was unknown, and we sought to estimate T_i along with filtered C_A and T from the noisy process measurement. The measurement equation is:

$$\mathbf{y_k} = 0.5[C_A \quad T]^T + \nu \tag{4.24}$$

where $\mathbf{y_k}$ is the available measurement, and ν is the measurement noise that was varied to study the performance of the estimator at different noise intensities. Simulations were performed for two different noise scenarios.

For the first scenario, we considered measurement noise $\nu \sim N(0, R_r)$ where $R_r = diag\ [0.01 \quad 0.01]$. The proposed estimator filtered the states, concentration (C_A) and temperature (T) of the reactor and estimated input feed temperature (T_i). The SIR filter was tuned using a process noise of a higher order than the actual process noise to ensure that the prior pdf was not too narrow while choosing the process noise. Measurement uncertainty of the SIR filter was chosen as the same order of the actual measurement noise. Considering both computation load and estimation accuracy, the number of particles for the filter is chosen to be 50 for the current case study. Filtered states and estimated input along with their actual values are shown in Figures 4.3 and 4.4. The figures suggest that the proposed method was able to filter the states and estimate the unknown input. However, as noisy estimation was observed while estimating temperature, a filter was used to improve the noisy estimate.

For the second scenario, measurement noise was doubled. Both estimated and actual states and input are shown in Figures 4.5 and 4.6. The performance of estimation deteriorated with additional noise intensity. The increased noise affects input estimation significantly. Thus, filtering the estimated input is required to improve the performance of the estimator.

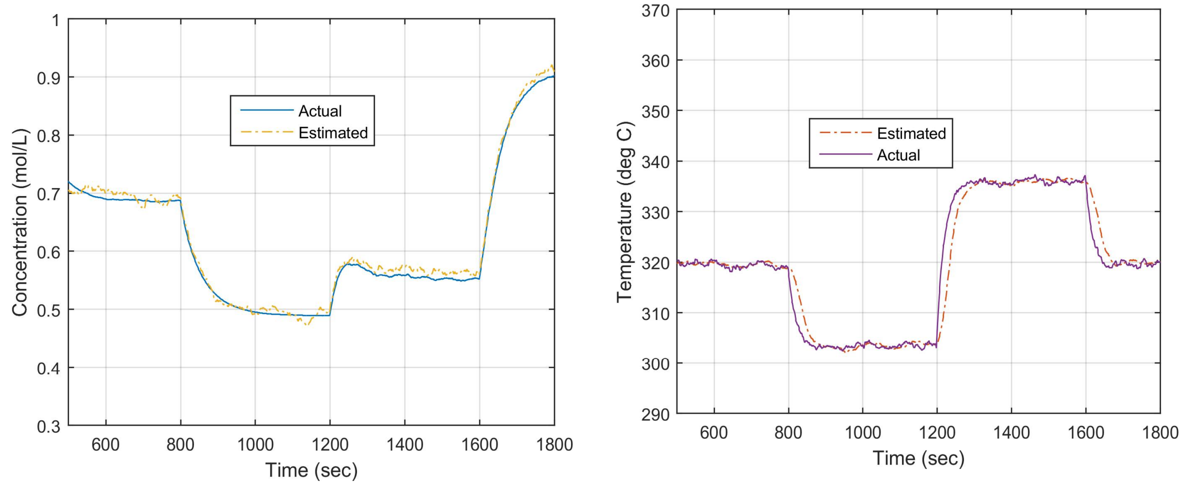

(a) Concentration plot (b) Temperature plot

Figure 4.3: Comparison of actual and estimated states of the CSTR system ($R_r = diag\ [0.01 \quad 0.01]$)

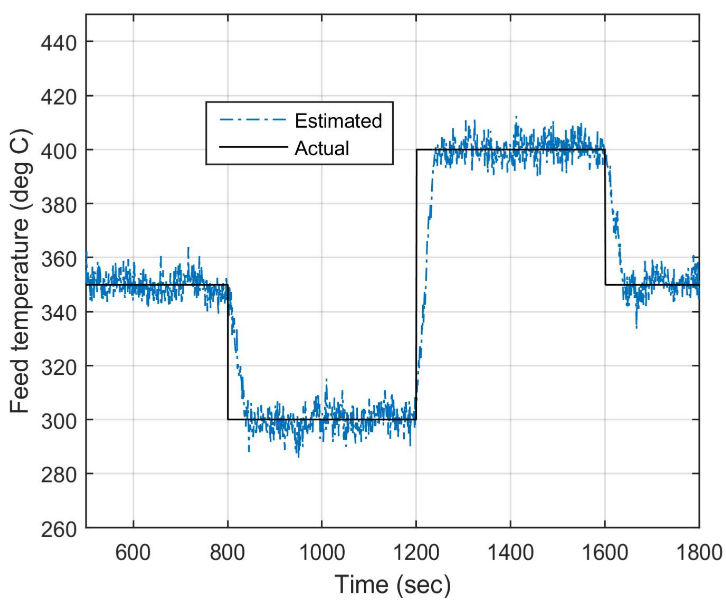

Figure 4.4: Comparison of the unknown input of the CSTR system with the estimated input signal ($R_r = diag\ [0.01 \quad 0.01]$)

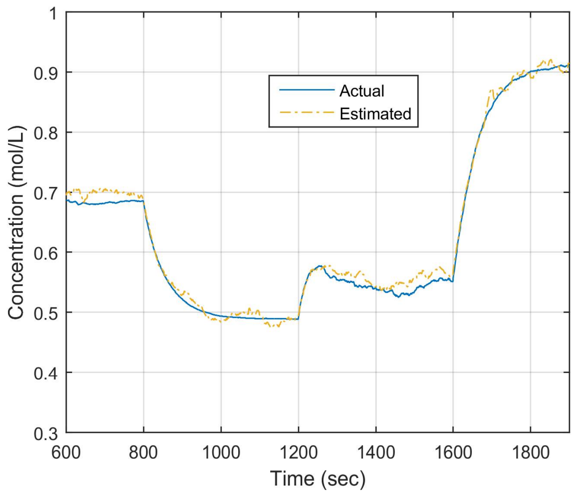

(a) Concentration plot

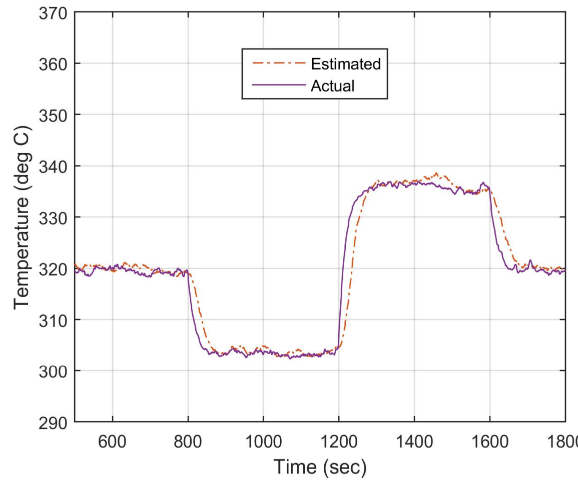

(b) Temperature plot

Figure 4.5: Comparison of actual and estimated states of the CSTR system ($R_r = diag\ [0.04 \quad 0.04]$)

4.4.2 Four tank pilot plant

A schematic diagram of a four-tank system is shown in Figure 4.7. Governing differential equations for this system were described by [Johansson, 2000] as follows:

$$\frac{dh_1}{dt} = -\frac{a_1}{A_1}\sqrt{2gh_1} + \frac{a_3}{A_1}\sqrt{2gh_3} + \frac{\gamma_1 k_1 v_1}{A_1} \tag{4.25}$$

$$\frac{dh_2}{dt} = -\frac{a_2}{A_2}\sqrt{2gh_2} + \frac{a_4}{A_2}\sqrt{2gh_4} + \frac{\gamma_2 k_2 v_2}{A_2} \tag{4.26}$$

$$\frac{dh_3}{dt} = -\frac{a_3}{A_3}\sqrt{2gh_3} + \frac{(1-\gamma_2)k_2 v_2}{A_3} \tag{4.27}$$

$$\frac{dh_4}{dt} = -\frac{a_4}{A_4}\sqrt{2gh_4} + \frac{(1-\gamma_1)k_1 v_1}{A_4}, \tag{4.28}$$

where h_i is the water level, A_i is the cross-section area, a_i is the cross-section area of the flow line coming out of the i-th tank. Applied voltage of the i-th pump is v_i,

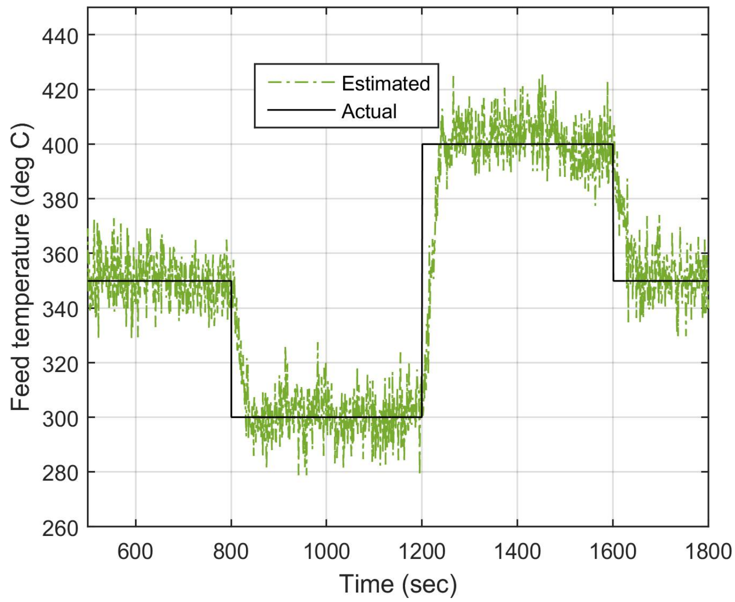

Figure 4.6: Comparison of the unknown input of the CSTR system with the estimated input signal ($R_r = diag\ [0.04 \quad 0.04]$)

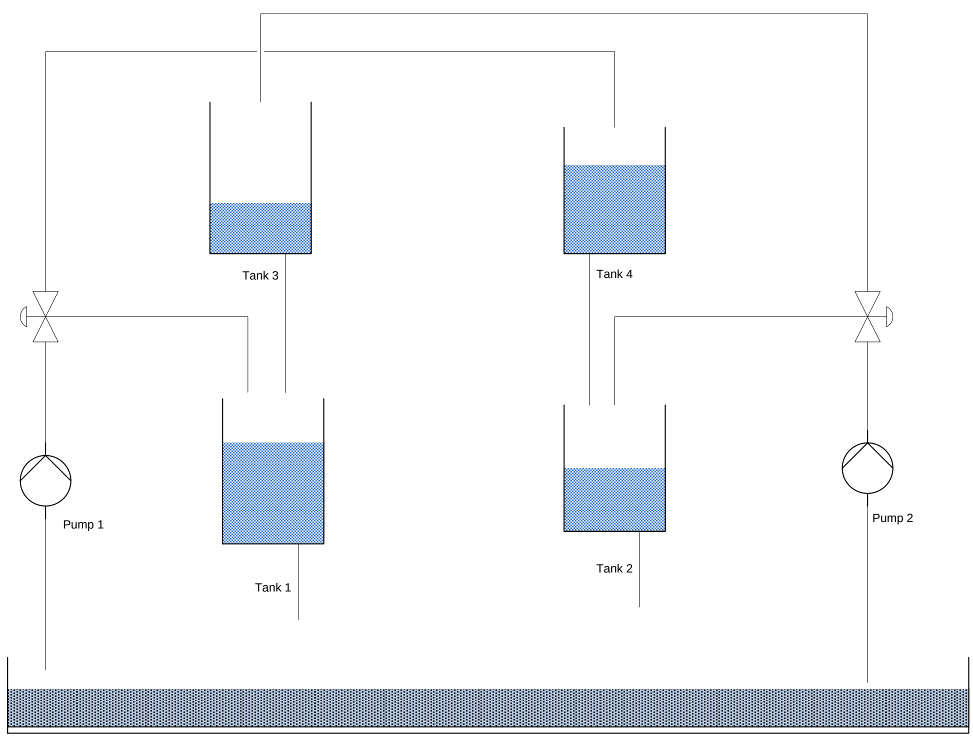

Figure 4.7: Schematic diagram of a Four tank system

Table 4.1: Dimensions of experimental setup

Variable	Unit	Op Pt
A_1, A_2, A_3, A_4	cm^2	392.7
a_1, a_2	cm^2	1.308
a_3, a_4	cm^2	0.829
k_c	$e/V/cm$	0.5
g	cm/s^2	981

$k_i v_i$ is the corresponding flow, and γ_1 and γ_2 are the parameters that determine the valve opening. For the current study, $\gamma_1 k_1 v_1$ and $\gamma_2 k_2 v_2$ are mentioned as u_l and u_r, respectively, and used as the process inputs. Equations 4.25-4.28 are the state transition equations and measurement matrix $\mathbf{C}$ is defined as follows:

$$\mathbf{C} = \begin{bmatrix} 1 & 0 & 0 & 0 \\ 0 & 1 & 0 & 0 \end{bmatrix}.$$

The experiment was performed on the four-tank plant located at the Chemical and Materials Engineering Department of University of Alberta. A mechanistic nonlinear model of the system was developed from the measured dimensions of the tank. The dimensions of the experimental setup are given in Table 5.1. States h_1 and h_2 are measured, and h_3 and h_4 are the unmeasured states. Position of the pumps u_l and u_r are the inputs of the system. Further, we assumed that the position of the right pump, u_r, was known, and the position of the left-side u_l was unknown. The proposed state and unknown input estimator was applied to estimate the hidden states h_3 and h_4, and unknown input u_l. Two sets of validations were performed for the four-tank system. For the first case study, measurements were simulated solving the nonlinear model with added measurement noise. Next, we used the data set collected from the laboratory setup to validate the estimator performance. In order to compare the results, we used the same input signals for the simulated model and the experiments.

4.4.2.1 Simulation study

In the simulated model we added different levels of noise to the system and checked the consistency and robustness of the proposed scheme. Equations 4.25 to 4.28 were solved to generate open loop state responses. Measurements were evaluated adding the measurement noise with the state variables h_1 and h_2. The SIR filter was tuned with 500 particles, and the proposed method was used to estimate the states and unknown inputs. Based on the intensity of the measurement noise, two different scenarios were considered. For the first scenario, a measurement noise $\nu \sim N(0, \sigma^2 \mathbf{I})$ was added where the noise variance $\sigma^2 \mathbf{I} = diag\ [0.1 \quad 0.1]\ cm^2$. In the second scenario, noise intensity was increased to $\sigma^2 \mathbf{I} = diag\ [0.5 \quad 0.5]\ cm^2$. Estimated and filtered states for these two scenarios are shown in Figures 4.8 and 4.9. From the figures, it is evident that even with the increased intensity of noise the proposed method was able to estimate the states fairly well. On the contrary, estimation of input was affected by the increased intensity of the noise. Positions of the left pump were estimated for both scenarios using the proposed algorithm. Estimated inputs for the two scenarios and actual inputs are shown in Figure 4.10. Figure 4.10 shows that noise in the measurement aggravates the estimated input. Though both of the estimated inputs follow the actual inputs, estimation deviated more in the higher noise scenario.

4.4.2.2 Experimental study

An open loop experiment was performed on the laboratory scale four tank system at the Process Dynamics and Control Lab of University of Alberta. Similar to the simulation study, it was assumed that only h_1, h_2, and u_r were available to the estimator. The estimator used available measurements and known input to estimate h_3, h_4, and u_l. As this is a pilot-scale setup, we expect that there is significant plant model mismatch and measurement noise in the system. Through validating the es-

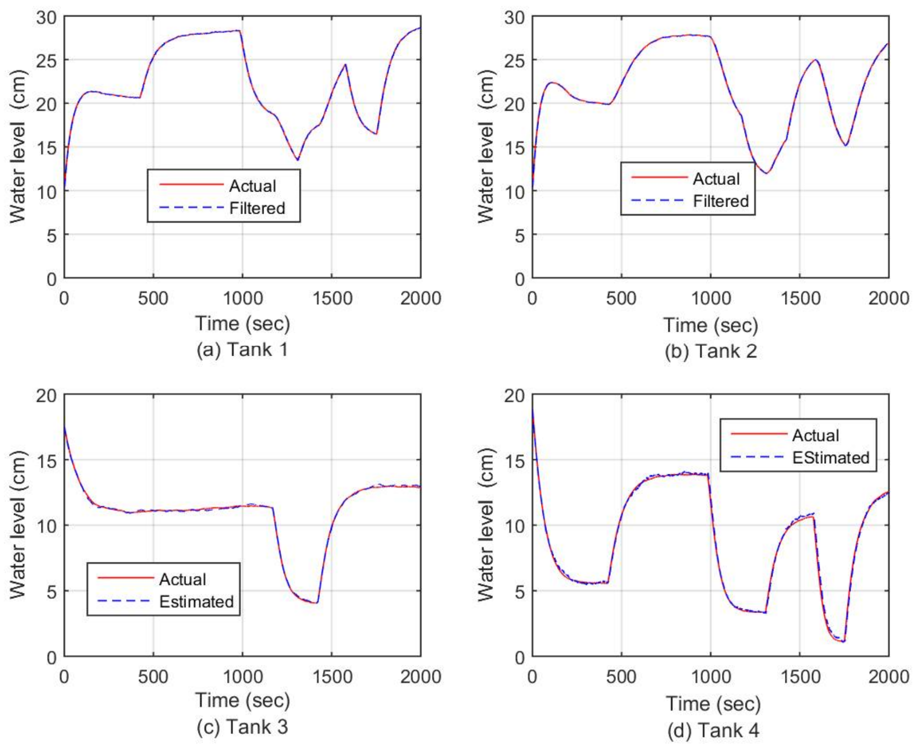

Figure 4.8: Comparison of actual and estimated states of the simulated four tank system (noise variance $\sigma^2\mathbf{I}$=$diag\ [0.1 \quad 0.1]\ cm^2$)

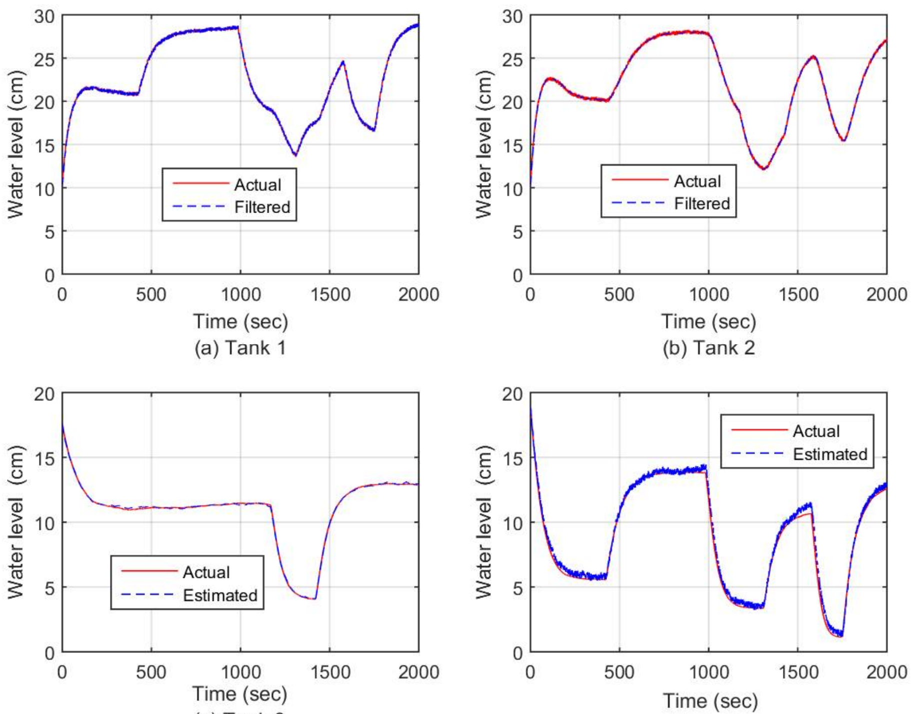

(a) Tank 1 (b) Tank 2 (c) Tank 3 (d) Tank 4

Figure 4.9: Comparison of actual and estimated states of the simulated four-tank system (noise variance $\sigma^2\mathbf{I}$=$diag$ $[0.5 \quad 0.5]$ cm^2)

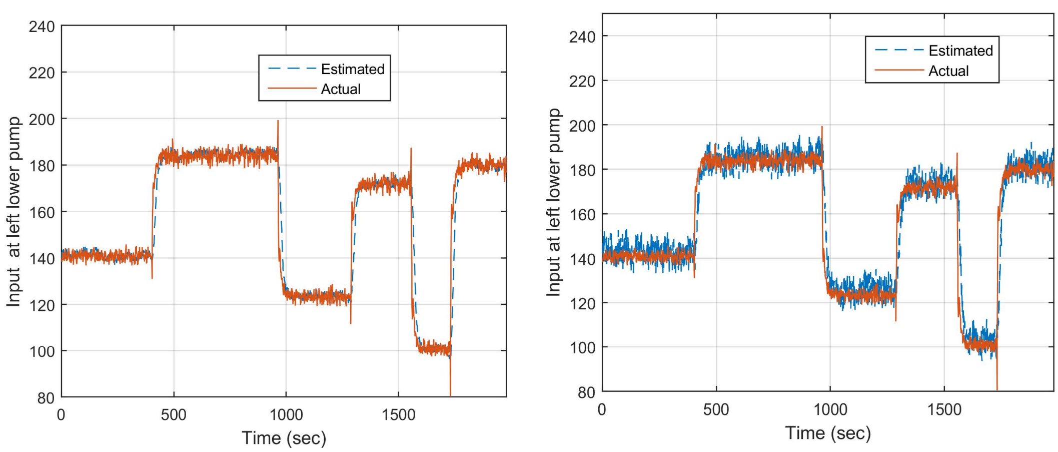

(a) At noise level ($\sigma^2\mathbf{I}$= diag $[0.1 \quad 0.1]$ cm^2) (b) At noise level ($\sigma^2\mathbf{I}$= diag $[0.5 \quad 0.5]$ cm^2)

Figure 4.10: Actual and estimated inputs of simulated four-tank system for different noise scenarios

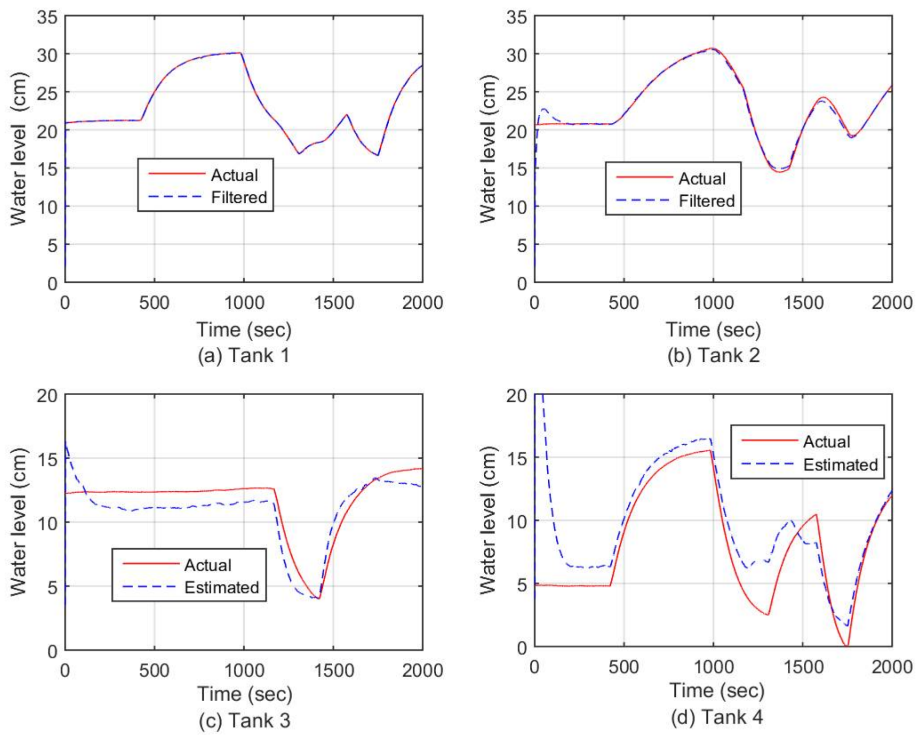

Figure 4.11: Comparison of actual and estimated states of the pilot-scale four-tank system

timator using this system, we want to demonstrate the robustness of the proposed method. The particle filter was tuned with 1000 particles to improve the performance of the estimator.

In the experiment, both the speed of the left and right pumps were varied as step inputs. Figure 4.11 shows the actual and estimated states of the process. Figure 4.12 shows the estimated and actual unknown inputs along with the known input to the process.

The results in Figures 4.11 and 4.12 reveal that the proposed method estimated states and unknown input correctly for most parts of the experiment. However, for some instances, estimated state and input deviated significantly from the experimental data. Deviations of the estimated states from the actual states are mostly due to plant model mismatch and impact of the deviations in the estimated input. Change

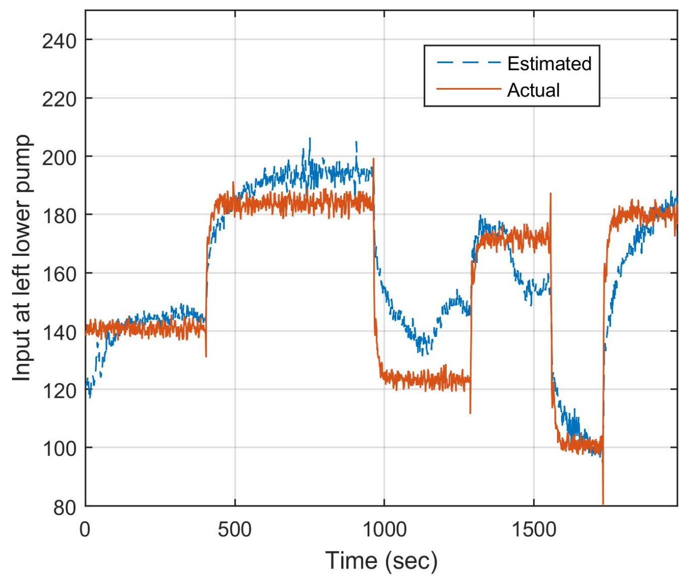

(a) Unknown Inputs

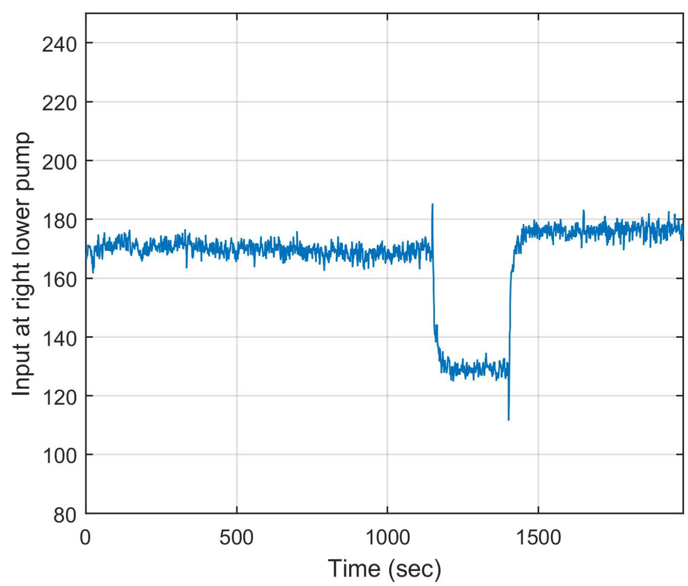

(b) Known input

Figure 4.12: Actual and estimated unknown inputs and known input for experimental study

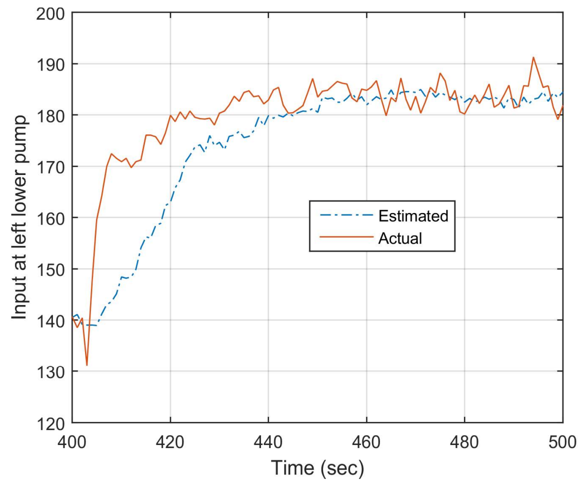

Figure 4.13: Dynamic tracking of the estimated input signal for simulated four tank system

in the speed of the right-side pump interacts dynamically with process states and unknown input. This interaction affects the estimate of the input and increases the error between the estimated state and the actual value.

4.4.2.3 Convergence of the Algorithm

As the proposed EM framework is an iterative approach, we sought to check the convergence of the estimator. Two different time frames, one from the simulation and the other from the experimental study, were considered to show the convergence of the estimated input. We considered the results of the low noise scenario of the simulation study. To study the convergence of this scenario, we considered a time frame from 400s to 460s, where a step change was made on input. Actual left-side pump input and the estimated signals for this time-frame are shown in Figure 4.13. Four time instances in this transition were selected to show the convergence behaviour. The squared percentage errors between the estimation and the actual input were calculated at these time instances and plotted against the iteration number. In Figure 4.14, the squared errors with iteration numbers for the selected time instances are plotted. In

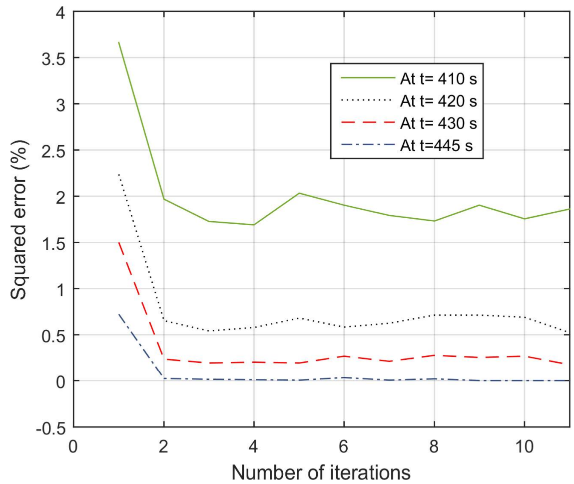

Figure 4.14: Change of error between estimated and actual input signal for simulated four-tank system

all three cases, the error decreased fairly quickly, and estimated the input converged to a steady value and remained stable.

For the experimental case study, we consider a time window from 1720 to 1900s, where a step change in input was made. Estimated input from experimental data along with the actual input are shown in Figure 4.15. We report the convergence profile at four time steps during this period. Percentages of the squared error for these instances are plotted against the iteration number in Figure 4.16. The estimated input converged to a steady value after the second iteration. The convergence shows a smooth profile. The estimation error is higher immediately after step changes were made. However, it quickly goes to a stable state.

4.5 Conclusions

An expectation maximization (EM) based methodology is proposed to estimate the states and unknown inputs of a nonlinear system simultaneously. States and inputs were iteratively corrected in two steps of an EM algorithm. The E-step approximated

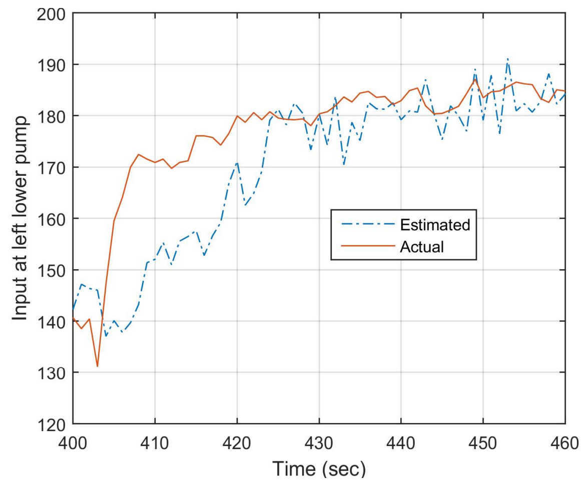

Figure 4.15: Dynamic tracking of the estimated input signal for four-tank system in experimental scenario

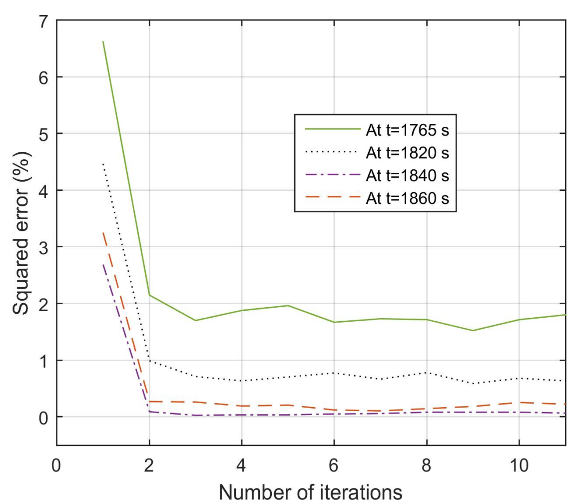

Figure 4.16: Change of error between estimated and actual input signal for simulated four-tank system in experimental scenario

the conditional posterior distribution of the states using a SIR filter. The M-step estimated the unknown input using the maximum likelihood estimation. In this study, we mainly focused on Gaussian distribution; however, the proposed algorithm is applicable to a non-Gaussian posterior, as a particle filter was used for estimating states. Both experimental and simulation studies were performed to demonstrate the efficacy of the proposed methodology. For all case studies, the proposed framework showed good results. Performance of the estimator degraded for the experimental case due to the presence of a plant model mismatch and measurement noise. As the estimator relies more on the measurements if noise in the measurement increases, the estimated input gets jittery. Filtering the estimated input signal can remove some of this jittery behaviour and give a better estimate of the input. Both the state and input estimates were affected by the interaction of the inputs and states.

Acknowledgement

The authors thank the Natural Sciences and Engineering Research Council (NSERC) of Canada for financial support.

Nomenclature

$\mathbf{A}, \mathbf{B}, \mathbf{C}, \mathbf{D}$ System matrices for the linear state space system

ΔH Reaction heat

Δu_k^d Step change in disturbance at time k ($unit$)

Δy_i^{ss} Change in steady state controller made to the i-th variable ($unit$)

ϵ Threshold value for two iterations

γ_i Valve opening of i-th pump

$\hat{u}_{k-1}^{+}$ Estimated input after M-step

$\hat{u}_k^d$ Estimated disturbance ($unit$)

$\hat{u}_{k-1}$ Estimated input at time step $k-1$

$\hat{x}_k$ Estimated state at time step k

$\hat{x}_k$ Estimated state ($unit$)

$\hat{y}_k$ Estimation of process variables from estimated state $\hat{x}_k$ at time step k

ν_k Measurement noise at time-step k

ρ Density of the reactant

$\sigma^2\mathbf{I}$ Variance of measurement noise of four tank system

σ_T^2 Noise variance of temperature ($^\circ$ C^2)

$\mathbf{A}$,$\mathbf{B}$ $\mathbf{C}$ and $\mathbf{E}$ Matrices of state space system

$\mathbf{F}$, $\mathbf{T}$, $\mathbf{K}_1$, $\mathbf{K}_2$, $\mathbf{H}$ Design matrices for UIO

A_i Cross section area of i-th tank of Four tank system

a_i Cross section are of the flow line coming out of ith tank of Four tank system

A_r Area of heat transfer

b_k Bias error ($unit$)

C_A Concentration of the reactant

C_p Specific heat of the reactant

C_{Ai} Feed concentration

e_k Estimation error ($unit$)

$E_{N,k}$ Error due to noise ($unit$)

G_i Gain of 'i-th' output

$G_{ij}(0)$ Step response at steady state

h_i Water level of ith tank of Four tank system

$k_0 e^{-E_A/T} C_A$ Reaction rate

$k_i v_i$ Flow of of i-th pump

m Number of total inputs

M_k,K_k Design matrices for Kalman based observer

N Total number of particles

n Number of states

P Monitoring horizon

p Number of measurements

Q Variance of process noise w_k

$q(x_k/x_{k-1}, Y_{k-1})$ Proposal distribution

Q_r Variance of process model mismatch of CSTR

q_r Flow rate of feed at CSTR

R Variance of measurement noise ν_k

R_r Variance of measurement noise of CSTR

T Temperature in the reactor

T_c Temperature of the cooling fluid

T_i Feed temperature

U Effective heat co-efficient

u_k^d Disturbance to the system ($unit$)

u_{k-1}^{d+} Estimated disturbance after M-step

u_{k-1}^{d-} Initial value of unknown disturbance at time step k

u_k^d Unknown input at time-step k

u_k^{in} Known input at time-step k

u_1 Cold water valve position (%)

u_2 Steam valve position (%)

u_3 Hot water valve position (%)

u_k Process inputs (*unit*)

u_l Left pump input of Four tank system

u_r Right pump input of Four tank system

V Volume of the feed at CSTR

v_i Applied voltage of i-th pump

v_k Measurement noise (*unit*)

w Unmodelled dynamics of CSTR

w_k Process noise (*unit*)

W_k Importance weight at time step k

w_k Process noise at time-step k

W_k^i Importance weight of i-th particle at time step k

x_k^i Random particle at time step k

$x_{k,resamp}^i$ Resampled particles

x_1 Tank volume

x_2 Output of valve transfer function

x_3 Enthalpy of tank

x_k Unknown state of the system (*unit*)

x_k Unknown states at time-step k

y_1 Level measurement (cm)

y_2 Flow measurement (m^3/s)

y_3 Temperature measurement ($°C$)

y_i^{ss} the steady state of the 'i-th' output variable (*unit*)

y_k Process measurement (*unit*)

y_k Process measurement at time-step k

$y_{i,high}$ Maximum safety limit of 'i'th output (*unit*)

$y_{i,k}$ Measurement of i-th' output at time k

$y_{i,low}$ Minimum safety limit of 'i'th output (*unit*)

z_k State of UIO (*unit*)

$u_{j,high}$ Minimum position of actuator (*unit*)

$u_{j,low}$ Maximum position of actuator (*unit*)

y_k^* predicted value of the variable y for at time sample *k-1* (*unit*)

Bibliography

[Andrieu and Doucet, 2003] Andrieu, C. and Doucet, A. (2003). Online expectation-maximization type algorithms for parameter estimation in general state space models. In *Acoustics, Speech, and Signal Processing, 2003. Proceedings.(ICASSP'03). 2003 IEEE International Conference on*, volume 6, pages VI–69. IEEE.

[Chen, 2003] Chen, Z. (2003). Bayesian filtering: From kalman filters to particle filters, and beyond. *Statistics*, 182(1):1–69.

[Corless and Tu, 1998] Corless, M. and Tu, J. (1998). State and input estimation for a class of uncertain systems. *Automatica*, 34(6):757.

[Dempster et al., 1977] Dempster, A. P., Laird, N. M., and Rubin, D. B. (1977). Maximum likelihood from incomplete data via the em algorithm. *Journal of the royal statistical society. Series B (methodological)*, pages 1–38.

[Dochain, 2003] Dochain, D. (2003). State and parameter estimation in chemical and biochemical processes: a tutorial. *Journal of process control*, 13(8):801–818.

[Fang and de Callafon, 2011] Fang, H. and de Callafon, R. A. (2011). Nonlinear simultaneous input and state estimation with application to flow field estimation. In *2011 50th IEEE Conference on Decision and Control and European Control Conference*, pages 6013–6018. IEEE.

[Fang and de Callafon, 2015] Fang, H. and de Callafon, R. A. (2015). Simultaneous input and state filtering: An ensemble approach. In *2015 54th IEEE Conference on Decision and Control (CDC)*, pages 437–442. IEEE.

[Fang et al., 2013] Fang, H., De Callafon, R. A., and Cortés, J. (2013). Simultaneous input and state estimation for nonlinear systems with applications to flow field estimation. *Automatica*, 49(9):2805–2812.

[Floquet et al., 2004] Floquet, T., Barbot, J.-P., Perruquetti, W., and Djemai, M. (2004). On the robust fault detection via a sliding mode disturbance observer. *International Journal of control*, 77(7):622–629.

[Friedland, 1969] Friedland, B. (1969). Treatment of bias in recursive filtering. *Automatic Control, IEEE Transactions on*, 14(4):359.

[Gillijns and De Moor, 2007] Gillijns, S. and De Moor, B. (2007). Unbiased minimum-variance input and state estimation for linear discrete-time systems. *Automatica*, 43(1):111–116.

[Gopaluni, 2008] Gopaluni, R. (2008). A particle filter approach to identification of nonlinear processes under missing observations. *The Canadian Journal of Chemical Engineering*, 86(6):1081–1092.

[Güntürkün et al., 2014] Güntürkün, U., Reilly, J. P., Kirubarajan, T., et al. (2014). Recursive hidden input estimation in nonlinear dynamic systems with varying amounts of a priori knowledge. *Signal Processing*, 99:171–184.

[Henson and Seborg, 1997] Henson, M. A. and Seborg, D. E. (1997). *Nonlinear process control*. Prentice Hall PTR Upper Saddle River, New Jersey.

[Hsieh, 2000] Hsieh, C.-S. (2000). Robust two-stage kalman filters for systems with unknown inputs. *IEEE Transactions on Automatic Control*, 45(12):2374–2378.

[Imsland et al., 2007] Imsland, L., Johansen, T. A., Grip, H. F., and Fossen, T. I. (2007). On non-linear unknown input observers–applied to lateral vehicle velocity estimation on banked roads. *International Journal of Control*, 80(11):1741–1750.

[Imtiaz et al., 2006] Imtiaz, S. A., Roy, K., Huang, B., Shah, S. L., and Jampana, P. (2006). Estimation of states of nonlinear systems using a particle filter. In *Industrial Technology, 2006. ICIT 2006. IEEE International Conference on*, pages 2432–2437. IEEE.

[Jampana et al., 2010] Jampana, P., Shah, S. L., and Kadali, R. (2010). Computer vision based interface level control in separation cells. *Control Engineering Practice*, 18(4):349–357.

[Johansson, 2000] Johansson, K. H. (2000). The quadruple-tank process: A multivariable laboratory process with an adjustable zero. *IEEE Transactions on control systems technology*, 8(3):456–465.

[Julier and Uhlmann, 2004] Julier, S. J. and Uhlmann, J. K. (2004). Unscented filtering and nonlinear estimation. *Proceedings of the IEEE*, 92(3):401–422.

[Kalman, 1960] Kalman, R. E. (1960). A new approach to linear filtering and prediction problems. *Journal of basic Engineering*, 82(1):35–45.

[Kandepu et al., 2008] Kandepu, R., Foss, B., and Imsland, L. (2008). Applying the unscented kalman filter for nonlinear state estimation. *Journal of Process Control*, 18(7):753–768.

[Kitanidis, 1987] Kitanidis, P. K. (1987). Unbiased minimum-variance linear state estimation. *Automatica*, 23(6):775–778.

[Korbicz et al., 2007] Korbicz, J., Witczak, M., and Puig, V. (2007). Lmi-based strategies for designing observers and unknown input observers for non-linear discrete-time systems. *Technical Sciences*, 55(1).

[Lee and Park, 2012] Lee, K.-S. and Park, T.-G. (2012). New results on fault reconstruction using a finite-time converging unknown input observer. *Control Theory & Applications, IET*, 6(9):1258.

[Luenberger, 1971] Luenberger, D. (1971). An introduction to observers. *IEEE Transactions on automatic control*, 16(6):596–602.

[Mattavelli et al., 2005] Mattavelli, P., Spiazzi, G., and Tenti, P. (2005). Predictive digital control of power factor preregulators with input voltage estimation using disturbance observers. *Power Electronics, IEEE Transactions on*, 20(1):140.

[Mejri et al., 2013] Mejri, S., Tlili, A. S., and Braiek, N. B. (2013). Particle filter for state and unknown input estimation of chaotic systems. *Proceedings Engineering & Technology-Vol*, 4:67–72.

[Mohd Ali et al., 2015] Mohd Ali, J., Ha Hoang, N., Hussain, M. A., and Dochain, D. (2015). Review and classification of recent observers applied in chemical process systems. *Computers and Chemical Engineering*, 76:27–41.

[Patwardhan et al., 2012] Patwardhan, S. C., Narasimhan, S., Jagadeesan, P., Gopaluni, B., and Shah, S. L. (2012). Nonlinear bayesian state estimation: A review of recent developments. *Control Engineering Practice*, 20(10):933–953.

[Qu and Hahn, 2009] Qu, C. C. and Hahn, J. (2009). Computation of arrival cost for moving horizon estimation via unscented kalman filtering. *Journal of Process Control*, 19(2):358–363.

[Radke and Gao, 2006] Radke, A. and Gao, Z. (2006). A survey of state and disturbance observers for practitioners. In *American Control Conference, 2006*, pages 6–pp. IEEE.

[Rawlings and Bakshi, 2006] Rawlings, J. B. and Bakshi, B. R. (2006). Particle filtering and moving horizon estimation. *Computers & chemical engineering*, 30(10-12):1529–1541.

[Söderström, 2012] Söderström, T. (2012). *Discrete-time stochastic systems: estimation and control*. Springer Science & Business Media.

[Spurgeon, 2008] Spurgeon, S. K. (2008). Sliding mode observers: a survey. *International Journal of Systems Science*, 39(8):751–764.

[Sundaram and Hadjicostis, 2008] Sundaram, S. and Hadjicostis, C. N. (2008). Partial state observers for linear systems with unknown inputs. *Automatica*, 44(12):3126.

[Tanner and Wong, 1987] Tanner, M. A. and Wong, W. H. (1987). The calculation of posterior distributions by data augmentation. *Journal of the American statistical Association*, 82(398):528–540.

[Vries et al., 2010] Vries, D., Keesman, K. J., and Zwart, H. (2010). Luenberger boundary observer synthesis for sturm–liouville systems. *International journal of control*, 83(7):1504–1514.

[Wang et al., 2016] Wang, X., Liang, Y., Pan, Q., and Wang, Y. (2016). Measurement random latency probability identification. *IEEE Transactions on Automatic Control*, 61(12):4210–4216.

[Wang et al., 2014] Wang, X., Liang, Y., Pan, Q., Zhao, C., and Yang, F. (2014). Design and implementation of gaussian filter for nonlinear system with randomly delayed measurements and correlated noises. *Applied Mathematics and Computation*, 232:1011–1024.

[Wang et al., 2017] Wang, X., Song, B., Liang, Y., and Pan, Q. (2017). Em-based adaptive divided difference filter for nonlinear system with multiplicative parameter. *International Journal of Robust and Nonlinear Control*, 27(13):2167–2197.

[Wei and Tanner, 1990] Wei, G. C. and Tanner, M. A. (1990). A monte carlo implementation of the em algorithm and the poor man's data augmentation algorithms. *Journal of the American statistical Association*, 85(411):699–704.

[Xiong and Saif, 2003] Xiong, Y. and Saif, M. (2003). Unknown disturbance inputs estimation based on a state functional observer design. *Automatica*, 39(8):1389–1398.

[Zarei and Poshtan, 2010] Zarei, J. and Poshtan, J. (2010). Design of nonlinear unknown input observer for process fault detection. *Industrial & Engineering Chemistry Research*, 49(22):11443–11452.

[Zhao et al., 2013] Zhao, Z., Huang, B., and Liu, F. (2013). Parameter estimation in batch process using em algorithm with particle filter. *Computers & Chemical Engineering*, 57:159–172.

[Zia et al., 2008] Zia, A., Kirubarajan, T., Reilly, J. P., Yee, D., Punithakumar, K., and Shirani, S. (2008). An em algorithm for nonlinear state estimation with model uncertainties. *IEEE Transactions on Signal Processing*, 56(3):921–936.

Chapter 5

Predictive Warning System for Nonlinear Process

Abstract: A robust warning generation method for non-linear systems is presented for forecasting abnormal situation in process systems. In contrast to traditional method, the proposed method issues warning based on the predicted signal. A process is considered in normal state when a feasible solution can be found that satisfies all input and output constraints. A constraint separation optimization algorithm was used to check the existence of feasible solution under various disturbance effects. An open loop dynamic model, process states and inputs at a given instance are used to predict the future states of the process over a prediction horizon. Predicted states and safety limits were used to define output constraints, while actuator capacity and process inputs defined input constraints. All the output and input constraints need to be satisfied for a safe operation. The proposed method was demonstrated using a continuous stirred tank reactor (CSTR) with different disturbance scenarios. The results show that the proposed method is able to detect a violation of a safety limit significantly earlier compared to the methods base on monitoring the measured signals.

5.1 Introduction

A well designed warning system is critical in chemical processes for safe operation. The motivation of the present work is to design a warning system that is capable of providing a lead time for the operator to take necessary corrective actions, when a process system is impacted by disturbances. In an earlier study [Khan et al., 2014], we focused on designing a predictive warning system for a linear process system. The scope of work for that study was limited to steady state and time-delay region of the system. In practical cases, most of the processes exhibit non-linear behaviour. Also the entire dynamic region of the system is of interest. In this work, we propose a systematic methodology to generate predictive warnings for a nonlinear system for the entire dynamic region of the process system.

When a disturbance enters into a process, process states deviate from the normal operating point. The control system counteracts this phenomenon and tries to bring the process back to the original set point. If a controller had infinite capacity to manipulate the actuators, it could always bring the process back to safety. However, in practical cases, an actuator operates within a certain range and hence a controller's action is limited by the actuator's capacity. Depending on the magnitude of the disturbance, a controller may or may not be able to bring the process back to the safe operating point. If the effect of disturbance is large, process states may cross safety limits. For some cases, controllers will not be able to bring the process inside safety limits. We seek a predictive scheme to identify these cases and issue an alert to the operator before the measured variable actually crosses the safety limit.

In the present study, a warning system is combined with controller design. The basic philosophy of the work is to use the predictive feature of advanced control technology to generate a warning for a non-linear system.

[Primbs et al., 1999] discussed two well known approaches for nonlinear optimum control: control Lyapunov function and receding horizon control. They concluded that each approach has its own strength based on the on-line or off-line calculation required. They also suggested an approach to combine both approaches to harness the maximum benefit. [Albalawi et al., 2017] presented a good review of the current research direction that combines control system design with safety considerations. [Varga et al., 2009] used predictive alarm management to generate warnings. They used a simulator-based approach to detect the last controllable point of the system in a particular trajectory. Lyapunov's indirect stability analysis of the state variables are used to detect the boundary of the controllable region of the process. Alarm is generated when states lie outside the controllable region. A Lyapunov based model predictive controller (LMPC) was used by [Zarei and Poshtan, 2010] to propose different safety schemes. All the proposed schemes varied the upper bound of the Lyapunov function to achieve the improved rate that drives the closed loop state to a safe operating region. An MPC with an adaptive learning rate was proposed by [Aswani et al., 2013]. The proposed scheme decoupled the safety and control performances in their framework. The Lyapunov approach is more suitable for off-line calculation, as suggested by [Primbs et al., 1999]. Our current goal is to generate warnings in real-time as such on-line calculation is necessary. A receding horizon or moving horizon estimate is an attractive choice to predict future outputs and generate a warning in real-time based on the predictive signal. [Ahooyi et al., 2016] proposed a model predictive safety (MPS) scheme that uses moving horizon estimates to generate a predictive warning. They generated warnings based on the controller's capacity to negate an extreme value of a predicted state. In practice, process variables are interconnected and hence, counteracting one extreme state using one manipulated variable may cause other variables to exceed the safety limit. The present study is motivated to improve this scheme for the multiple input multiple output interactive system. Moreover, we seek to use all predicted states over the moving horizon to define safety constraints instead of considering only one extreme point.

Safe operation of a process is determined by the existence of a feasible solution of all states within the safety constraints. In [Khan et al., 2014], a linear programming was used to check to determine if the controller is able to satisfy all linear constraints of the system. Determining a feasible solution for a nonlinear system is a difficult problem. [Chinneck, 2007] described different methodologies to check feasibility. Most of the algorithms work very well for identification of a feasible region of linear system. Feasibility of a nonlinear system is still an open problem. A sampling based approach is described by [Banerjee and Ierapetritou, 2005] to identify a feasible solution. Their proposed method is computationally inefficient for on-line calculations as a computationally expensive genetic algorithm was used to determine the feasible solution. The computational load of the genetic algorithm slows down the warning generation process.

[Schnabel, 1982] proposed a constraint separation method to determine the feasible solution of multiple non-linear and linear constraints. They separated the non-linear constraints from the linear constraints. Non-linear constraints were combined to formulate an objective function. Existence of a positive minimum of the objective function suggests an infeasible solution. Application of the method is shown for static non-linear constraints. We used this method to check the feasibility of dynamic non-linear constraints.

The rest of the article is organised as follows: in Section 2, the proposed methodology is presented and different modules of the methodology are described. In Section 3, the proposed method is demonstrated on a nonlinear continuous stirred tank reactor (CSTR) and finally Section 4 gives some concluding remarks.

5.2 Predictive warning system

5.2.1 Theory

Consider a dynamic model of a nonlinear system of the following form:

$$\begin{aligned} x_{k+1} &= f(x_k, u_k, d_k), \\ y_k &= g(x_k), \end{aligned} \tag{5.1}$$

where $x \in \mathbf{R}^{n_x}$ is the unknown states, $y \in \mathbf{R}^{n_y}$ is the process measurements, $u \in \mathbf{R}^{n_u}$ is the manipulated variables, and $d \in \mathbf{R}^{n_d}$ is disturbances to the system. When a disturbance is introduced to the system, it affects the system outputs. If the system is an open loop, large disturbances will drive the system states outside the normal operating limits. Under closed loop control, one of two possible scenarios may occur, based on the system dynamics. The first possible scenario is that process measurements start to rise and may exceed the upper/lower safety threshold, despite control actions. In the second scenario, the controller regulates the manipulated variables and nullifies the disturbance effect, and is capable of keeping all system states within the threshold limits. These two scenarios are shown in Figure 5.1.

For the system, l step ahead prediction of a measured output is $\hat{y}_{k+l}$ and effect of the control action is $\Delta y_{k+l,c}$; upper and lower thresholds of measured variable y are y_h and y_l respectively. Necessary safety conditions for the output constraints are as follows:

$$y_l \leq \hat{y}_{k+l} + \Delta y_{k+l,c} \leq y_h \tag{5.2}$$

where l=$1, 2, ..., L$, and L is large enough to capture the system dynamic response up to the steady state. Output constraints will always be satisfied if Δu_{k+L} is unbounded. For all practical applications the actuator's capacity is limited and is defined

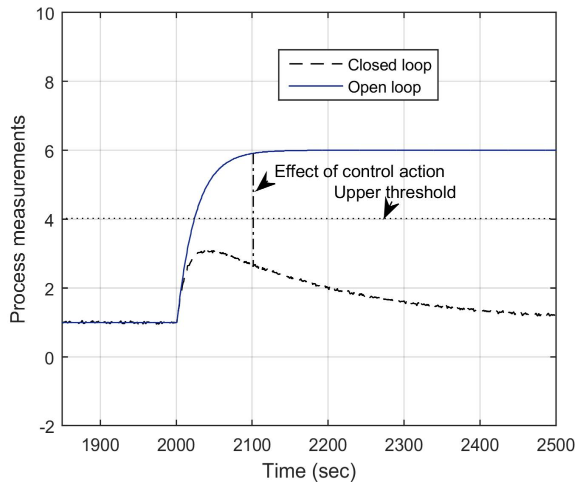

Figure 5.1: Possible abnormal scenarios when disturbance affect the process measurement

as input constraints as follows:

$$u_l \leq u_k + \Delta u_{k+l} \leq u_h, \tag{5.3}$$

where u_l and u_h are the lower and upper limits of the actuator. Based on these conditions, we provide the following definitions for predictive warning in a generalized system.

Definition 1: Consider a system with n_y outputs and n_u manipulated variables. In the normal state (i.e, 'no warning state') the system must satisfy the following feasibility conditions. For a bounded disturbance $\|d_k\| < \infty$, at any time step k,

$$\begin{aligned} y_{i,l} \leq \hat{y}_{i,k+l} + \Delta y_{i,k+l} \leq y_{i,h}, \\ u_{j,l} \leq u_{j,k} + \Delta u_{j,k+l} \leq u_{j,h}. \end{aligned} \tag{5.4}$$

subject to

$$\begin{aligned} x_{k+1} &= f(x_k, u_k, d_k), \\ y_k &= g(x_k), \end{aligned} \tag{5.5}$$

where $i = 1, 2, \ldots, n_y$, and $j = 1, 2, \ldots, n_u$; $l = 1, 2, \ldots, N$ and N is sufficiently large that at $k + N$ time step the system reaches a new steady state.

5.2.2 Implementation of predictive warning system

The proposed model based warning scheme works in two steps. In the first step, an open loop predictor predicts the dynamic response of the system. If the predicted response shows a violation of the safety limits and identifies a potential abnormal event, the system is further investigated in the next step. In the second step, a feasibility check is performed to determine if all safety constraints can be satisfied simultaneously. Safety constraints are defined based on the system safety limits and controllers' capacity.

A flow chart of the proposed warning generation protocol is shown in Figure 5.2. When a disturbance enters the system, it affects the states and is reflected by the change in measurements. Impact of the disturbance on the future time steps is predicted using a moving horizon estimator (MHE). The MHE uses the system model, disturbance model and current measurements and the disturbance input. If predicted states over the 'monitoring horizon' do not exceed the safety limit, a 'no warning' status is set and the monitoring system progresses to the next time step.

If one or more predicted states exceed the safety limits, the warning system checks whether the controllers have enough capacity to mitigate the effect. Inequality constraints are formulated for all predicted states. A feasibility analysis is performed to

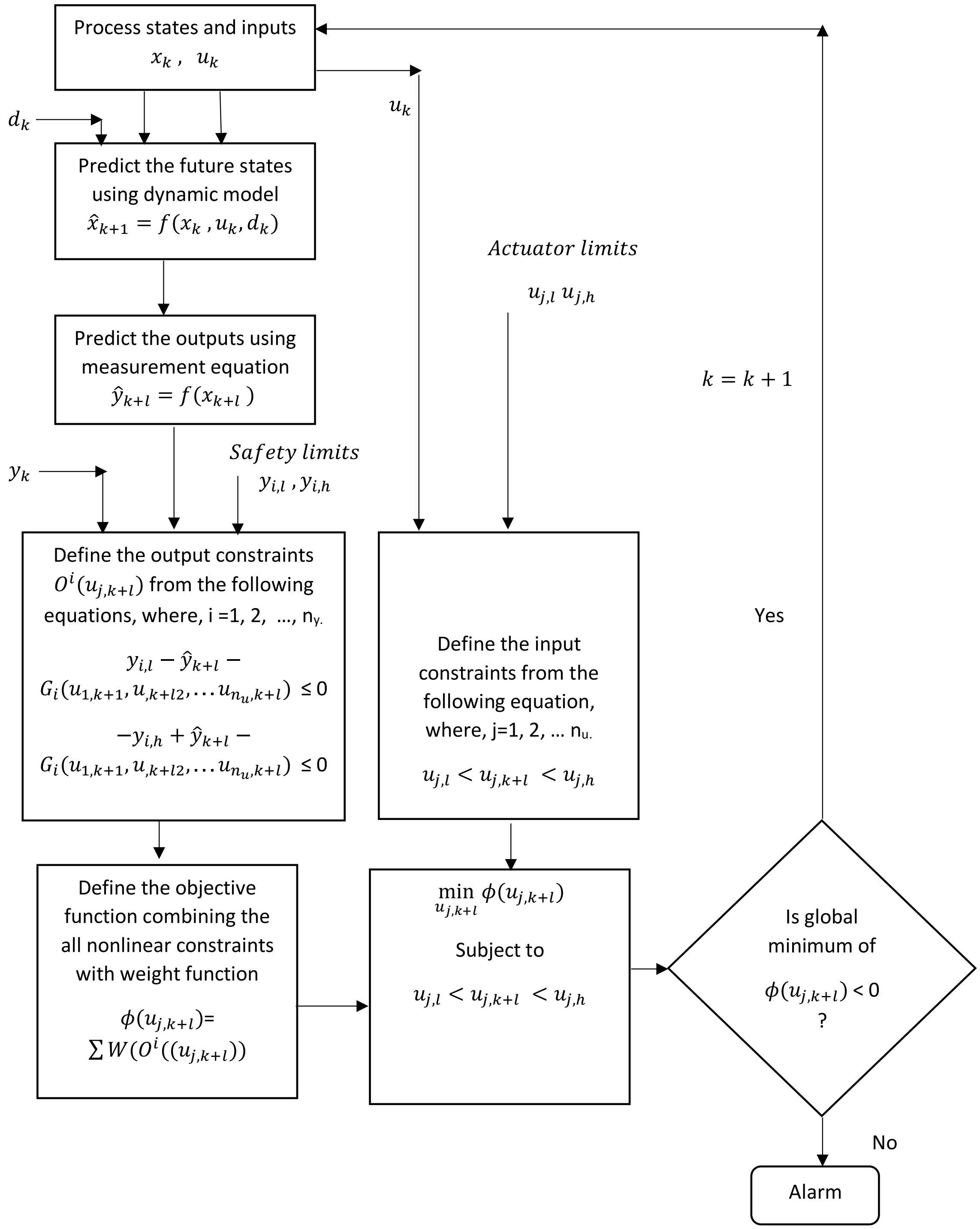

Figure 5.2: Implementation steps of proposed alarm system

determine whether they can be satisfied simultaneously. This analysis is performed using a constraint separation optimization method, which formulates an objective function using the non-linear constraints and keeps the linear inequalities as constraints. Global minimum of the objective function is determined subject to all the linear constraints. A non-negative global minimum of the objective function implies that there is no feasible solution that satisfies all the inequality constraints. Thus a 'warning' is issued to the operator, when a non-negative minimum is determined for the objective function. In the following sections, descriptions of the different modules of the predictive warning system are presented in detail.

5.2.3 Open loop prediction to check a safety condition

Consider the non-linear system in Equation 5.1. One-step ahead prediction of states can be found as:

$$\mathbf{x_{k+1}} = f(\mathbf{x_k}, \mathbf{u_k}, \mathbf{d_k}), \tag{5.6}$$

where, $\mathbf{x_k}$ $\mathbf{u_k}$ and $\mathbf{d_k}$ are the state variables, manipulated variables and disturbances respectively. We assume that the process is at a steady state before disturbance affects the system.

Assume that a disturbance entered the system at time step k. The disturbance will cause the system states to change. If there is no controller in the system, the one step ahead 'open-loop response' of the system can be predicted using the system model as follows:

$$\hat{x}_{r,k+1} = f(x_{r,k}, u_{k,1}, u_{k,2}, ..., u_{k,n_u}, d_{k,1}, d_{k,2}, ..., d_{k,n_p}) \tag{5.7}$$

where r=$1, 2, ..., n_x$. This equation can be used successively to evaluate l-step ahead prediction of states as follows:

$$\hat{x}_{r,k+l} = f(x_{r,k+l-1}, u_{k,1}, u_{k,2}, ..., u_{k,n_u}, d_{k,1}, d_{k,2}, ..., d_{k,n_p}) \tag{5.8}$$

where $l = 2, 3, ...L$ and L is the length of the 'monitoring horizon'. From Equations 5.7 and 5.8 we have prediction profiles for each variable. Future outputs can be evaluated from the predicted states as follows:

$$\mathbf{y_{k+l}} = g(\mathbf{x_{k+l}}), \tag{5.9}$$

where non-linear mapping $g : R^{n_x} \rightarrow R^{n_y}$ describes the relation between states and measurements.

Open loop predicted states indicate a possible outcome of the states without any control action. The predicted states are checked against the safety limits of the system. If all predicted variables are within safety limits, that indicates that the disturbance will not cause a violation of safety limits and the system will remain in a normal state, even in presence of disturbance. However, if any of the predicted states violates safety conditions, further analysis is performed to check whether the effect of the disturbance can be mitigated by the controller.

5.2.4 Safety check for closed loop system

The controller's ability to keep the system within safety limits is checked in this step. This is done independent of the controller. Using a non-linear feasibility analysis algorithm, it is determined if there is exists a feasible solution within the input and output safety limits of the system (i.e. Definition 1). If there is a feasible solution, 'no warning' will be issued by monitoring system; otherwise, a warning will be issued. Following the notations discussed earlier, $\Delta y_{i,k+l,c}$ is a function of all the control actions at time step $k + l$; output constraints can be written as the following two inequalities:

$$y_{i,l} - \hat{y}_{i,k+l} - G_i(u_{1,k+l}, u_{2,k+l}, ...u_{n_u,k+l}) \leq 0, \tag{5.10}$$

$$\hat{y}_{i,k+l} - G_i(u_{1,k+l}, u_{2,k+l}, ...u_{n_u,k+l}) - y_{i,h} \leq 0, \tag{5.11}$$

where, $i = 1, 2, ...n_y$, and G_i is a nonlinear function describing the effect of control action on i-th output. Input constraints are described as:

$$u_{j,1} \leq u_{j,k+l} \leq u_{j,h}. \tag{5.12}$$

If all the output and input constraints described above are satisfied simultaneously, we conclude that the controller has the capacity to bring the process back to a safe operating region. This feasibility check is carried out successively for each time step in the 'monitoring horizon'. If all the constraints are linear, the problem can be formulated as a linear optimization problem, and linear programming can be used to check for feasible solution. However, from Equations 5.10, 5.11 and 5.12, it is evident that, though input constraints are linear, output constraints are nonlinear for any non-linear system. Hence, feasibility checking of all the constraints is a non-trivial problem. In our current study a feasibility test is performed through the constraint separation method described by [Schnabel, 1982].

5.2.5 Feasibility analysis using constraint separation method

Consider a nonlinear constraint of the form in Equation 5.10,

$$
\begin{aligned}
y_{1,l} - \hat{y}_{1,k+l} - G_1(u_{1,k+l}, u_{2,k+l}, ...u_{n_u,k+l}) \leq 0,\\
or \\
O(u_{j,k+l}) \leq 0,
\end{aligned}
\tag{5.13}
$$

along with $2n_u$ number of linear constraints as follows: =

$$
u_{j,1} \leq u_{j,k+l} \leq u_{j,h}, \tag{5.14}
$$

where $j = 1, 2, ..n_u$, $l = 1, 2, ..L$ and O is the non-linear function of $u_{j,k+l}$ that describes the non-linear constraint in Equation 5.10. To determine whether there exists a feasible solution of all the constraints, an optimization problem can be formulated as follows:

$$
\begin{aligned}
\min_{u_{j,k+l}} \quad & O(u_{j,k+l}) \\
\text{subject to} \quad & u_{j,1} \leq u_{j,k+l} \leq u_{j,h}.
\end{aligned}
\tag{5.15}
$$

Now, if the global minimum of the optimization problem is positive, it clearly indicates that Equation 5.13 cannot be satisfied with the given linear constraints. Thus a feasible solution of all the constraints is not possible. Now we will expand this result for m number of non-linear constraints O^i where, $i = 1, 2..m$. However, inclusion of more non-linear constraints will lead to a discontinuous objective function of the following form:

$$
\begin{aligned}
\min_{u_{j,k+l}} \quad & \phi(u_{j,k+l}) = \sum_{i=1}^{m} O^{i+}(u_{j,k+l}) \\
\text{subject to} \quad & u_{j,1} \leq u_{j,k+l} \leq u_{j,h}.
\end{aligned}
\tag{5.16}
$$

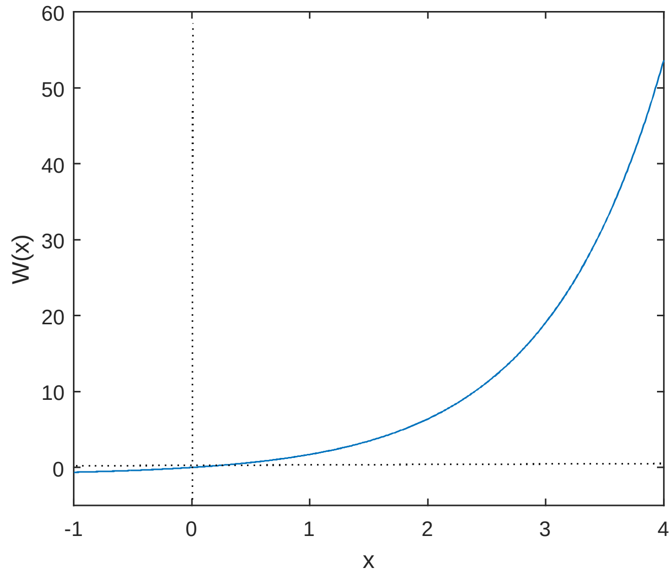

Figure 5.3: Responses of a typical weight function

where

$$O^{i+}(u_{j,k+l}) = \begin{cases} O^i(u_{j,k+l}) & O^i(u_{j,k+l}) > 0 \\ 0 & O^i(u_{j,k+l}) \leq 0 \end{cases} \tag{5.17}$$

Due to discontinuity in the objective function, evaluation of the global minimum using standard optimization procedure is difficult. [Schnabel, 1982] proposed the use of a continuous weight function. The property of the weight function is such that it penalizes a positive input and rewards a negative input. Different types of weight functions are suggested by the work of [Schnabel, 1982]. For our current study, we used a weight function from the exponential family. A typical shape of weight function is shown in Figure 5.3. Using weight function, Equation 5.18 is redefined as:

$$\begin{aligned} \min_{u_{j,k+l}} \qquad & \phi(x) = \sum_{i=1}^{m} W(O^i(u_{j,k+l})) \\ \text{subject to} \qquad & u_{j,1} \leq u_{j,k+l} \leq u_{j,h}. \end{aligned} \tag{5.18}$$

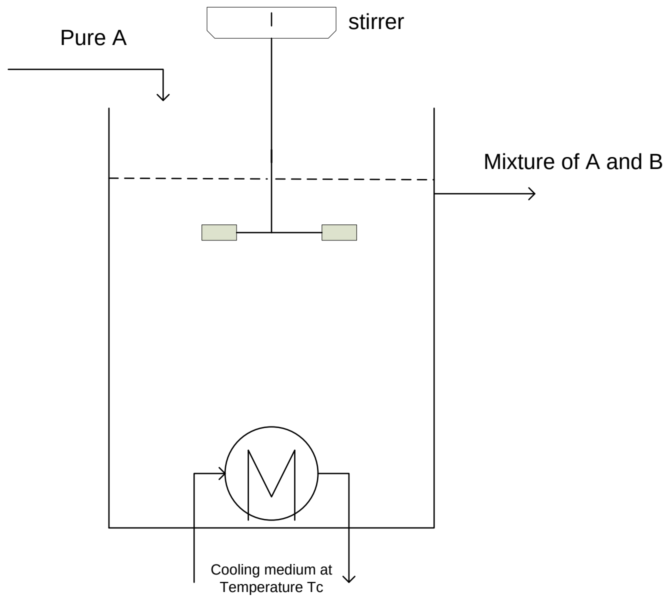

Figure 5.4: Schematic diagram of a CSTR

Optimization is performed with a gradient descent nonlinear optimizer to evaluate the global minimum of function $\phi(u_{j,k+l})$. A positive value of the objective function indicates that one or more constraints are violated. However, when a negative minimum is found, it indicates that a feasible solution can be found.

5.3 Case study

The proposed predictive warning system is demonstrated on a continuous stirred tank reactor (CSTR) model. A schematic diagram of a CSTR is shown in Figure 5.4. Governing equations of the CSTR are described as follows:

$$\frac{dC_A}{dt} = \frac{q}{V}(C_{Ai} - C_A) - k_0 e^{-E_A/T} C_A + w_1 \tag{5.19}$$

$$\frac{dT}{dt} = \frac{q}{V}(T_i - T) - \frac{\Delta H}{\rho C_p} k_0 e^{-E_A/T} C_A - \frac{UA}{\rho C_p V}(T - T_c) + w_2, \tag{5.20}$$

Table 5.1: Parameters of CSTR

Variable	Unit	Value
V	$Litre$	100
k_0	s^{-1}	1.2×10^9
dH	$Jmol^{-1}$	-5×10^4
ρ	$gLitre^{-1}$	1000
C_p	$Jg^{-1}K^{-1}$	0.239
U	$Jcm^2s^{-1}K^{-1}$	83.3
A	cm^2	10
T_c	K	305
E_A/R	K	8750

where C_A is the concentration of the reactant, T is the temperature in the reactor, q and V are flow-rate and volume and C_{Ai} and T_i are the feed concentration and temperature respectively. The reaction rate is $k_0 e^{-E_A/T} C_A$, ΔH is the reaction heat, ρ is the density, C_p is the specific heat, A is the area of heat transfer, U is the overall heat co-efficient and T_c is the temperature of the cooling fluid. $w = [w_1 \; w_2]^T$ represents the plant model mismatch of the system. In this case we assumed w was random Gaussian. The operating range of process inputs and different parameters of the system were chosen from the work of [Henson and Seborg, 1997] and are stated in Table 5.1. These parameters remain the same throughout the case study. Nonlinear state equations were solved by the differential equation editor (DEE) of Simulink and were used as the process plant. Measurement noise was added to the states and measurement equation is expressed as follows:

$$\mathbf{y_k} = [C_A \quad T]^T + \nu \tag{5.21}$$

where, $\mathbf{y_k}$ is the process measurement and ν is the measurement noise. Measured outputs C_A and T were controlled by two PID controllers. Controllers regulated the feed concentration C_{Ai} and feed temperature T_i to achieve the desired concentration

C_A and temperature T of the reactant. Feed concentration was varied between 0 and 1 and feed temperature was varied between 300°C and 500°C. A step change in feed flow q was considered as disturbance to the plant. Different scenarios were defined based on the size of the step disturbance.

5.3.1 Demonstration of the warning system

The proposed predictive warning system had been demonstrated for three different disturbance scenarios. From many case simulations, these scenarios were selected to show the three possible outcomes when a disturbance affects the system. These are: (i) disturbance size is small and does not cause a violation of the safety threshold, even if there is no control action; (ii) disturbance is large enough to cause a violation for an open loop system; however, the controller has the capacity to nullify the effect; (iii) a large disturbance that perturbs the system significantly. These three scenarios were created changing the step size of feed flow. The proposed warning scheme was applied to these three simulated cases and the consistency of the alarm system outcomes (i.e., 'no alarm', 'alarm') was checked against the actual closed loop signal.

For all the scenarios, the plant was initially brought to a steady state at C_A=0.7 and T=330K using two PID controllers. Controllers govern the manipulated variables: feed concentration C_{Ai} and temperature T_i. The ranges of these manipulated variables are :

$0 \leq C_{Ai} \leq 1$ and $200\ K \leq T_i \leq 500\ K$.

The lower safety threshold of concentration C_A and temperature T were set at 0.6 and 320 K respectively. Feed flow q was set at 1.667 $litre/s$, till plant steady state was achieved by the controller. After a steady state was achieved, feed flow was decreased to a lower value to introduce a disturbance to the system.

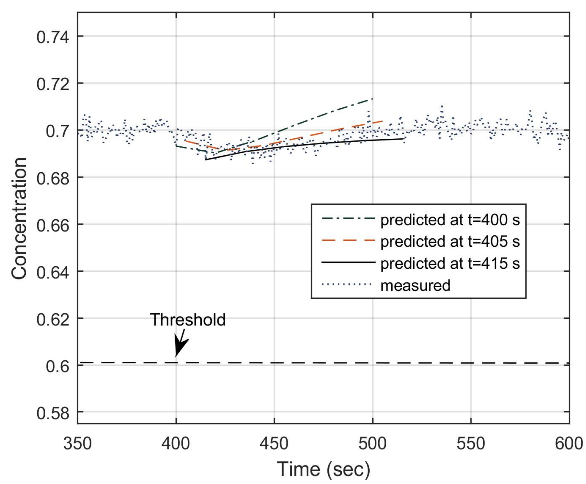

(a) Concentration plot

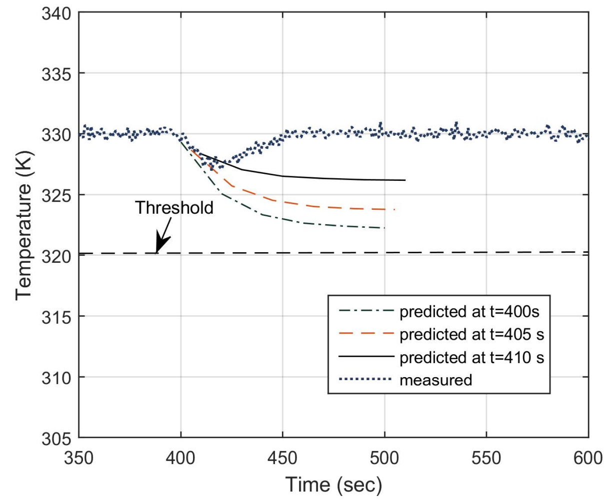

(b) Temperature plot

Figure 5.5: Predicted open loop states and closed loop measurements of the CSTR when feed flow is changed from 1.6 to 1 $litre/s$

For the first scenario, feed flow was decreased to 1 $litre/s$. Open loop predictions of concentration and temperature for different time instances are shown in Figures 5.5a and 5.5b. The results showed that the predicted temperature and concentration at the monitoring horizon (400s to 500s) remain within the safety limits and no alarm was issued. Measured concentration and temperature validated the 'no warning' state and are shown in Figures 5.5a and 5.5b.

For the second scenario, feed flow was changed to 0.8 $litre/s$ after the steady state was achieved. Open loop predictions of concentration and temperature for this scenario are shown in Figures 5.6a and 5.6b. Results show that the open loop predicted temperature exceeds the safety threshold. Hence, the warning system proceeds to the next stage to check if all the input and output constraints can be satisfied in a closed loop scenario. Input constraints are defined from the upper and lower thresholds of the manipulated variables. Output constraints are defined from the safety thresholds and open loop predictions of states. To reduce the computational load, predictions are sampled every 20 seconds and five samples are used to define five output constraints

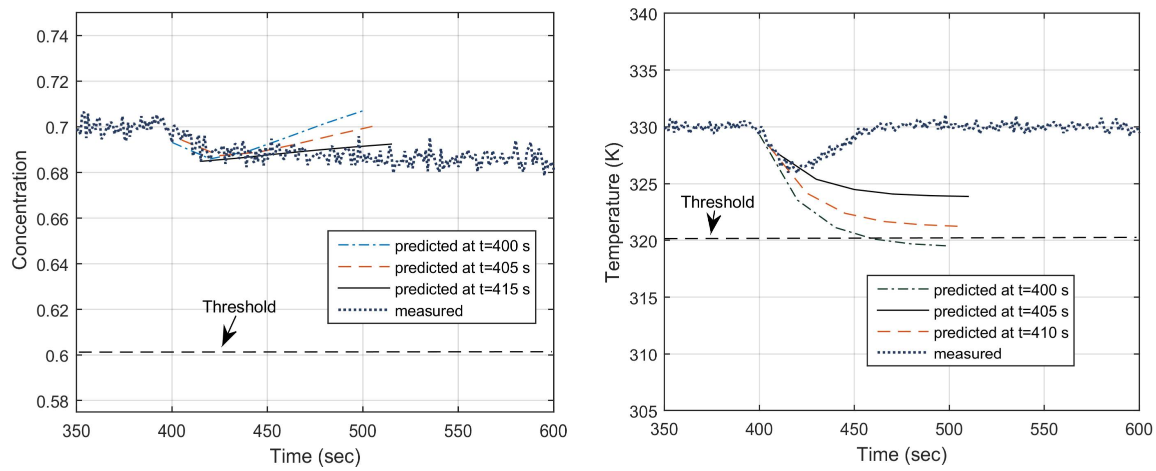

(a) Concentration plot (b) Temperature plot

Figure 5.6: Predicted open loop states and closed loop measurements of the CSTR when feed flow is changed from 1.6 to 0.8 $litre/s$

for each measured variable. Hence, concentration constraints and temperature constraints are defined. In the feasibility analysis, it was checked to determine whether all the input and output constraints could be satisfied simultaneously. The proposed constraint separation method was used to perform this analysis at each time instant. A weighting function was used to penalize a positive minimum and reward a negative minimum. It was initially set as $w_1(x) = e^{4x} - 1$. The solution of the optimization function for the given constrained conditions for each time instant is shown in Figure 5.7. It was found that the minimum for the optimization function remained negative for each time instant. This result suggests that controllers have sufficient capacity to nullify the disturbance; the system remained at the 'no warning state'. Measured variables for this scenario are shown in Figures 5.6a and 5.6b. Figures show that both concentration and temperature started to decrease after a disturbance was introduced. However, the controllers were able to counteract the effect and brought the measured variables to their original positions. Thus, measured variables support the 'no alarm' state from the warning system.

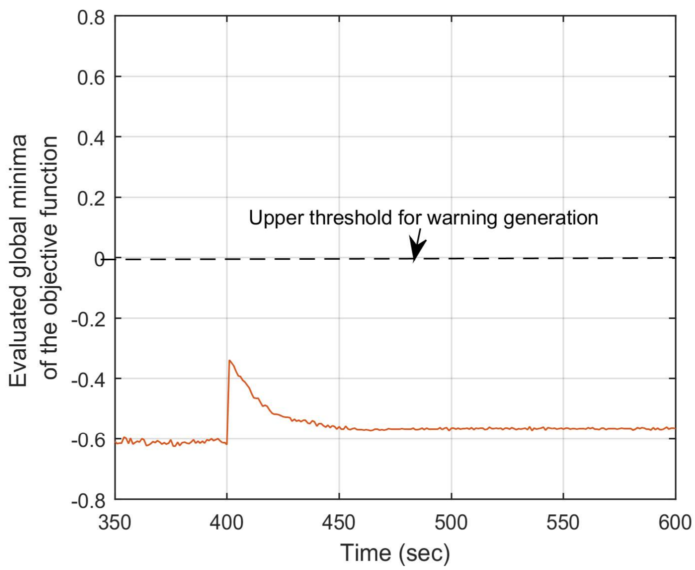

Figure 5.7: Global minima evaluated for a feasible solution when flow rate is changed to 0.8 $litre/s$.

For the third scenario, a higher level of disturbance was introduced by changing the flow from 1.667 $litre/s$ to 0.2 $litre/s$ at $t = 400$ s. Predicted concentration and temperature for this case are shown in Figures 5.8a and 5.8b. Though the predicted concentration remained above the lower threshold, the predicted temperature violated the lower threshold. Similar to the previous scenario, the controller's ability to nullify this disturbance was checked using the feasibility analysis algorithm.

Three weighting functions were used for making the system more robust. The global minimum for this case is shown in Figure 5.9. It was found that after the disturbance was introduced, the global minimum showed a positive value, which indicates a violation of one or more safety conditions. Thus, a warning was issued to the operators for this scenario. The warning system is validated from the process measurements shown in Figures 5.8a and 5.8b. The results show that the temperature exceeded the safety threshold at $t = 425s$. Thus, using the proposed method, a warning was issued 25 s earlier, compared to the conventional method. The predictive warning system issued

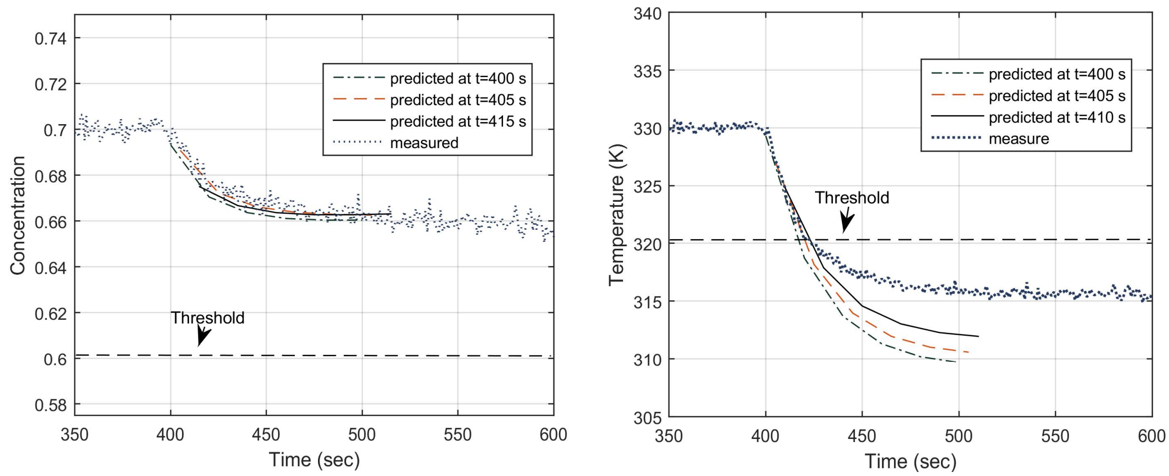

(a) Concentration plot

(b) Temperature plot

Figure 5.8: Predicted open loop states and closed loop measurements of the CSTR when feed flow is changed from 1.6 to 1 $litre/s$

a warning at $t = 400s$, as soon as the disturbance entered the system.

5.3.2 Performance of the proposed method using different weight functions

The variable separation method uses a weighting function to smooth the discontinuity in an objective function. The weighting function was chosen such that it penalizes a positive value and rewards a negative optimized solution. As different nonlinear safety constraints contribute in the objective function, there is a possibility that a small positive value from certain constraints may not be realizable as one can be neutralized by a number of negative solutions. To eliminate that possibility, the weighting function was changed after a negative outcome from the objective function was obtained. For the case study, the weight function was initially set as, $w_1(x)$=$e^{4x} - 1$. After a negative outcome of the objective function was observed, this weight function was changed to $w_2(x)$=$e^{8x} - 1$. This procedure was repeated twice to improve the robustness of the overall 'warning generation' procedure. Consider the third scenario

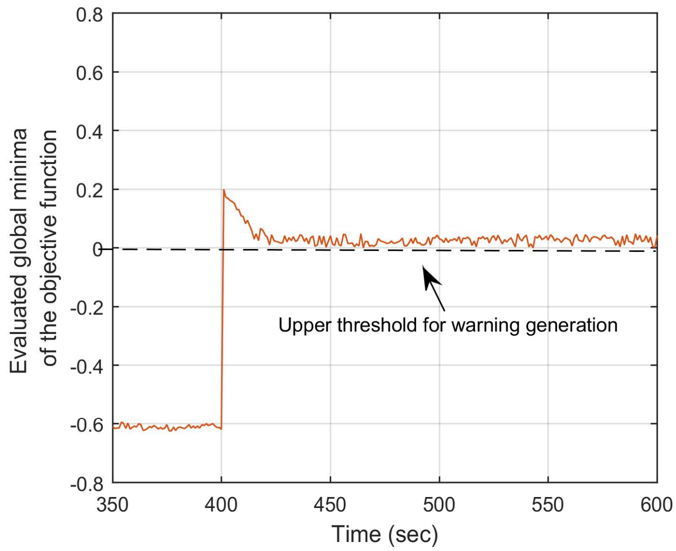

Figure 5.9: Global minima evaluated for a feasible solution when flow rate is changed to 0.2 $litre/s$.

of the previous section, where the disturbance was large enough to take the process measurement below the lower threshold. The plant was initially steadied at 0.7 and 330 K. At the steady state, feed flow was changed from 1.6 to 0.2 $litre/s$. A robust result was obtained in the previous case study by successively changing the weight function when a negative minimum was observed. Three different fixed weight functions were used. These functions are:

$w_1{=}e^{4x} - 1$;

$w_2{=}e^{8x} - 1$;

$w_3{=}e^{12x} - 1$.

Steps of the weight functions are shown in Figure 5.10. Global minima of the objective functions are evaluated and passed through the weight functions at each instant. Evaluated minima at the output of the different weights and alarm generation threshold are shown in Figure 5.11a, 5.12a and 5.13a. A warning is generated when output at the weight function shows non-zero values. Generated alarm profiles from the different weight functions are shown in Figure 5.11b, 5.12b and 5.13b.

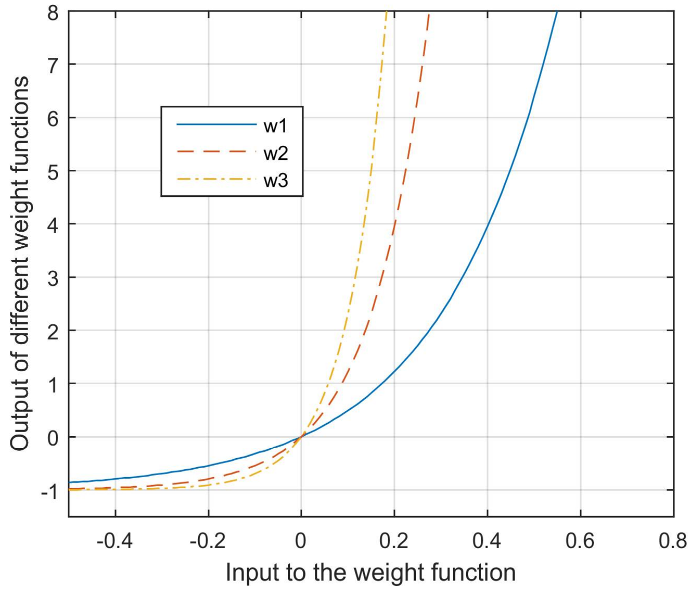

Figure 5.10: Responses of the different weight functions

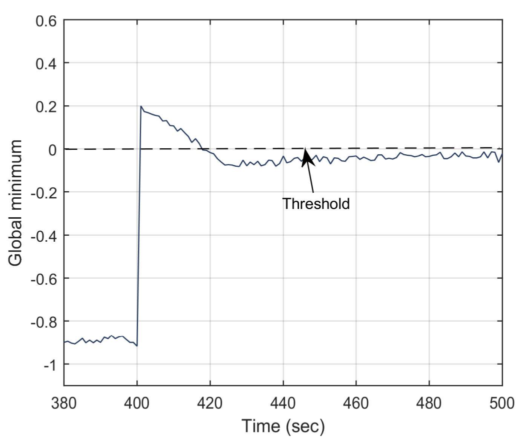

(a) Evaluated global minimum using w_1

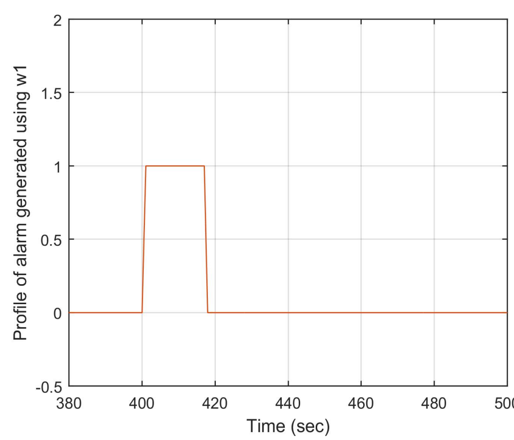

(b) Generated warning using w_1

Figure 5.11: Global minimum and alarm profile using w_1

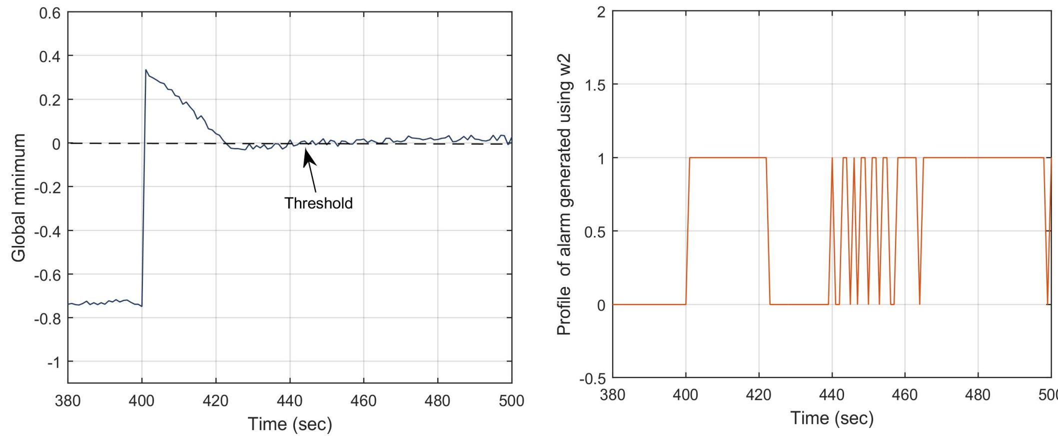

(a) Evaluated global minimum using w_2

(b) Generated warning using w_2

Figure 5.12: Global minimum and alarm profile using w_2

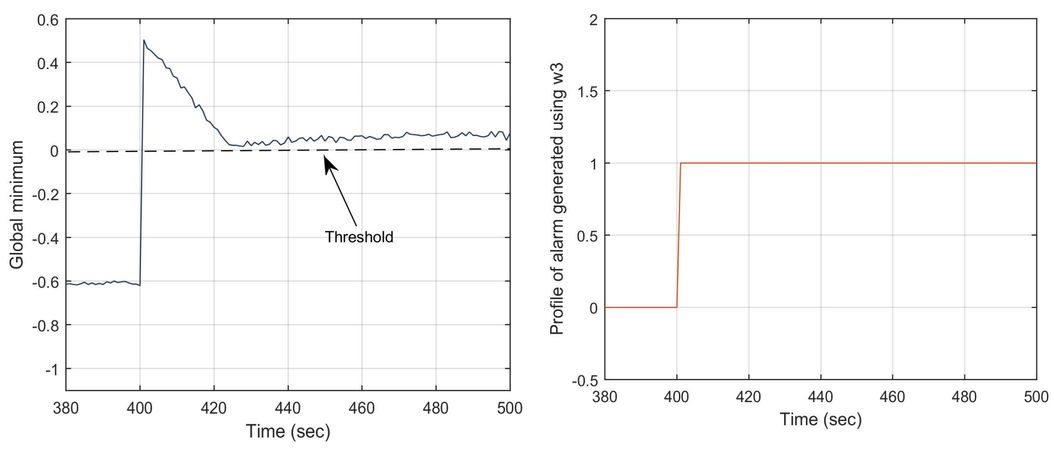

(a) Evaluated global minimum using w_3

(b) Generated warning using w_3

Figure 5.13: Global minimum and alarm profile using w_3

The alarm profile from w_1 shows a 'no warning state' after $418s$, even though measurements show a violation of the safety condition. For weight function w_2, there was alarm chattering, as for some instances the positive minimum was nullified by the other negative minima. The third curve shows the same alarm profile found using weight function w_3. It shows a sustained alarm, which is consistent with the observed measurement. Execution time of the proposed warning generation system is also an important factor. Execution time increases with the use of steeper weight functions. Thus, accuracy and execution time both need to be considered when selecting an initial weight function and its gradual increase for warning generation.

5.4 Conclusions

A predictive warning generation system for a nonlinear system was presented. The warning was generated analysing the predictive states, current measurement, safety limits and available controllers' capacity. Future states were predicted from the open-loop process model using a nonlinear receding horizon predictor. Predicted states were used to identify a possible violation of safety limits. Once a potential abnormal outcome was detected, a feasibility analysis was performed to check whether the existing controller was capable of negating the effect of disturbance.

Performance and robustness of the proposed method was demonstrated through a case study with different scenarios. The proposed method was able to issue an early warning significantly earlier compared to monitoring a measured signal. In this paper, we also deal with identification of a feasible solution of nonlinear constrained system. In the proposed monitoring system, constraint separation based optimization method was used to perform this task. The constraint separation method uses weight function which was changed iteratively to improve the robustness. The ability of this weight function to generate a warning was also studied. Results showed that accuracy of the warning system increases with the use of steeper weight functions.

Acknowledgement

The authors thank Natural Sciences and Engineering Research Council (NSERC) for financial support.

Bibliography

[Ahooyi et al., 2016] Ahooyi, T. M., Soroush, M., Arbogast, J. E., Seider, W. D., and Oktem, U. G. (2016). Model-predictive safety system for proactive detection of operation hazards. *AIChE Journal*, 62(6):2024–2042.

[Albalawi et al., 2017] Albalawi, F., Durand, H., and Christofides, P. D. (2017). Process operational safety via model predictive control: Recent results and future research directions. *Computers & Chemical Engineering*.

[Aswani et al., 2013] Aswani, A., Gonzalez, H., Sastry, S. S., and Tomlin, C. (2013). Provably safe and robust learning-based model predictive control. *Automatica*, 49(5):1216–1226.

[Banerjee and Ierapetritou, 2005] Banerjee, I. and Ierapetritou, M. G. (2005). Feasibility evaluation of nonconvex systems using shape reconstruction techniques. *Industrial & engineering chemistry research*, 44(10):3638–3647.

[Chinneck, 2007] Chinneck, J. W. (2007). *Feasibility and Infeasibility in Optimization:: Algorithms and Computational Methods*, volume 118. Springer Science & Business Media.

[Henson and Seborg, 1997] Henson, M. A. and Seborg, D. E. (1997). *Nonlinear process control*. Prentice Hall PTR Upper Saddle River, New Jersey.

[Khan et al., 2014] Khan, M. A. I., Imtiaz, S. A., and Khan, F. (2014). Early warning system for chemical processes with time delay and limited actuator capacity. *Industrial & Engineering Chemistry Research*, 53(12):4763–4772.

[Primbs et al., 1999] Primbs, J. A., Nevistić, V., and Doyle, J. C. (1999). Nonlinear optimal control: A control lyapunov function and receding horizon perspective. *Asian Journal of Control*, 1(1):14–24.

[Schnabel, 1982] Schnabel, R. B. (1982). Determining feasibility of a set of nonlinear inequality constraints. *Algorithms for Constrained Minimization of Smooth Nonlinear Functions*, pages 137–148.

[Varga et al., 2009] Varga, T., Szeifert, F., and Abonyi, J. (2009). Detection of safe operating regions: a novel dynamic process simulator based predictive alarm management approach. *Industrial & Engineering Chemistry Research*, 49(2):658–668.

[Zarei and Poshtan, 2010] Zarei, J. and Poshtan, J. (2010). Design of nonlinear unknown input observer for process fault detection. *Industrial & Engineering Chemistry Research*, 49(22):11443.

Chapter 6

Conclusions and Future Recommendations

6.1 Contributions

The current research was performed to develop a predictive warning generation scheme for chemical processes with unknown disturbances. Warning was generated using predictive states from the moving horizon predictor of MPC. The predictive scheme was initially developed for restrictive cases; later the scheme was modified for more general cases, relaxing the constraints. The research was completed fulfilling the goals defined in chapter 1. Contributions and outcomes of the thesis is summarized below:

(i) In chapter 2, an experimental study is performed to evaluate the control performance of PID-free MPC as supervisory controller. In-house DMC was designed on a pilot scale plant of CSTH and control performance of the controller was compared with its competitor structures. Based on the ISE value, PID-free MPC showed superior performance in set-point tracking of the temperature.

(ii) Control frequency plays an important role while executing PID-free controller. Effect of control frequency on PID-free MPC was also studied in chapter 2, through a comparative study of the control performance of DMCs designed with different control frequencies.

(iii) In chapter 3, predictive warning generation system was designed for linear process with unknown disturbance. This work improved an earlier warning scheme of [Khan et al., 2014] including unknown input observer. Luenberger and Kalman-based observers were designed and used in the warning scheme to estimate the disturbance. Proposed scheme was applied to a virtual plant described in [Thornhill et al., 2008]. Results showed robust performance while generating warning. Kalman-based scheme showed improved performance compared to Luenberger-based scheme while estimating the disturbance in the noisy scenarios.

(iv) As, the proposed scheme in chapter 3 is an extension of an earlier work, a comparison of the performances of the two schemes is provided. The results of the proposed scheme was consistent with the previous work. However, lead-time of the warning generation reduced with the introduction of the unknown disturbance.

(v) In chapter 4, an EM-like particle filter based simultaneous state and unknown disturbance estimation framework was developed. The proposed framework was applied to simulated models of CSTR and four-tank system, and an experimental data of a pilot-scale plant of a four-tank system. The results showed consistent estimation of states and inputs for all cases.

(vi) Convergence analysis of the estimated input was performed for both simulation and experimental cases. The results showed that, proposed algorithm converged to the estimated inputs after few iterations.

(vii) In chapter 5, warning generation of a nonlinear system is presented using moving horizon predictor and feasibility analysis. Moving horizon was used to predicted the process states. The predicted states, safety limits and actuator capacity was used to formulate the output and input constraints. A feasibility analysis was used to determined if all the input and output constraints were satisfied using the existing controllers' capacity. Constraint separation method was used to perform the feasibility analysis.

(viii) Proposed warning scheme of chapter 5 was applied to a nonlinear CSTR model. For different cases, proposed method was able to generate warning consistently. Weight function plays a significant roles in constraint separation method. Hence, performance of the warning system for different weight functions was also studied.

6.2 Future recommendations

Predictive warning generation for nonlinear system is still an open problem. In this thesis, we systematically developed predictive scheme initially for linear process with unknown input; later was extended for nonlinear system. Some areas of further research is listed below:

(i) For simultaneous estimation of hidden states and unknown disturbances, we considered only step-type additive disturbance. Estimation scheme for multiplicative and ramp-type disturbance needs further investigation. Estimation of the unknown disturbance was hampered, when there was model mismatch. Improving the estimation scheme for that case needs further consideration.

(ii) Warning generation scheme proposed in chapter 5, used known disturbance. Estimation scheme of the chapter 4 needs to be integrated with the warning scheme to improve it further.

Bibliography

[Khan et al., 2014] Khan, M. A. I., Imtiaz, S. A., and Khan, F. (2014). Early warning system for chemical processes with time delay and limited actuator capacity. *Industrial & Engineering Chemistry Research*, 53(12):4763.

[Thornhill et al., 2008] Thornhill, N. F., Patwardhan, S. C., and Shah, S. L. (2008). A continuous stirred tank heater simulation model with applications. *Journal of Process Control*, 18(3-4):347 – 360.